DOI:10.14753/SE.2022.2630

THE INTERPLAY OF PLATELETS AND FIBRIN IN FIBRINOLYSIS: *EX VIVO* AND *IN VITRO* STUDIES

PhD Thesis

Veronika Judit Farkas

Molecular Medicine Doctoral School

Semmelweis University

Supervisor: Krasimir Kolev, MD, D.Sc

Official reviewers: Bodó Imre, MD, Ph.D

Bagoly Zsuzsa, MD, Ph.D

Head of the Final Examination Committee: Gyula Domján, MD, Ph.D

Members of the Final Examination Committee: György Blaskó, MD, D.Sc

Gábor Bőgel, MD, Ph.D

Budapest

2021

DOI:10.14753/SE.2022.2630

TABLE OF CONTENTS

THE LIST OF ABBREVIATIONS 4

1. INTRODUCTION 7

1.1. Platelets 9

1.1.1. Platelet adhesion 11

1.1.2. Activation 12

1.1.2.1. Signaling pathways activated by adhesive and soluble platelet agonists 13

1.1.2.2. Shape change 16

1.1.2.3. Integrin activation by inside-out signaling 16

1.1.2.4. Granule secretion 16

1.1.2.5. Membrane reorganization 18

1.1.3. Aggregation 20

1.1.4. Influence on fibrin structure, clot retraction 21

1.1.5. Regulation of fibrinolysis 22

1.1.6. Distinct platelet populations of the hemostatic plug 23

1.2. Cyclophilin D 28

1.2.1. The structure of the mitochondrial Cyclophilin D 28

1.2.2. The role of CypD in the regulation of mitochondrial bioenergetics 28

1.2.3. Pharmacological modulation of MPTP and CypD function 30

1.2.4. MPTP opening in platelets 31

2. OBJECTIVES 34

2.1. Platelet content of arterial thrombi 34

2.2. Effects of CypD and CsA on the morphology and function of platelets 34

2.3. Structural properties of cancer-associated venous thrombi 34

DOI:10.14753/SE.2022.2630

3. METHODS 35
3.1. Investigations of platelet content of arterial thrombi 35
3.1.1. Patients 35
3.1.2. Thrombus collection 35
3.1.3. Scanning electron microscopic (SEM) imaging of arterial thrombus composition 36
3.1.4. Statistical procedures 36
3.2. Investigations on the effects of CypD and CsA on platelet morphology and function 37
3.2.1. Animals 37
3.2.2. Preparation of platelets 37
3.2.3. Morphological imaging of platelets by scanning electron microscope (SEM) 38
3.2.4. Morphological imaging of platelets by transmission electron microscope (TEM) 39
3.2.5. Platelet functional assays – adhesion and spreading 40
3.2.6. Platelet functional assays – aggregation assay 40
3.2.7. Platelet functional assays – tissue factor-induced clotting assay 41
3.2.8. Platelet functional assays – turbidimetry assay of fibrinolysis 41
3.2.9. Statistical procedures 42
3.3. Investigations of the structural properties of venous thrombi formed in human pancreatic tumor-bearing mice 42
3.3.1. Cells and mouse tumor model 42
3.3.2. Thrombosis model 43
3.3.3. Scanning electron microscopic (SEM) imaging of venous thrombus composition 43
3.3.4. Statistical procedures 44

DOI:10.14753/SE.2022.2630

4. RESULTS 46
4.1. Platelet content of arterial thrombi 46
4.2. Effects of CypD and CsA on platelet morphology and function 49
4.2.1. Morphological alterations of platelets activated by ’strong’ stimuli 49
4.2.2. Structural features of fibrin formed in the presence of ’strongly activated’ platelets……54
4.2.3. Platelet functions as a response to ’mild’ stimuli 56
4.2.4. Fibrin structure modification in the presence of platelets activated by ’mild’ stimuli……..60
4.2.5. Effects of platelets on the tissue factor-induced clotting of plasma 62
4.2.6. Impact on fibrinolytic susceptibility 63
4.3. Structural properties of venous thrombi formed in human pancreatic tumor-bearing mice 66
5. DISCUSSION 68
5.1. Platelet content of arterial thrombi 68
5.2. Effects of CypD and CsA on platelet morphology and function 70
5.3. Structural properties of venous thrombi formed in human pancreatic tumor-bearing mice 76
6. CONCLUSIONS 78
7. SUMMARY 79
8. ÖSSZEFOGLALÁS 80
9. BIBLIOGRAPHY 81
10. BIBLIOGRAPHY OF THE CANDIDATE’S PUBLICATIONS 118
10. 1. Publications related to the PhD thesis 118
10. 2. Publications not related to the PhD thesis 118
11. ACKNOWLEDGEMENTS 120

DOI:10.14753/SE.2022.2630

THE LIST OF ABBREVIATIONS

AC	adenylate-cyclase
AIS	acute ischemic stroke
ANT	adenine nucleotide translocase
ASA	acetylsalicylic acid
Bk	bongkrekic acid
CAD	coronary artery disease
CalDAD-GEFI	Calcium and diacylglycerol regulated guanine nucleotide exchange factor I
CI	cell index
CRP	C-reactive protein
CsA	Cyclosporin A
CypA	Cyclophilin A
CypD	Cyclophilin D
$CypD^{-/-}$, KO	Cyclophilin D knock-out
DAG	1,2-diacylglycerol
DMSO	dimethyl-sulphoxide
DTS	dense tubular system
et	ethanol
FcRγ	Fc receptor γ chain
FI-XIII	coagulation factors I-XIII
FI-XIIIa	activated coagulation factors I-XIIIa
FK, FK-506	tacrolimus
Gla	γ-carboxyglutamate
GPCR	G-protein-coupled receptor
GPIa/IIa, IIb/IIIa, VI, Ib-IX-V	glycoprotein receptors Ia/IIa, IIb/IIIa, VI, Ib-IX-V
Hgb	Hemoglobin
IP_3	inositol-1,4,5-trisphosphate
ITAM	immunoreceptor tyrosine-based activation motif
IVC	inferior vena cava
MPT	mitochondrial permeability transition
MPTP	mitochondrial permeability transition pore

NSTEMI	non ST-elevation myocardial infarction
PAD	peripheral artery disease
PAI-1	plasminogen activator inhibitor-1
PAR1,3,4	protease-activated receptor 1,3,4
PBS	phosphate buffered saline
PDF	probability density function
p_{distr}	p-value from Kuiper-test for distributions
PI3K	phosphoinositide 3-kinase or phosphatidylinositol 3-kinase
PLA2, Cß,Cγ2	phospholipase A2, Cß, Cγ2
(H)Plt	(human) platelet
p_{med}	p-value resulting from one-tailed hypothesis testing for medians
PPIase	peptidyl-prolyl *cis-trans* isomerase
PPP	platelet-poor pooled plasma
PS	phosphatidylserine
Rap1b	Ras-related protein 1b
RBC	red blood cell(s)
RIAM	Rap1-interacting adaptor molecule
RhoA	Ras homolog family member A
ROS	reactive oxygen species
rtPA	recombinant tissue-type plasminogen activator
SD	standard deviation
SE	standard error of mean
SEM	scanning electron microscope
sGC	soluble guanylate-cyclase
sPlt	relative platelet content/surface occupancy
Src kinase	eukaryotic sarcoma tyrosine-kinase
STEMI	ST-elevation myocardial infarction
STIM1	stromal interaction molecule 1
Syk kinase	spleen tyrosine kinase
TC	total platelet cross-section area

TEM	transmission electron microscope
TF	tissue factor
TFPI	tissue factor pathway inhibitor
Th	thrombin
TO	total area of membrane-bearing organelles
tPA	tissue-type plasminogen activator
TP	thromboxane A2 receptor
TRIS	Tris-(Hydroxymethyl)-aminomethane
TRPC	transient receptor potential canonical channels
TXA_2	thromboxane A_2
t10, t50	time to reach 50% or 10% of maximal turbidity
uPA	urokinase-type plasminogen activator
vWF	von Willebrand Factor
WBC	white blood cell
WT, $CypD^{+/+}$	wild type
Z_i, Z_0	impedance at an individual time point or at the start of the experiment
#O	number of observations

DOI:10.14753/SE.2022.2630

1. INTRODUCTION

According to the World Health Organization statistics, cardiovascular diseases remain among the major causes of death. Ischaemic heart disease is responsible for 16% of the world's total deaths, showing a greatly increasing trend since 2000. Stroke is the second leading cause of mortality, with approximately 11% of total deaths (1). The third most prevalent form of cardiovascular disorders is peripheral artery disease generating a severe burden on health care (2).

These medical conditions have a common underlying pathology: arterial thrombus formation leading to vessel occlusion and tissue hypoxia. Platelets have a long-known role in the formation of arterial thrombi, and most therapeutic designs of primary and secondary prevention rely on targeting these cell fragments. The rising incidence of cardiovascular disorders despite the many pharmacological options indicates gaps in our knowledge about some aspects of platelet physiology. For instance, their response to heterogeneous local activator signals remains ambiguous. Unraveling the exact molecular mechanisms regulating platelet function can improve our understanding of this complicated process and enable the further development of anti-platelet drugs.

Our work described in this thesis focused on i) the clinical determinants of relative platelet content of arterial thrombi formed in coronary, peripheral artery disease, and acute ischemic stroke, and ii) the specific role of cyclophilin D (CypD) in platelet activation.

To put our work in perspective, this chapter provides an introduction to basic platelet physiology. This is followed by the description of CypD function and its relation to platelet activation.

Although deep vein thrombosis and its most serious complication, pulmonary embolism are not included in the WHO's list of top 10 causes of death, venous thromboembolism is the third leading vascular disease with over one million estimated VTE events or related deaths per year in six countries of the EU (3). The pathomechanism differs from arterial thrombus formation; Virchow's triad describing the precipitating factors of DVT includes venous stasis, vessel wall injury and hypercoagulability. The last risk factor is often associated with malignant diseases, e.g. pancreatic cancer (4).

The examination of venous thrombi formed in the presence of pancreatic cancer may enable the fine-tuning of anticoagulant therapy in affected patients. Thus, the last part of

DOI:10.14753/SE.2022.2630

our work focused on the study of venous thrombus composition in human pancreatic tumor-bearing mice.

1.1. Platelets

Platelets (or thrombocytes) are enucleated discoid blood cells (1-2 μm in diameter with 0,5 μm thickness) produced primarily in the bone marrow from polyploid megakaryocytes during thrombopoiesis and continuously released into the circulation (5). The hematopoietic stem cells are activated by thrombopoietin released from the liver as an answer to low blood platelet counts (6) or in inflammatory states (reactive thrombopoiesis, stimulated by interleukin-6 (7)). The shedding of long-branching cytoplasmic protrusions leads to the formation of proplatelets that further develop and divide into platelets (5). Circulating platelets are non-reactive and interact passively with the endothelial layer of the vessels, partly due to the endothelial cell-derived platelet activation inhibitors (e.g. secreted nitric oxide, prostacyclin, or CD39, an ecto-ADPase) (8, 9).

These smallest blood cells have a short lifespan (7-10 days) in circulation before being phagocytosed in the spleen or liver (10). They have been found to take part in many physiological and pathological processes during their short life. Embryonic development (11), inflammation (12), tumor cell growth (13), and cancer metastasis formation (14) all require certain platelet functions, but these cells are primarily viewed as key mediators of hemostasis.

The platelet-dependent process preventing blood loss from an injured vessel is called primary hemostasis, as it precedes the formation of a fibrin clot through the actions of the plasmatic coagulation factors (secondary hemostasis). Platelets create a temporary platelet plug that – together with vasoconstriction – closes the wound until the secondary hemostasis stabilizes the thrombus with the help of a developing fibrin network (Fig.1). The distinction between these two processes is quite arbitrary as the role of platelets is not limited to the initial stage; there are multiple links between the cellular and the plasmatic coagulation systems. (i) Platelets serve as a site for thrombin generation as they promote the functions of coagulation factors by providing an activation surface. (ii) They act as an anchor for the growing scaffold of the clot and modify the structure of the forming fibrin fibers through interactions between their membrane receptors and the extracellular proteins. (iii) They can regulate both the formation and the dissolution of this hemostatic protein network (fibrinolysis) through the secretion of substances from their granules.

DOI:10.14753/SE.2022.2630

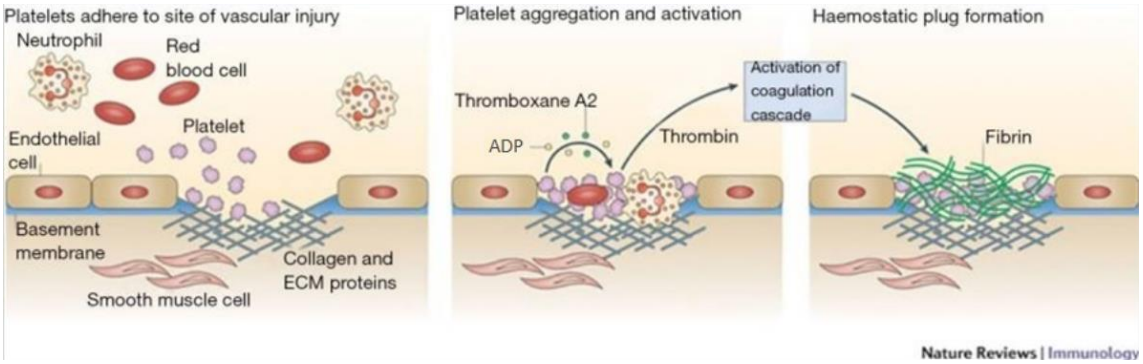

Figure 1. Schematic depiction of the hemostatic plug formation. Adapted from (15). For a detailed description see text.

Their hemostatic functions can be divided into three distinct phases: *adhesion* to subendothelial collagen of the injured vessel wall through specific receptors, *activation* resulting in intracellular signal transduction causing membrane and cytoskeletal reorganization and vesicle secretion, and the *aggregation* of numerous platelets with the help of plasma proteins (Fig. 2.). The steps of these phases are successive but happen with certain overlaps and redundancies.

On one hand, platelets are indispensable in the formation of a primary hemostatic clot to stop blood loss at the site of vascular injury, on the other, their hemostatic roles can turn pathological: they play a crucial role in the development of often life-threatening arterial thrombi. Although many details of their activation – e.g. the mechanisms of platelet adhesion, aggregation, vesicle secretion, microvesicle formation, and clot retraction/stabilization – are well outlined and are targeted by various anti-platelet drugs, some aspects of their functions are not fully elucidated.

The gaps in our current knowledge mainly concern the distinction between normal and pathological processes. The therapeutic goal in arterial thrombotic diseases is to inhibit unnecessary thrombus formation without increased risk of bleeding while maintaining the ability of platelets to contribute to normal hemostasis.

DOI:10.14753/SE.2022.2630

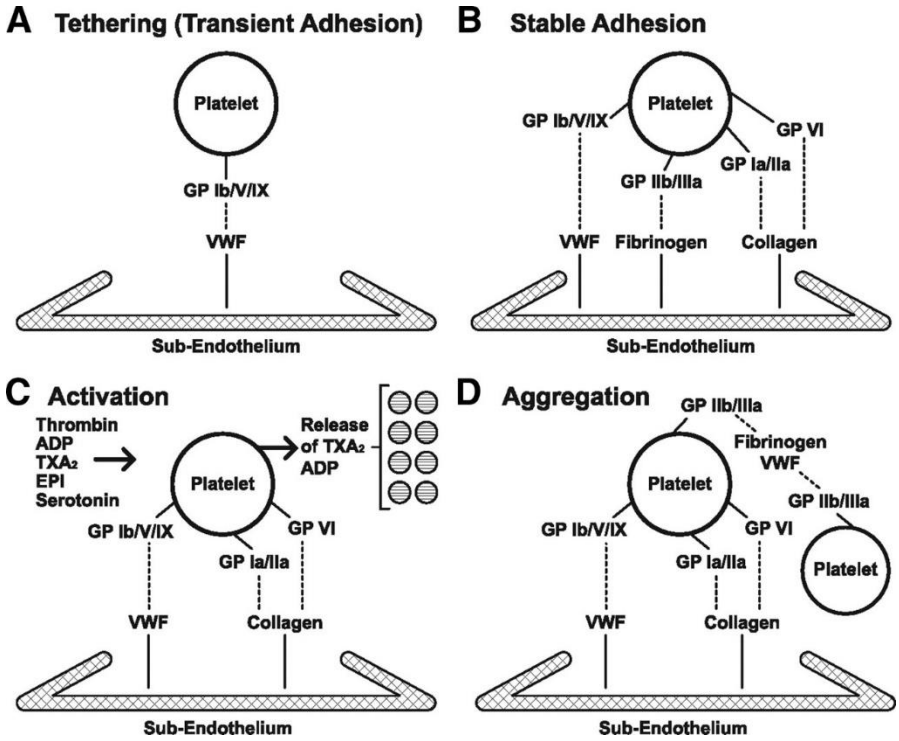

Figure 2. Stages of platelet adhesion, activation, and aggregation. Adapted from (16).

GPIb/V/IX, GPIIb/IIIa, GPVI: glycoprotein receptors, VWF: von Willebrand Factor, TXA_2: thromboxane A_2, EPI: epinephrin. For a detailed description see text.

1.1.1. Platelet adhesion

At the site of vascular injury, resting circulating platelets come in contact with and adhere to the highly reactive components of the subendothelial layers of the vessel wall. There are two major (collagen and von Willebrand Factor, vWF) and several minor (fibronectin (17), laminin (18), and thrombospondin (19)) adhesive substrates that participate in the process.

The initial, reversible interaction with exposed extracellular matrix proteins helps capture the platelets and trigger their activation (20). In the arteries, under high shear and extremely rapid blood flow, the tethering and rolling of platelets are enabled by the interaction of glycoprotein receptors Ib-IX-V (GP Ib-IX-V) with vWF (21). vWF is a multimeric plasma protein synthesized by endothelial cells and megakaryocytes (22) with several functional domains that offer binding sites for subendothelial matrix proteins (e.g. collagen, sulfated glycoproteins). It becomes immobilized through its collagen binding sites in A1 and A3 domains on the site of vessel wall damage (23, 24)

and stretched out by the high shear forces of arterial blood (25). The GPIbα receptor of the GPIb/IX/V complexes that can be found in high density in the platelet membrane forms a large number of bonds with the A1 domains of the multivalent vWF. As the interaction is characterized by rapid on- and off-rates, it results only in transient association (21). New membrane projections, filopodia form and participate in platelet translocation or rolling along the immobilized vWF (21, 26, 27). Their role is critical in decelerating and maintaining platelets in close contact with the exposed subendothelium allowing integrin-mediated arrest, the secondary phase of platelet adhesion.

Additionally, platelets bind directly to subendothelial collagen, and this interaction is one of the most potent initiators of platelet activation and aggregation (28). The GPVI receptor, similarly to GPIbα has a low affinity for collagen and is unable to mediate stable platelet adhesion by itself. This receptor contributes to the signaling events that start platelet activation processes and switch on the integrin receptors α2bß3 and α2ß1 responsible for the next phase (29, 30). In turn, the collagen-binding of the α2ß1 receptor reinforces GPVI signaling (31, 32).

For the irreversible, stable adhesion, receptors with relatively slower bond formation rates are needed (21). These integrins, the α2ß1, and α2bß3 need to be converted to a high-affinity state through conformational change induced by inside-out signaling (see detailed in section 1.1.2.3.) (33, 34). The binding of subendothelial matrix proteins through members of the integrin family adhesion receptors can stabilize the adhesion, as they have a very slow rate of bond dissociation (21).

The loss of the protective endothelial layer at the site of vessel wall damage enables the contact between subendothelial tissue factor (TF)-bearing cells and the circulating FVII to initiate secondary hemostasis. Here, still on the surface of TF-bearing cells, through the activation of factors IX, X, V, and the formation of a prothrombinase complex, a trace amount of thrombin is formed, which contributes to the activation of adhered platelets (35).

1.1.2. Activation

The activation phase is initiated by insoluble and soluble platelet agonists through a network of intracellular signaling pathways. These result in shape change, integrin

activation, vesicle secretion, membrane reorganization of the platelets, and clot retraction.

1.1.2.1. Signaling pathways activated by adhesive and soluble platelet agonists

Platelets can be activated by many soluble and adhesive mediators through different signaling pathways, generally leading to the elevation of cytosolic calcium levels or the decrease of cAMP. Inhibitory mediators, on the other hand, act by increasing cAMP, or cGMP levels (PGI_2, prostacyclin, or NO from the endothelial cells, respectively (36)) (Fig. 3.).

The earlier receptor signaling pathways are activated by adhesive ligands collagen and vWF. The signaling pathways initiated by the vWF binding of the GPIb-IX-V (37) receptor complex include the stimulation of nonreceptor tyrosine kinases, such as Src family kinase Lyn (38) and lead to downstream activation of the phosphoinositide 3 - kinase (PI3K)-Akt (39), the mitogen-activated protein kinase (40), the LIM kinase 1 (LIMK1) (41) and the cGMP-dependent protein kinase pathways (42).

The collagen receptor GPVI is coupled to the Fc receptor γ chain (FcRγ) (43), and its stimulation also involves Lyn activation, which phosphorylates the immunoreceptor tyrosine-based activation motif (ITAM) in the FCRγ (44), enabling spleen tyrosine kinase (Syk) binding and activation. Consequently, phospholipase Cγ2 (PLCγ2) is activated and hydrolyzes phosphatidylinositol 4,5-bisphosphate (PIP_2) into 1,2-diacylglycerol (DAG) and inositol-1,4,5-trisphosphate (IP_3) (45, 46). DAG and IP_3 lead to the activation of protein kinase C and the release of calcium into the cytosol, respectively (47). The other main collagen receptor, the integrin α2ß1 acts synergistically with GPVI (32) and also operates through Syk phosphorylation and PLCγ2 activation (48). The calcium signal then triggers many changes within the platelets, altogether termed as activation. This includes thromboxane (TXA_2) production, the release of granule contents (e.g. ADP), integrin activation, and phospholipid scrambling.

TXA_2, a short-lived platelet activator, is not being stored in platelet granules; instead, its synthesis is triggered by phospholipase A2 (PLA2) activation, which results in the release of arachidonic acid from the sn-2 position of phospholipids (49). Cyclooxygenase 1 and thromboxane synthase then convert arachidonic acid to TXA_2,

which after its release acts as an autocrine and paracrine amplifier of platelet activation signals (50).

Along with ADP (stimulating P2Y1/P2Y12 receptors), TXA_2 acts as a positive feedback mediator, further increasing the intracellular [Ca^{2+}] through its TP receptor (51). These and other soluble agonists (thrombin, serotonin, platelet-activating factor) elicit intracellular signaling by binding to their G-protein-coupled receptors (GPCRs) and activating heterotrimeric guanine nucleotide-binding proteins (G proteins) (51). G_q activation is coupled to the formation of second messengers IP_3 and DAG and causes Ca^{2+}-release, while G_i acts by inhibiting the synthesis of potent platelet inhibitory seconder messenger cAMP. The $G_{12/13}$ pathway activates RhoA and Rho kinase, promoting the phosphorylation of the myosin light chain and actin-myosin-dependent contraction (52). The signals of the glycoprotein receptors GpIb and GPVI are supported and amplified through these soluble mediators to achieve optimal platelet activation (53). This often requires synergy or cooperativity of different receptor pathways, e.g. G_i (through G_i-coupled P2Y12 receptor) and G_q (through G_q-coupled P2Y1 receptor) pathways are both necessary for ADP-induced platelet activation (51), and the TXA_2 receptor TP is coupled to both G_q and $G_{12/13}$ (54).

Thrombin also has two G-protein-coupled receptors on human platelets, the protease-activated receptor 1 and 4 (PAR1 and PAR4) (55). PAR1 has a much higher affinity for thrombin than PAR4 (56). The proteolytic cleavage of a PAR catalyzed by thrombin leads to the formation of a new N-terminal tethered ligand that activates the receptor (57) and consequently platelets through G_q, G_i, and $G_{12/13}$ signal transduction pathways (58). The calcium release induced by PAR receptors is a result of phospholipase Cß (PLCß) activation (51). GPIbα is also able to bind thrombin, and the thrombin-induced signaling acts synergistically with PAR signaling (59).

Calcium has a central role in platelet activation (60). It can be mobilized from the endoplasmic reticulum (via IP_3 receptors), can enter the cells via the stromal interaction molecule 1 and Orai1 channels (store-operated Ca^{2+} entry) (61), or nonselective TRPC cation channels (with a significant role in phosphatidylserine (PS) exposure, see detailed in section 1.2.4.) (62). Furthermore, it can be released from the mitochondria through the formation of mitochondrial permeability transition pore (MPTP, see detailed in section 1.2.2.), leading to supramaximal Ca^{2+} signals (63, 64). In single

platelets, there is a marked difference in the calcium signal initiated by GPCR or by ITAM-linked receptors: ADP and thrombin evoke oscillatory, spiking Ca^{2+} rises (65), while stimulation by collagen results in a continuous Ca^{2+} elevation (66). Thus the differential exposure to agonists can alter the magnitude and duration of the Ca^{2+} signal and lead to differences in platelet response (see detailed in sections 1.1.6. and 1.2.4.).

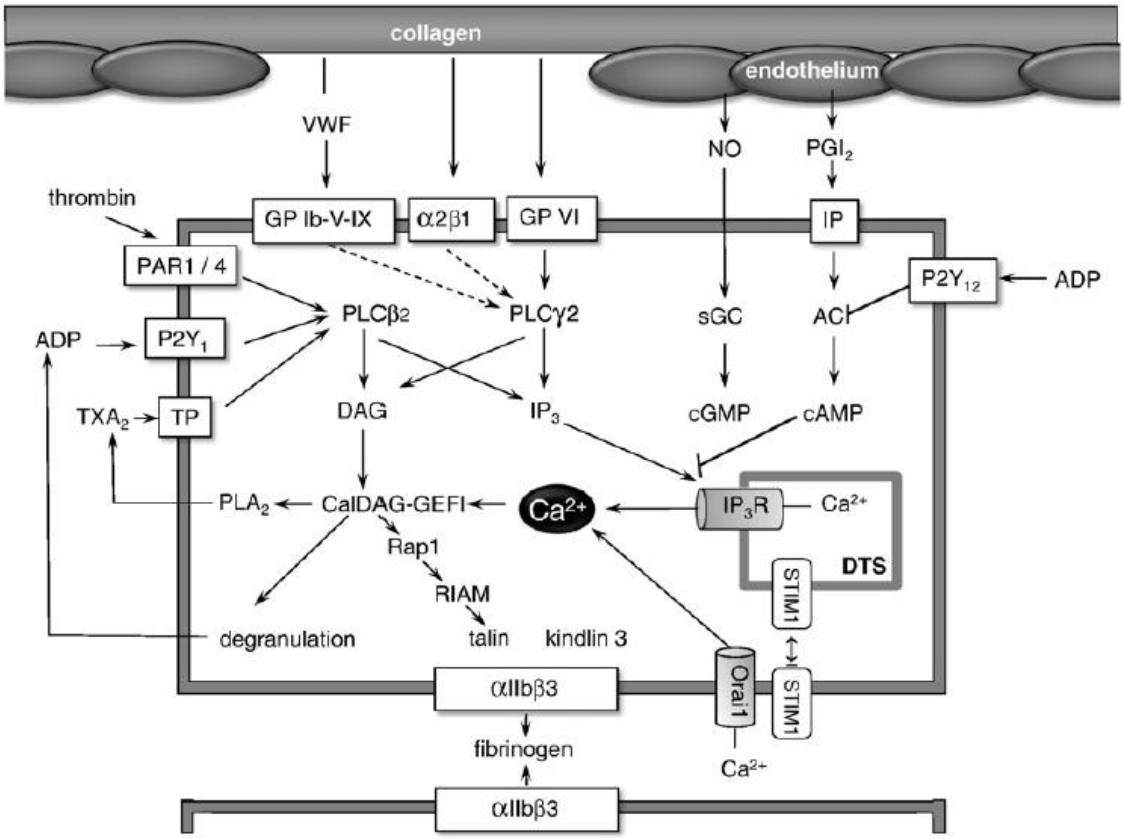

Figure 3. Main platelet receptors and signaling in platelet activation. Adapted from (67). VWF: von Willebrand Factor, NO: nitrogen-monoxide, PGI_2: prostacyclin, GPIb/V/IX, GPVI: glycoprotein receptors Ib/V/IX, VI, αIIbß3, α2ß1: integrin receptors, IP: prostacyclin receptor, PAR1/4: protease-activated receptor 1, 4, $P2Y_1$, $P2Y_{12}$: ADP receptors, TXA_2: thromboxane A_2, TP: thromboxane A_2 receptor, PLA2, Cß2, Cγ2: phospholipase A2, Cß2, Cγ2, sGC: soluble guanylate-cyclase, AC: adenylate-cyclase, DAG: diacylglycerol, IP_3(R): inositol-1,4,5-trisphosphate (receptor), cAMP, cGMP: cyclic adenosine/guanosine-monophosphate, CalDAG-GEFI: Calcium and diacylglycerol regulated guanine nucleotide exchange factor I, DTS: dense tubular system, Rap1b: Ras-related protein 1b, RIAM: Rap1-interacting adaptor molecule, STIM1: stromal interaction molecule 1. For a detailed description see text.

1.1.2.2. Shape change

The discoid shape of resting platelets is stabilized by the cross-linked cytoplasmatic actin network and a so-called marginal band organized by microtubules (68, 69). When the cells adhere to the injured vessel wall, they must go through a shape change to quickly cover the open wound by increasing their contact area. This spreading of platelets includes the flattening and thinning of the cells and the formation of spikelike and sheetlike plasma membrane protrusions (called filopodia and lamellipodia, respectively) (27, 70, 71). The interaction of fibrinogen and the α2bß3 integrin appears to be a dominant factor in initiating these processes, but the ligation of major collagen receptors (GPVI or α2ß1), as well as PAR4 activation, are also able to affect the rearrangement of actin that builds up these structures (72). Later, when a blood clot containing a fibrin network is created, platelets further reinforce the structure by forming stress-fiber-like actin structures (clot retraction) (73, 74).

1.1.2.3. Integrin activation by inside-out signaling

The integrin receptor α2bß3 resides in a bent inactive form in resting platelets which exhibits low affinity for ligands fibrinogen and vWF. This conformation is stabilized by the interactions between the cytosolic regions of the α and ß subunits in the proximity of the cell membrane (75). Upon stimulation, Ca^{2+} and DAG activate the Ca^{2+} and diacylglycerol regulated guanine nucleotide exchange factor I (CalDAG-GEFI) (76) and the protein kinase C/PI3K pathway. As a consequence, a small GTP binding protein, Rap1b is activated, which builds an' activation complex' with Rap1-interacting adaptor molecule (RIAM) and talin (77) (Fig. 3.). This complex enables talin to bind to the ß3 tail of the integrin receptor and connect it with actin and actin-binding proteins (78). The talin-integrin α2bß3 connection disrupts the clasp between the α and ß subunits (79) and results in the stretching of the extracellular domains exposing the ligand-binding sites of the receptor (80).

1.1.2.4. Granule secretion

Following adhesion, the subsequent signaling initiates the controlled release of bioactive molecules contained in platelet granules. The three distinguished types of granules, α-granules, dense- (or δ-) granules, and lysosomes (or λ-granules) are formed

in megakaryocytes and go through maturation in proplatelets (81, 82). The secreted substances from immobilized platelets act para- and autocrine to drastically amplify the platelet activation process; they stimulate the activation of nearby circulating platelets and thereby evoke secondary secretion. Granular release is differential (not all types of granules are necessarily secreted at once) and can selectively modulate the microenvironment of the activated platelets (83). At lower agonist levels, the α- and δ-granules are exocytosed individually, while at higher levels of stimulation, compound exocytosis is characteristic, starting with the fusion of α-granules (84).

The α-granules are the most abundant of platelet granules, with 50-80/platelet (85) and contain both membrane-associated receptors (e.g. α2bß3 and P-selectin) and more than 300 soluble proteins (86). These can regulate a wide variety of processes, such as angiogenesis (e.g. vascular endothelial growth factor), inflammation (e.g. interleukin-8), wound healing (e.g. vitronectin, platelet-derived growth factor, transforming growth factor ß) and hemostasis (e.g. vWF, fibronectin, thrombospondin 1, protein C, tissue factor pathway inhibitor (TFPI)) (87). Some factors are pro-thrombotic (thrombospondin-1, multimeric vWF(88), fibrinogen, coagulation factors FII, V, XI, XIII, high molecular-weight kininogen); others are anti-coagulatory (TFPI, protein S, protein C), or anti-fibrinolytic (plasminogen activator inhibitor-1 (PAI-1)) (87, 89, 90).

Dense granules, the second most abundant platelet granules with 3-8/platelet, mainly contain bioactive amines (e.g. serotonin and histamine), high concentration of cations (e.g. $Ca^{2+,}$ $Mg^{2+,}$ K^{+}), adenine nucleotides (e.g. ADP), polyphosphates, and pyrophosphates (91). The most prominent amplifier of initial platelet activation, ADP binds to purinergic receptors. $P2Y_1$ receptor binding mediates Ca^{2+}-mobilization, shape change, and transient aggregation through G_q-coupled phospholipase Cß2 (PLCß2) activation (92). Activation of the $P2Y_{12}$ receptor (and subsequent G_i signaling) potentiates platelet secretion and sustains irreversible aggregation (92). Stimulation of both receptors simultaneously is required to initiate the synthesis of the short-lived prostanoid, thromboxane A_2 (TXA_2) (93). TXA_2 binds to a thromboxane receptor that activates G_q and $G_{12/13}$ signaling pathways (94). Another adenine nucleotide, ATP is also released from the dense granules and stimulates $P2X_1$ receptors leading to Ca^{2+}-influx and consequent shape change and secondary granule secretion (92, 95). Another dense granule-derived activator, serotonin binds to 5-HT2A-receptors and, through Gq-

mediated signals, can help amplify platelet response together with ADP (96). Polyphosphates originating from the dense granules of platelets consist of 60-100 monomers and can be present as linear or as precipitated, membrane-associated nanoparticles (97-99). They act as proinflammatory and procoagulant mediators; linear polyphosphates stimulate the activation of FV (100) and FXI (101) and hinder the inhibitory effect of tissue pathway inhibitor (TFPI) on FXa and FVIIa (100). Initially, the activation of FXII through negative charges was thought to be mostly stimulated by bacteria-derived polyphosphates. Linear polyphosphates indeed have a lower potential because of their smaller size, but the nanoparticle form bound to platelet surface with the help of Ca^{2+} is also able to trigger contact system activation (99, 102).

Lysosomes (1-3/platelet) have an acidic intraluminal pH and store hydrolytic enzymes (e.g. ß-hexosaminidase) (103). To release their content, greater stimulation is necessary than for α- and δ-granules. The exact role of these enzymes is not yet completely understood but is thought to contribute to the regulation of thrombus formation and remodeling of the extracellular matrix (90, 104).

1.1.2.5. Membrane reorganization

Activated platelets regulate the plasmatic or secondary hemostasis in more than one way. A critical part in the interplay between platelets and the coagulation system is the exposure of phosphatidylserine (PS) – and to a lesser extent phosphatidylethanolamine – on platelets (105). These anionic phospholipids are originally situated mostly in the inner layer of the plasma membrane of resting platelets and are readily transported to the outer layer upon sufficiently high and persistent calcium signal (62). The collapse of the original lipid asymmetry is caused by the activation of a scramblase (anoctamin 6 or transmembrane protein 16F (106)) and the inactivation of an aminophospholipid translocase (107). This "agonist-induced" pathway of PS exposure is distinct from the "apoptosis-induced" activation pathway (108). The exposed anionic phospholipids can interact with the γ-carboxyglutamic acid (Gla) domains in the K-vitamin-dependent coagulation factors (FII, FVII, FIX, FX, protein C, and S) (109). The tenase (with FIXa as the active serine protease and FVIIIa as a cofactor) and prothrombinase (with the serine protease FXa and the cofactor FVa) complexes of the coagulation system can assemble on this negative surface with the help of Ca^{2+}, leading to a burst of thrombin

which cleaves fibrinogen to fibrin (110) (Fig.4.). The catalytic efficiency of the proteases in the tenase and prothrombinase complexes increases by several orders of magnitude on the lipid surface (111-113). The PS surface serves multiple functions: i) a localized catalytic surface is produced that restricts coagulation to the site of endothelial damage, ii) reaction rate is accelerated by the increased enzyme and substrate concentration on the membrane surface (114), iii) trimolecular complexes of enzyme, substrate, and cofactor enable proper juxtaposition of active site and scissile bond, and iv) the ordering of prothrombin cleavage reaction ensures sufficient thrombin concentrations (115). Alternatively, PS might bind to discrete regulatory sites on both factors Xa and Va to allosterically alter their proteolytic and cofactor activities (116).

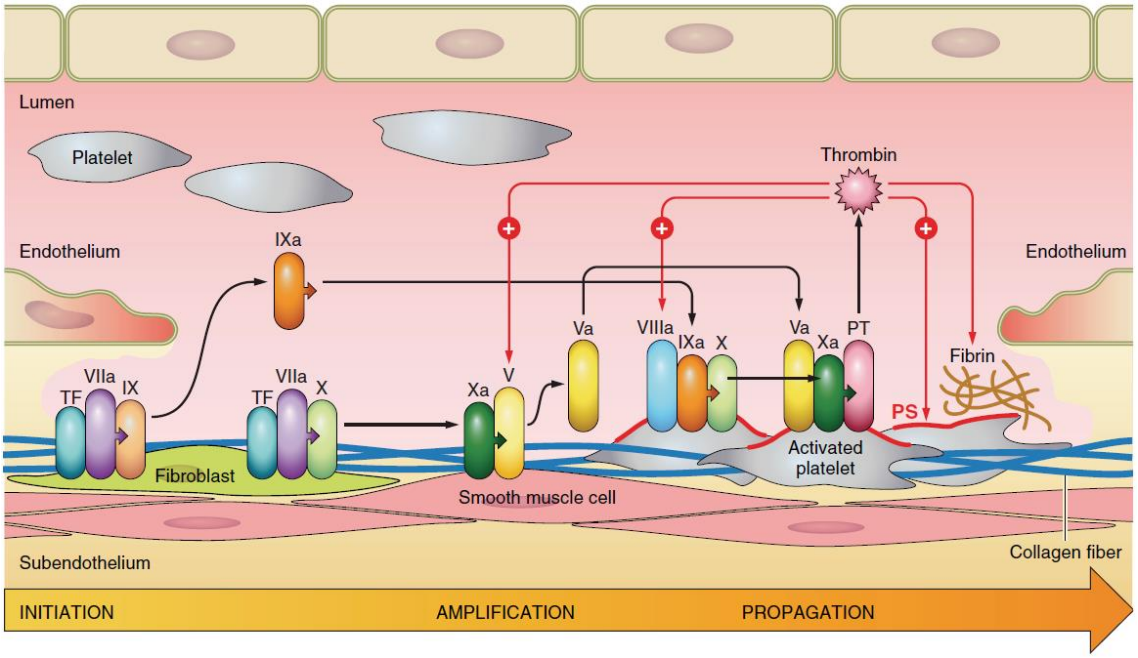

Figure 4. Role of cellular surfaces in the activation of plasmatic coagulation factors during hemostatic coagulation. The initiation of the coagulation cascade starts on the surface of TF-expressing subendothelial cells and leads to the activation of FIX and FX. Traces of thrombin activate the cofactors (FVIII and FV) of the tenase and prothrombinase complexes, respectively, in the amplification phase of coagulation. These complexes form on the surface of PS-exposing platelets during the propagation phase leading to the burst of thrombin and fibrin formation. FIX, X, V: coagulation factors, FVIIa, Va, IXa, VIIIa, Xa: activated coagulation factors, TF: tissue factor, PT: prothrombin, PS: phosphatidylserine. Adapted from (117).

Platelets can also release membrane vesicles formed by their cell membrane (microvesicles) or endosomal compartments (exosomes) (118). These small particles are together referred to as extracellular vesicles, although they appear to be heterogeneous and have a very diverse cargo (e.g. lipids (119), interleukins (120), mitochondria (121)). This enables the modulation of physiological and pathological processes, such as inflammation (120, 122, 123) and cancer growth through cell-to-cell communication (124, 125), as well as the exchange of molecules between cells (123). They can exert both pro- (126, 127) and anticoagulant (128, 129) and even fibrinolytic (130) effects on hemostasis and their overall action appears to be dependent on the activating stimulus leading to their release (131).

1.1.3. Aggregation

After a platelet monolayer is formed on the exposed subendothelial protein, platelet-platelet interaction called aggregation allows building a hemostatic platelet plug. The receptors and adhesive ligands involved in this complex and dynamic process depend on the shear rates present at the site of injury (132). Three distinct mechanisms can initiate aggregation on the first layer of adherent platelets. In solution or at low shear rates (<1000 s^{-1}) observed in veins platelets become predominantly bridged by the symmetric binding of α2bß3 receptors by fibrinogen. Although this can happen independently of vWF in experiments performed in flow chambers (133), in vivo mice studies showed that platelet aggregation is also vWF dependent under venous conditions (134). As the shear rates increase to the arterial range, between 1000 s^{-1} and 10000 s^{-1}, a two-step process develops, that also involves vWF-GPIb-IX-V mediated interaction (135). The initial step is the translocation of discoid, non-activated platelets on adherent discoid platelets through the formation of membrane tethers induced by shear stress (136). These reversible adhesive contacts depend on vWF-GPIbα and reversible fibrinogen-α2bß3 interactions (137-139). In the narrow space of aggregating platelets, soluble agonists (e.g. ADP, thrombin, TXA_2) can accumulate and induce activation, shape change, and degranulation of platelets. The activation results in the irreversible change of α2bß3 integrin to a high-affinity state and thus, a stable bond between platelets (140). Additionally, fibronectin also appears to contribute to aggregation (by

binding to α2bß3) in a major way (141), as thrombi still form in the absence of vWF and fibrinogen (142).

1.1.4. Influence on fibrin structure, clot retraction

Many external factors affect the formation, structure, and properties of the fibrin scaffold that stabilizes the platelet plug, and platelets themselves are one of them. Increasing the activity of the serine protease thrombin that catalyzes fibrinogen-fibrin conversion has the greatest impact. Prothrombin activation to thrombin is highly enhanced on the surface of platelets as a result of their membrane reorganization and PS exposure. The increased thrombin activity leads to faster fibrin polymerization and thereby to clots with thinner fibers, more branch points, and smaller pores between the fibers (143, 144). Platelet FXIIIa then stabilizes the fibrin scaffold by introducing covalent cross-links between adjacent fibrin monomers (145, 146) reducing fiber thickness (144) and porosity of clots (147). The release of polyphosphates can also change the fibrin strands near activated platelets and make them thicker (148).

The structure of the forming fibrin network is also modified by the strong adhesive forces between platelets and the fibers. As the conformation of the integrin α2bß3 changes during platelet activation, its binding to the extracellular fibrin(ogen) (149) is enabled, which initiates outside-in signaling (150). The actin-myosin-based contractile system of platelets activated by the Ca^{2+}-signal promotes a shape change (151). As α2bß3 is connected to the intracellular actin cytoskeleton via talin (152), the contractile forces generated within the cells are translated to the extracellular fibrin placing the fibers under tension (153). This so-called' clot retraction' enables contact signaling between the cells, stiffens fibrin, and increases its density in the platelet-rich areas of the thrombi (74).

Platelets are not the only cellular elements in the forming thrombi with a connection to the fibrinogen and the fibrin network. Erythrocytes (red blood cells, RBCs) also interact with fibrinogen through a receptor related to the α2bß3 integrin of platelets (154-156). As the contracting platelets pull the fibrin scaffold tighter, fibrin compresses the RBCs bound to the forming thrombus. This leads to their shape change from the classical biconcave to polyhedral enabling their close compaction in the pores between the fibrin fibers (157). These tightly packed RBCs build a nearly impermeable seal mimicking the

barrier of the endothelial cell lining of vessels (157, 158). Thus, clot contraction is an indispensable step in reestablishing vessel wall integrity and inhibiting further blood loss. The erythrocytes may also provide a surface for the assembly of coagulation factors through their membrane PS (159) and further modify the structure of fibrin through increasing thrombin concentration (160). In vitro studies show that their capture in the fibrin matrix reinforces the structure by promoting the formation of thinner, more resistant fibers against fibrinolysis (161) and by decreasing the accessibility of fibers through the created diffusion barrier. The role of RBCs might have a bigger impact in the veins, as thrombi formed under venous flow conditions contain lots of erythrocytes (162), although several studies observed a considerable amount of RBCs in arterial thrombi as well (157, 163, 164).

1.1.5. Regulation of fibrinolysis

Platelets contain a host of factors that regulate fibrinolysis. The dissolution of the fibrin network within the vasculature is catalyzed by the serine protease plasmin, which is activated through the proteolytic cleavage of its inactive proenzyme (165), plasminogen by a plasminogen activator (e.g. tissue-type plasminogen activator – tPA (166), urokinase-type plasminogen activator – uPA (167), FXIIa (168)). Fibrinolysis is tightly regulated by the structure of the fibrin network as well as by plasminogen activation and plasmin inactivation; all of which are affected by platelets (169).

Platelet FXIIIa increases the fibrinolytic resistance of thrombi by creating covalent cross-links between fibrin fibers and between fibrin and α2-antiplasmin, the principal inhibitor of plasmin (170). Clot retraction also leads to the condensation of the cross-linked α2-antiplasmin (171). Platelet-rich clots bind less tPA (172), and extrude both plasminogen and its activator through clot retraction (173), hindering plasminogen activation. Interestingly, the clustering of lysing fibers in the platelet-rich regions of clots increases local fibrin-bound tPA concentration and a second, late phase acceleration of fibrinolysis can be observed (174).

The resistance against tPA-mediated lysis of platelet-rich thrombi can be further explained by the high number of fibrinolytic inhibitors within platelets, that are readily secreted upon stimulation. Platelet-derived plasminogen activator inhibitor-1 (PAI-1), the serine protease inhibitor of both tPA and uPA accounts for the majority of

circulating PAI-1 (175) and can be found in a 2-3 fold higher concentration in arterial thrombi containing platelet dense regions (176), compared to venous thrombi (177, 178). Upon strong activating signals (see detailed in sections 1.1.6. and 1.2.4.) this serpin is translocated to the outer leaflet of the platelet membrane by an α2bß3 integrin- and fibrin-dependent mechanism. A 60% fraction of PAI-1 is fully released while the remaining 40% is bound to the platelet surface (179). The secreted PAI-1 has a short half-life (180) and is stabilized by vitronectin (181), an adhesive glycoprotein that binds PAI-1 to fibrin forming a bridge between them (182). The α-granules contain other serpins (e.g. platelet C1 inhibitor (183), protease nexin-1 (184)), and histidine-rich glycoprotein (185) that can regulate fibrinolysis, but their relative contribution and importance are still obscure. The thrombin activatable fibrinolytic inhibitor reduces the availability of tPA and plasminogen binding sites on fibrin by removing the C-terminal lysine residues (186) and can also be released from the α-granules in sufficient concentrations to down-regulate fibrinolysis (187).

Polyphosphates originating from the dense granules elicit numerous effects not only on coagulation, but also on fibrinolysis. Through the alteration of the structure of the fibrin scaffold, they delay tPA-mediated lysis (188) by decreasing the binding of plasminogen and tPA to fibrin (148). They also show profibrinolytic properties as they activate FXII (189), which then stimulates fibrinolysis by generating plasmin itself (190, 191). Moreover, they have been shown to bind uPA with high affinity and enhance plasminogen activation by this activator (192).

1.1.6. Distinct platelet populations of the hemostatic plug

Circulating platelets are not uniform, their morphology and function are heterogeneous with a still uncertain link between the two. Individual megakaryocytes – from which platelets mature – already differ considerably in the expression levels of cytoplasmic and membrane proteins (193, 194). Their environment also has an influence on the transcriptome of the developing platelets, which then undergo further changes during their maturation. Resting platelets, that vary in their intrinsic properties (e.g. size, age, protein composition (132)) come in contact with various extrinsic factors in their surroundings during their activation (e.g. exposure to agonists, contact with other cells, local rheology (30, 195, 196)) that further differentiate these cells. Differences in the

extent of their activation have already been displayed by electron microscopy images in the 1960s (197, 198).

As reviewed by J . W. M. Heemskerk et al. (199) at least two distinct platelet populations develop at the site of vascular wall injury:' procoagulant' platelets that promote thrombin generation and fibrin formation building a dense inner core closest to the opening in the endothelial layer, and a 'discoid' platelet group in the outer shell of the thrombus responsible for aggregation and clot retraction (Fig.5.). These populations differ in their surface properties, their role in the coagulation process, and their activation state which strongly depend on local activator concentrations. This regional heterogeneity develops quickly after vessel wall damage and persists for at least an hour (200).

In a hemostatic plug, the platelets arriving first to the site of injury come in contact with collagen in the damaged vessel wall. This stimulus promotes platelet activation with the release of α-granules (evidenced by the P-selectin positivity of these cells), the formation of pseudopods and lamellipodia, and the exposure of PS on their surface. As a result of the PS exposure, these platelets have an increased ability to bind coagulation factors on their negative surface (201). They are also able to release PS-containing microparticles further amplifying procoagulant response (202, 203). Consequently, thrombin generation also occurs mainly here, on the surface of these' procoagulant' platelets closest to the injury and the highest subendothelial TF concentration. It seems to be the primary factor (along with collagen (204)) in platelet activation in the innermost region, where 60% of the volume is comprised of very tightly packed' procoagulant' platelets. Despite its outward diffusion, thrombin does not extend the full width of the core before declining below critical concentration (205). The developing thrombin gradient is also mirrored in the distribution of fibrin within the plug. It concentrates mostly on the site of injury stabilizing the hemostatic thrombus, while also extending into the vessel wall (200).

These platelets are less adhesive as their GPIbα and GPVI receptors are cleaved by members of a disintegrin and metalloprotease family in a process called glycoprotein shedding (206). Their capability to aggregate is also decreased because of the secondary inactivation of the α2bß3 integrin receptors after occupation with a ligand such as

fibrinogen (207), which comes with the modulation of certain epitopes in the protein (208).

These platelets later assume a characteristic balloon shape with a protruding' cap' on their membrane with high amounts of aminophospholipids (209) and bound α-granular proteins (210) and plasmatic coagulation factors (211). Platelet FXIII (212) and plasma-derived plasminogen are also mostly found in this area (213), as well as the secreted PAI-1, that co-localizes here with its cofactor vitronectin (179). Because of their morphological resemblance of cells undergoing necrosis, they were also termed' necrotic' (108).

A subset of' procoagulant' platelets bind α-granular proteins (FV (214), fibrin(ogen), thrombospondin, fibronectin, vWF (215)) on their surface and have a' coated' appearance (216). This assembly of secretion products and plasmatic factors on the outer membrane of the cells was experimentally identified after stimulation with collagen and thrombin but did not happen in all PS-exposing platelets, however, there seems to be at least a partial overlap between these two platelet populations (214, 217).

Although aging, apoptotic platelets also expose PS and have procoagulant potential, this phospholipid transfer relies on a distinct signaling pathway and is anoctamin-6 independent (108, 218).

DOI:10.14753/SE.2022.2630

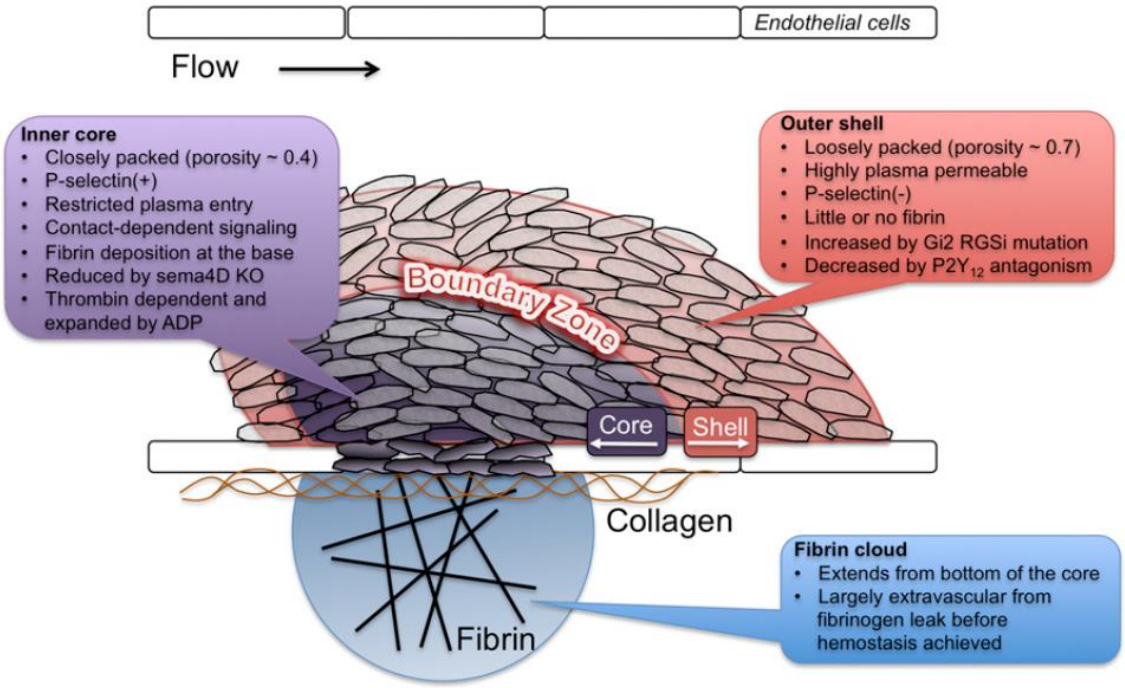

Figure 5. Hierarchical organization of the hemostatic thrombus. Adapted from (200). KO: knock out. Sema4D: semaphorin 4D is a cell surface molecule enabling contact-dependent signaling between adjacent platelets. Gi2 RGSi mutation: Gi2α is insensitive to feedback inactivation by regulators of G-protein signaling (RGS) creating a gain-of-function platelet phenotype with increased duration of ADP receptor, $P2Y_{12}$ signaling. For a detailed description see text.

The increased packing density of the central platelets reduces the penetration of soluble plasma molecules, e.g. inhibitors of thrombin, so that they cannot effectively constrain thrombin activity in the central parts of the plug, but ADP released from the activated platelets is small enough to reach peripheral areas, where a different subpopulation of platelets create an outer shell. Here, the platelets recruited by ADP (and presumably TXA_2) are P-selectin negative, indicating their lack of granule release and show no PS-exposure. They take up a discoid form and are more loosely packed, therefore they may be more prone to detach from the aggregate. They expose activated α2bß3 integrin on their surface and bind fibrin and other platelets. Thus, the' discoid' platelets are responsible for clot retraction. As the platelet-fibrin clot becomes denser, contact-

DOI:10.14753/SE.2022.2630

signaling of the platelets is also enabled. The size of the outer shell is probably limited by the declining ADP concentrations preventing unnecessary occlusion of the affected vessel (200).

DOI:10.14753/SE.2022.2630

1.2. Cyclophilin D

1.2.1. The structure of the mitochondrial Cyclophilin D

Cyclophilin D (CypD), a member of the cyclophilin family of peptidyl-prolyl, *cis-trans* isomerases (PPIase), is encoded by the *Ppif* gene and is a cytoplasm-translated globular protein with a molecular weight of ~22 kDa (219). The mature protein (~19 kDa) forms after the removal of its mitochondrial targeting sequence (220, 221) and resides in the mitochondrial matrix until activation when the protein binds to the inner mitochondrial membrane (222, 223). According to the structural analysis of the cyclophilin family, CypD's structure consists of 8 antiparallel ß sheets and 2 α-helices enclosing the sheets (224). The name' cyclophilin' signals the molecule's ability to bind to Cyclosporin A (CsA, see later in section 1.2.3.) (225, 226), which is enabled by an additional short α-helical turn containing the active site residue tryptophan (W121) (224). Two highly conserved pockets near the active site, the proline interaction surface pocket (S1) and the substrate interaction surface pocket (S2) contribute to substrate specificity, binding, and turnover, while the less characterized "backface" of the molecule mediates the many protein-protein interactions of CypD (224, 227).

1.2.2. The role of CypD in the regulation of mitochondrial bioenergetics

The physiological function and exact mechanism of action of CypD remain elusive to this day, but its significant role in the regulation of mitochondrial function is confirmed by decades of research. It appears to supervise mitochondrial ATP-synthesis, the activity of the electron transport chain , and controls the opening of the mitochondrial permeability transition pore (MPTP) (228).

Reducing equivalents ($NADH+H^+$ and $FADH_2$) originating from the oxidation of nutrients act as electron donors for complex I and II of the electron transport chain in the inner mitochondrial membrane, that transfer these electrons through a series of redox reactions to further electron acceptors (ubiquinone, complex III, cytochrome c, complex IV and finally oxygen). The complex I, III, and IV of the electron transport chain harvest the energy freed by these redox reactions to create an electrochemical gradient (mitochondrial membrane potential, $\Delta\psi_m$) through the inner mitochondrial membrane . Through the transport of protons into the intermembrane space develops a

proton motive force that drives the ATP synthesis of the F_oF_1-ATP synthase. The substrates of the ATP production, ADP, and inorganic phosphate are transported to the site of utilization by the adenine nucleotide translocase (ANT) and the mitochondrial phosphate carrier, respectively.

In various experimental setups CypD appeared to support the formation of supercomplexes (containing complexes I, III, and IV), or' respirasomes' that enhance the generation of the proton gradient across the inner mitochondrial membrane (229, 230). On the other hand, assembly of' synthasomes' (comprising of oligomerized ATP synthase, ANT, and phosphate carrier) to increase the efficiency of ATP production were found to be inhibited by CypD action (231).

The effectivity of this elaborate system relies on a tight coupling of the electron transport chain and ATP synthase activities (232). The regulation of the mitochondrial coupling controls the cell's substrate utilization, ATP production, and affects cellular physiology and health (233). If a mitochondrion is uncoupled, the proton motive force is dissipated, and ATP synthesis is repressed (234-236).

The mitochondrial permeability transition pore (MPTP), first described by Hunter and Hayworth (237-239) is a regulator of coupling. It is described as a high-conductance, relatively unselective pore, that upon voltage-dependent opening enables the movement of molecules of maximum 1.5 kDa molecular weight through the inner mitochondrial membrane. The trigger of the pore opening appears to be the accumulation of Ca^{2+} in the matrix, with many factors influencing the required Ca^{2+}-threshold, acting as sensitizers (e.g. reactive oxygen species – ROS (240, 241), low $[H^+]_{matrix}$, low $\Delta\psi_m$ (242), long-chain fatty acids (243), and ANT modulators atractyloside, carboxyatractyloside (244, 245)), or desensitizers (Mg^{2+}, ATP, ADP, high $[H^+]_{matrix}$ and ANT inhibitor bongkrekic acid (246)) of the process (247).

The mitochondrial permeability transition (MPT) is accompanied by the osmotic influx of water to the mitochondrial matrix collapsing the mitochondrial membrane potential and resulting in swelling of the cell organ. The impaired capability of the mitochondria to produce ATP deteriorates the ion homeostasis of the cell, generally resulting in cell necrosis. A transient opening of the pore is also possible, which is hypothesized to act as a release valve lowering the $[Ca^{2+}]$ in the mitochondrial matrix (248, 249).

The exact molecular structure of the MPTP is still uncertain, although many candidates have been proposed throughout the years, among those CypD. As several other mitochondrial proteins (e.g. mitochondrial phosphate carrier (227, 250), ANT (251, 252), the translocator protein of 18 kDa (253), the voltage-dependent anion channel (254, 255)), CypD's role as a potential structural element of the pore was also disproved, as its genetic deletion did not cause the complete elimination of MPTP activity (256, 257). It did, however, alter its regulation, namely the pore's sensitivity to Ca^{2+}, inorganic phosphate, and ROS is reduced if CypD expression decreases (258, 259). More recently, the c subunit of the F_oF_1-ATP synthase appeared to be the strongest candidate as the main structural element (260, 261), but again its fate followed that of the previous contenders (262-264).

All these failed attempts to find a sole pore-forming protein have led researchers to hypothesize the existence of multiple components. The deletion of the c-subunits of the F_oF_1-ATPase (265) or alternatively, the deletion of three ANT isoforms (ANT1, 2, 4) both resulted in some remaining MPTP activity, but the conductance measured by patch-clamp analysis appeared distinct from the classical MPTP (264). The theory arising from these findings is that both ANT and the F_oF_1-ATPase can form permeability pores in the mitochondrial membrane, and the assembly or disassembly of an ATP synthasome might regulate the MPTP depending on bioenergetic needs. According to this hypothesis, the role of CypD is to stimulate synthasome disassembly when certain signals are present (e.g. high Ca^{2+}, low ADP concentrations, ROS formation, etc.) to promote MPTP opening (231). Further work is necessary to clarify the relative contribution of these proteins to the formation of the pore.

1.2.3. Pharmacological modulation of MPTP and CypD function

Cyclosporin A (CsA) is a fungal cyclic undecapeptide and a known immunosuppressive agent used to treat post-transplant organ rejection (267, 268) and several autoimmune diseases (269-272). The adverse effects associated with its clinical use include thrombotic complications (273, 274). The therapeutic applications were originally based on its inhibitory effect on calcineurin, a calcium/calmodulin-dependent Ser/Thr protein phosphatase that normally upregulates the interleukin 2 expression of T cells and thereby mediates the cellular immune response (275, 276). CsA binds to its intracellular

receptor cyclophilin A (CypA) and the formed CsA-CypA complex inhibits calcineurin phosphatase activity. Without dephosphorylation, the nuclear factor of activated T cells cannot translocate to the nucleus to stimulate the transcription of inflammatory genes (277). More recent works indicate modulatory effects on the cell of the innate immune system as well (278-280). CsA also binds CypD with high affinity through hydrophobic interactions as well as hydrogen bonds (281, 282), and inhibits the PPIase activity (220, 228, 283).

Bongkrekic acid (Bk) is a highly unsaturated tricarboxylic fatty acid, a bacterial toxin (produced by *Burkholderia gladioli* pathovar *cocovenenans*), which causes food-borne poisoning (284). Bk and its synthetic derivatives can be used in experiments aimed to study MPTP because of its inhibitory effect on the ANT. ANT is locked in its' m' (matrix-oriented) conformation when bound to Bk and thereby MPT pore formation becomes inhibited (246, 285).

1.2.4. MPTP opening in platelets

The phosphatidylserine exposure on the platelet surface is MPTP dependent and proposed to be an indirect result of the [Ca^{2+}] elevation (286).

It requires a prolonged and substantial rise in the intracellular [Ca^{2+}], which can be reached only through certain 'strong' platelet activators (199). Adhesion to collagen in the vessel wall can cause appreciable PS exposure, but for it to be detectable in a substantial fraction of platelets, additional stimulation is necessary. Through the simultaneous stimulation of both PLCγ (via GPVI or α2bß3) and PLCß (via PAR1/4) isoforms, a sufficient Ca^{2+} signal can be achieved for the formation of 'procoagulant' platelets. Co-stimulation by collagen and thrombin – that happens primarily through GPVI and PAR1 receptors, respectively – seems to be the most successful (287-289) as together they are able to activate receptor-operated Ca^{2+} entry mechanisms that are inactive upon singular stimulation. TRPC channels and the Na^{+}/Ca^{2+} exchanger are involved in this process resulting in Na^{+} influx and consequential sustained [Ca^{2+}] elevation (62).

Another highly efficient inductor is the combination of thrombin and ROS signal (e.g. H_2O_2) (63). Reactive oxygen species (ROS) are formed by the partial reduction of oxygen and are natural by-products of aerobic metabolism. The term describes several

factors, such as superoxide anion (O_2^-), hydrogen peroxide (H_2O_2), hydroxyl radical (OH^-), and hypochlorous acid (HOCl). Platelets can be both the target and the source of ROS. They are continuously exposed to them even under physiological conditions, as cells of the vessel wall provide a low flux of ROS (290, 291). Platelets themselves are also able to produce a significant amount of ROS upon stimulation, suggesting autocrine or paracrine roles in platelet activation (292). Moreover, many pathological situations are associated with oxidative stress and elevated ROS levels, e.g. inflammation (293), atherosclerosis (294, 295), diabetes (296, 297). ROS can stimulate MPTP formation through cross-linking of cysteine thiol groups in the regulatory components of MPTP (298).

Other agonists, such as vWF (299), fibrinogen, ADP, thrombospondin (300) can also boost PS exposure of collagen-stimulated platelets by increasing the Ca^{2+} signal via their respective receptors but are unable to cause a sufficient rise in the [Ca^{2+}] on their own.

In addition to the Ca^{2+} signal arising from calcium release from intracellular stores or import from the extracellular space, the opening of the mitochondrial permeability transition pore is also an absolute requirement in the process (301).

According to the recent model of N. Abbasian et al. (64) multiple Ca^{2+} signaling events determine whether a platelet becomes procoagulant or not. Platelet agonists initiate the release of Ca^{2+} from intracellular Ca^{2+} stores, or the extracellular space leading to the elevation of cytosolic Ca^{2+} concentration ($[Ca^{2+}]_{cyt}$). This is followed by a passive calcium influx through the mitochondrial calcium uniporter, increasing the $[Ca^{2+}]_{mit}$ levels. This initial increase in $[Ca^{2+}]_{cyt}$ and the consequent rise of $[Ca^{2+}]_{mit}$ varies between platelets depending on the activating signal. Only platelets simultaneously stimulated with ’strong’ agonists can reach the minimum threshold that results in the opening of the mitochondrial PTP. The MPTP opening then triggers a ’supramaximal’ Ca^{2+} signal in the cytosol that is necessary for the formation of a ’procoagulant’ platelet (64). Their studies indicate, that a Ca^{2+} elevation estimated at approximately 166 μM is reached. The low Ca^{2+} sensitivity of anoctamin-6 might explain why such a high concentration is needed for PS exposure (302, 303).

The threshold for MPTP opening is modulated by the sensitizing effects of CypD (304), consequently, many investigations have been carried out to define the role of CypD in

platelet function. Using ’strong’ activators (thrombin and collagen-analog convulxin, or H_2O_2) in in vitro setups, these studies proved the critical function of CypD in various processes. The formation of ’coated’ platelets was hindered by CypD inhibition with CsA (as well as in the presence of the ANT-inhibitor Bk) (305). Genetic ablation of CypD (63, 301), as well as pharmacological inhibition (CsA) (207), resulted in decreased PS exposure. The epitope modulation and inactivation of α2bß3 were also found to be abrogated in $CypD^{-/-}$ or CsA-treated platelets (207, 306). Membrane vesiculation and the attenuation of clot retraction are also CypD dependent (63), just like the shape change stimulated by these activators (306).

Several studies also applied in vivo experiments, where the consequences of the loss of CypD function were assessed during thrombus formation triggered by photochemical (63) or ferric chloride ($FeCl_3$)-induced endothelial injury (307). In the photochemical experimental model both germ-line deletion of CypD (63) and platelet-specific knock-out of the gene (306) result in accelerated thrombosis. The $FeCl_3$-induced endothelial damage on the other hand leads to hampered thrombus formation in the case of CypD deletion (307).

DOI:10.14753/SE.2022.2630

2. OBJECTIVES

2.1. Platelet content of arterial thrombi

In the first part of this work, our goal was:

1. To determine the platelet content of arterial thrombi from different locations
2. To identify clinical determinants of platelet occupancy.

2.2. Effects of CypD and CsA on the morphology and function of platelets

Although the studies mentioned in section 1.2.4. have provided invaluable insight on the critical roles of CypD in platelet activation, a number of important details are still unknown. To address these questions and expand our knowledge in the field, our aims were the following:

1. To monitor changes in platelet structure triggered by ’strong’ platelet agonists
2. To study the role of CypD in ’mild’ stimulus-induced platelet activation
3. To improve our understanding of the effects of MPTP-dependent and -independent molecular pathways of CsA in platelet aggregation
4. To introduce an impedance-based method to follow real-time platelet adhesion and spreading
5. To characterize the impact of CypD on the lytic susceptibility of platelet-fibrin composite clots.

2.3. Structural properties of cancer-associated venous thrombi

In the last part of our study, our aim was:

1. To determine the RBC content of venous thrombi formed in human pancreatic tumor-bearing mice
2. To characterize the fibrin structure of these thrombi.

DOI:10.14753/SE.2022.2630

3. METHODS

3.1. Investigations of platelet content of arterial thrombi

3.1.1. Patients

Between 2014 and 2016, 208 consecutive patients (66 coronary artery disease, CAD patients; 64 peripheral artery disease, PAD patients, and 78 acute ischemic stroke, AIS patients) were prospectively enrolled.

3.1.2. Thrombus collection

Coronary (CAD) patients with symptoms of STEMI or NSTEMI that met the inclusion criteria (definite diagnosis of acute myocardial infarction, eligibility for percutaneous coronary intervention, no previous thrombolytic therapy, TIMI thrombus grade≥3) were referred to primary percutaneous coronary intervention. Pretreatment with 500 mg aspirin, 5000 IU intravenous bolus of unfractionated heparin, abciximab (if there was no absolute contraindication), and 600 mg clopidogrel was administered to all patients. Those already on anti-platelet therapy on a regular basis received a reduced dose. This was immediately followed by the revascularization process: angiography and thromboaspiration were performed from radial or femoral access with QuickCat (Spectranetics Int., Leusden, Netherlands), Export (Medtronic Inc, Minneapolis, MN), or Eliminate (Terumo, Gifu, Japan) aspiration catheters.

Thrombendarterectomy (with Fogarty catheter) or semi-closed endarterectomy (with Vollmar ring stripper) were performed on patients presenting with acute symptoms of peripheral artery thrombosis (PAD) under local or general anesthesia. The inclusion criteria were: definite radiographic and clinical diagnosis of arterial occlusion and eligibility for surgery. Thrombi formed in bypass-grafts or emboli stemming from lesions proximal to the site of occlusion were not handled separately in the study. During vascular reconstruction 150 IU/kg systemic heparin was given before clamping (308).

In AIS, thrombi were removed via stent thrombectomy from acutely occluded large vessels of the circle of Willis. All patients with a definite diagnosis of AIS eligible for mechanical thrombectomy were included during the study period providing that a clot

was successfully removed. Prior to mechanical thrombectomy recombinant tissue-type plasminogen activator was administered to patients who were eligible for intravenous thrombolysis.

The study was approved by the institutional and regional ethical board (Ref.#8/2014/18.09.2014) and informed written consent was obtained from all participants or their legal guardians. The research also conforms to the principles outlined in the Declaration of Helsinki.

3.1.3. Scanning electron microscopic (SEM) imaging of arterial thrombus composition

Samples were placed into 100 mM Na-cacodylate pH 7.2 buffer for 24 h at 4 °C immediately after extraction and after repeated washes with the same buffer fixed in 1% (v/v) glutaraldehyde for 16 h. The dehydration of the samples carried out in a series of ethanol dilutions (20%-96% v/v), a 1:1 mixture of 96% (v/v) ethanol/acetone, and pure acetone followed by critical point drying with CO_2 in E3000 Critical Point Drying Apparatus (Quorum Technologies). The specimens were mounted on adhesive carbon discs and sputter-coated with gold in SC7620 Sputter Coater (Quorum Technologies). Randomly selected images from separate parts of thrombi were taken with scanning electron microscope EVO40 (Carl Zeiss) and the manufacturer's software to control for composition heterogeneity (309). Altogether 10 images were taken of each thrombus with SEM EVO40 (Carl Zeiss GmbH, Oberkochen, Germany), using 5000x magnification. Surface occupancy of cellular components and fibrin network was determined in typically 5 images (exceptionally 4) at the lower magnification after dividing the images to 864 equal-sized square regions of interest using Photoshop 7.0.1 CE (Adobe, San José, CA, USA) and based on morphological characteristics each region was classified as occupied by fibrin, platelets or other blood cells. Thrombus composition was then calculated as a percentage of regions occupied by each component out of the total area of the image as previously described (310).

3.1.4. Statistical procedures

Each patient was characterized by an array of routine clinical data and surface occupancy data from t_j number of SEM images. During the analysis of the occupancy

data, the sections of a thrombus could not be treated as separate observations, because the intra-individual heterogeneity would have been neglected and the patients with larger sets of SEM data would be ascribed a higher weight in the conclusion derived. That is why the sets of occupancy data were treated as fuzzy samples. The degree of membership to the general population of any observation of patient number *j* in such a fuzzy sample was assumed to be $1/t_j$. The so formed fuzzy sample accounted for inter-individual heterogeneity in thrombus occupancy, because each patient would influence the conclusions equally.

A Kuiper statistical test for equality of distribution (311) and a one-tail statistical test for median equality (308) were used to identify differences in the characteristics of two one-dimensional continuous populations. Each of the populations was represented by independent and identically distributed samples of fuzzy observations. Bootstrap procedures that do not use any other parametric assumptions were implemented with 10,000 pseudo-realities, equal size generation over empirical cumulative distribution function as previously described (312).

3.2. Investigations on the effects of CypD and CsA on platelet morphology and function

3.2.1. Animals

WT and $CypD^{-/-}$ littermate mice (of C57Bl/6 J background, either sex, between 60 and 180 days of age) were housed in a room maintained at 20–22 °C on a 12 h light-dark cycle with food and water available ad libitum. Experiments were performed in accordance with the guidelines and regulations of the Code of Animal Welfare and Experimentation Rules of Semmelweis University (act #106/b//2013., IX. 26) and approved by the Animal Care and Use Committee of Semmelweis University.

3.2.2. Preparation of platelets

After anesthesia by the intraperitoneal injection of 400 mg/kg chloralhydrate, the inferior cava vein was made accessible by median laparotomy and terminal blood collection was performed. Blood samples were then collected into pre-prepared

Eppendorf tubes with 85 mM trisodium citrate, 66 mM citric acid, 80 mM glucose at an anticoagulant/blood ratio of 1:9.

Citrated human blood was obtained from healthy individuals. Platelet-rich plasma was prepared by centrifugation of samples at 150*g* for 10 min at 25 °C. Platelet-rich plasma was diluted 4-fold in 63 mM TRIS, 95 mM NaCl, 12 mM citric acid, 1 μM PGE_1, 1 U/ml apyrase, pH 6.5 and centrifuged at 600 g for 10 min at 25 °C. Platelets were resuspended in PBS (phosphate-buffered saline: 134 mM NaCl, 2.9 mM KCl, 20 mM Na_2HPO_4, 12 mM $NaHCO_3$, 1 mM $MgCl_2$, 5 mM glucose, pH 7.35), and the supernatant was discarded. Cell counts were determined using an Abacus Junior B Hematology Analyser (Diatron, Budapest, Hungary).

3.2.3. Morphological imaging of platelets by scanning electron microscope (SEM)

Washed platelets at 1.5×10^5/μl in PBS containing 2.5 mM $CaCl_2$ were placed on glass cover slips coated with 0.05 mg/ml collagen G (Biochrom AG, Berlin, Germany) in 150 mM NaCl 10 mM HEPES pH 7.4 overnight at 4 °C. Platelets were activated with 25 nM thrombin (Serva Electrophoresis GmbH, Heidelberg, Germany, further purified and characterized as described previously (313, 314)) for 0/15/30 min at 37 °C in the absence or presence of 2 μM CsA. In certain cases, 10 μM $CuSO_4$, 10 μM homocysteine, and 100 μM H_2O_2 (indicated as ROS whenever applied in the measurements) were also added. This ROS mix was selected to generate hydroxyl radicals through a copper/thiol-dependent chemistry (315, 316) at physiologically relevant concentrations of the components. Hydroxyl radical formation was confirmed with the fluorescent probe coumarin-3-carboxylic acid (317).

For the preparation of fibrin clots, 6 μM fibrinogen (human, plasminogen depleted from Calbiochem, LaJolla, CA, USA) was supplemented with washed platelets at 0.5×10^5/μl in PBS containing 2.5 mM $CaCl_2$ and 250 ng/ml convulxin ± 1 μM CsA. In another experimental setup washed platelets were pretreated with 2 μM CsA/50 μM FK-506/20 μM Bk or their respective vehicles for 30 min at 37 °C. Fibrin clots were prepared by mixing 6 μM fibrinogen with platelets at 10^5/μl, 2.5 mM $CaCl_2$, and 10 μM ADP in the presence or absence of the previously described ROS mix. The samples were clotted with 15 nM thrombin for 2 h. Platelet activation and clot formation were terminated using 3% glutaraldehyde in 100 mM Na-cacodylate pH 7.2. Further

treatment of the fixed samples, as well as generation and analysis of images, was carried out as described in section 3.1.3. (318).

The morphometric analysis of these clots included the measurement of fibrin fiber diameters followed by evaluation of their distribution using scripts running under the Image Processing Toolbox of MatLab R2015a (Mathworks, Natick, MA). A grid was drawn over the image with 10–15 equally-spaced horizontal lines and all fibers crossed by them were included in the analysis. The diameters were measured by manually placing the pointer of the Distance tool over the endpoints of transverse cross-sections (always perpendicularly to the longitudinal axis of the fibers) of 300 fibers from each image (2-6 images per clot type) (308, 309, 319).

3.2.4. Morphological imaging of platelets by transmission electron microscope (TEM)

Washed platelets at 3.3×10^5/µl in PBS containing 2.5 mM $CaCl_2$ were activated with 25 nM thrombin and 250 ng/mL convulxin at 37 °C. In certain cases, ROS ± 2 µM CsA was also added. After 2 h of activation, platelets were centrifuged at 1500 g for 5 min. Supernatants were discarded, samples were treated with 30 µl 3% glutaraldehyde in 100 mM Na-cacodylate pH 7.2 for 16 hours, followed by centrifugation as described above. The pellet was treated with 1% OsO_4 (in distilled water) for 6 hours at 4 °C. After washing with distilled water, the cells were suspended in 10 µl of 1% low melting-point agarose at 40 °C. After congelation, 1 mm^3 pieces were dehydrated in 20–96% (v/v), absolute ethanol, propylene oxide, then infiltrated and embedded in Durcupan ACM Epoxy Resin. Resin blocks were polymerized for 48 h at 60 °C and 80 nm sections were made using Leica UC7 ultramicrotome (Leica Microsystems, Wetzlar, Germany). Sections were mounted on 100-mesh nickel grids coated with Formvar (SPI-Chem, West Chester, PA, USA), contrasted with 1% (w/v) aqueous uranyl acetate and 0.08% (w/v) lead citrate, and examined using a Philips Morgagni 268D electron microscope (FEI, Eindhoven, Netherlands) at an accelerating voltage of 100 kV. Images were analyzed using siViewer 5.1 (Olympus Soft Imaging Solutions, Münster, Germany) and ImageJ (NIH, Bethesda, MD) software. From TEM images depicting individual platelet cross-sections, the total area of membrane-bearing organelles (TO) as well as total platelet cross-section area was measured (TC).

Normalized organelle area was calculated as TO/(n × TC) for each evaluated image, where n is the number of detected organelles.

3.2.5. Platelet functional assays – adhesion and spreading

Cell adhesion and surface spreading were monitored in E-plates (ACEA Biosciences, Ind., USA) in an xCELLigence System (Roche Applied Science, Indianapolis, USA) (320, 321). During the attachment of cells, an increase in the impedance can be registered, which depends on the local ionic environment, the number, and spreading of cells adhered to the surface of the electrodes at the bottom of wells. The change in impedance is represented as Cell Index (CI), which is calculated as $CI = (Z_i - Z_0)/F$ where Z_i is the impedance at an individual time point, Z_0 is the impedance at the start of the experiment and F is a constant depending on the applied frequency.

Human platelets at 2×10^5/µl in PBS were pre-incubated with 2 µM CsA or 1% ethanol (as vehicle control) for 30 min at 37 °C.

PBS was added to each well and the impedance was detected for 1 h to obtain constant background values. Thereafter, 2.5 mM $CaCl_2$ ± 10 µM ADP was added and a second baseline was measured. After the addition of the pre-incubated platelets at 10^5/µl, the impedance was recorded at 10 kHz for 24 h, using only PBS-containing wells as control. Impedance curves were analyzed using the Curve fitting toolbox of Matlab 7.10.0.499 (R2010a) (The Mathworks, Natick, MA, USA) software to calculate maximal impedance and initial slope values.

3.2.6. Platelet functional assays – aggregation assay

Aggregation was monitored with a Carat-TX4 optical aggregometer (Carat Diagnostics, Budapest, Hungary) (322). Washed platelet count was adjusted to 2×10^5/µl by dilution with PBS containing 2.5 mM $CaCl_2$ and 6 µM fibrinogen, and aggregation was induced by 10–50 µM ADP after 30 min of incubation with CsA, Bk or FK-506, or their vehicles. Aggregation was expressed as a percentage of maximal transparency measured with PBS. Aggregation curves were analyzed with the integrated software of the instrument to calculate initial slope and maximal aggregation values.

3.2.7. Platelet functional assays – tissue factor-induced clotting assay

Washed platelets (at a final count of 10^5/µl) were incubated for 30 min at 37 °C with 2 µM CsA, 50 µM FK-506 or 20 µM Bk or their vehicles (1% ethanol, 0.5% DMSO or 2 mM NH_4OH, respectively). FK506 (Tacrolimus) is a selective calcineurin inhibitor, also clinically used as an immunosuppressant (323). It acts by forming a complex with its intracellular binding protein (FK506-binding protein-12) enabling interaction with calcineurin (324). Using FK506, we can differentiate between the CypD- and calcineurin-dependent effects of CsA. After pre-activation with 10 µM ADP, platelet suspensions were mixed with citrated human pooled plasma at a ratio of 1:1 and supplemented with 12.5 mM $CaCl_2$. Clotting was initiated by the addition of 1200 × diluted recombinant thromboplastin Dia-PT R (Diagon Kft, Budapest, Hungary) and monitored at 37 °C in two assay settings. (i) Clotting time was measured in a KC-1A electromechanical coagulometer (Amelung, Lemgo, Germany). (ii) Clot formation was monitored by registering the absorbance at 340 nm with a CLARIOstar microplate reader in a turbidimetric assay (BMG LABTECH, Ortenberg, Germany), and clotting time defined as time to reach half-maximal absorbance.

3.2.8. Platelet functional assays – turbidimetry assay of fibrinolysis

tPA-driven lysis was studied in clots prepared from 6 µM fibrinogen supplemented with 0.5 µM plasminogen (isolated from human plasma(325)), 2.5 mM $CaCl_2$, 10 µM ADP, in certain cases ROS, human or murine platelets at $0/1/2 \times 10^5$/µL, and clotted with 16 nM thrombin for 60 min, in a total volume of 120 µl. Lysis was initiated by the addition of 100 µl of 50 µg/mL tPA to the clot surface. Clot formation and dissolution were followed by measuring the light absorbance at 340 nm at 37 °C with a Zenyth 200rt microplate spectrophotometer (Anthos Labtec Instruments GmbH, Salzburg, Austria). Lysis curves were analyzed with a self-designed script running under the Matlab software to determine the time needed to reduce the turbidity of the clot to a given fraction of the maximal (initial) value (t50 to reach $0.5A_{max}$, t10 to reach $0.1A_{max}$) as a quantitative parameter of fibrinolytic activity (326).

3.2.9. Statistical procedures

The distribution of fibrin fiber diameter data was analyzed using the algorithm described previously (318, 319): theoretical distributions were fitted to the empirical data sets and compared using Kuiper's test and Monte Carlo simulation procedures. On other datasets with three or more compared subsets, ANOVA was performed. For datasets with small sample sizes ($n < 9$), where the normal distribution of the evaluated numeric data could not be confirmed, non-parametric statistical tests were applied. The Kolmogorov-Smirnov test was chosen because of its robust power to compare distributions of two data sets independently of their distribution. For the comparison of three or more datasets, the Kruskal-Wallis test was used. All statistical tests were performed using GraphPad Prism 6.00 (GraphPad Software, La Jolla California USA) and the Statistical Toolbox 7.3 of Matlab. Data are presented as mean ± standard error of mean (SE), except for fibrin fiber diameter given as median and bottom–top quartile values.

3.3. Investigations of the structural properties of venous thrombi formed in human pancreatic tumor-bearing mice

3.3.1. Cells and mouse tumor model

Our collaborators in N. Mackman's lab generated luciferase-expressing BxPc-3 cells, injected the cells into the pancreas of mice, and used an inferior vena cava (IVC) stasis model to obtain thrombi. They provided the thrombi samples that we studied using scanning electron microscopy.

A human pancreatic cancer cell line BxPc-3 expressing the firefly luciferase reporter was used. The human pancreatic cancer cell line BxPc-3 was obtained from the American Type Culture Collection (Manassas, VA, USA). BxPc-3 cells were cultured in RPMI-1640 medium (Gibco, Waltham, MA, USA) with 10% fetal bovine serum (Omega Scientific, Tarzana, CA, USA) and 1% antibiotic–antimycotic (Gibco).

BxPc-3 cells were infected with a Cignal Lenti Positive Control (luc) vector containing the luciferase reporter gene (Qiagen, Hilden, Germany). The vector (multiplicity of infection of 25) was added to 1.0×10^4 BxPc-3 cells in a 96-well cell culture plate (Corning, Corning, NY, USA). Infected BxPc-3 cells were incubated for 24 h at 37 °C,

and cells containing the vector were selected in RPMI-1640 containing 5 μg mL^{-1} puromycin (Sigma Aldrich, St Louis, MO, USA) for 3 weeks. To confirm that the cells were expressing luciferase, BxPc-3 cells were incubated with Xenolight D-luciferin (150 μg/mL) (Perkin Elmer, Waltham, MA, USA) for 5 min at room temperature. Luciferase expression was measured with the IVIS Kinetic *in vivo* imaging system (Caliper Life Science, Waltham, MA, USA).

Crl:NU-*Foxn1*^{nu} male mice (nude mice) aged 6–8 weeks were purchased from the animal service core facility at the University of North Carolina at Chapel Hill. Luciferase-expressing BxPc-3 cells (2.0 x 10^6 cells per 40 μL of phosphate-buffered saline/matrigel [1:1]) were injected into the pancreas, and tumors were grown for 7–10 weeks. Luciferase expression was measured with the IVIS Lumina *in vivo* imaging system (Caliper Life Science) every week. When the orthotopic tumors gave a signal count of ≥ 2.0 x 10^5, mice were scheduled for a thrombosis experiment. Some of the variations in tumor size was attributable to differential growth rates of the tumors and delay in scheduling the thrombosis experiments. Mice with tumors weighing ≥ 2 g were used for all of the thrombosis experiments. All animal studies were approved by the University of North Carolina at Chapel Hill Animal Care and Use Committee and complied with National Institutes of Health guidelines.

3.3.2. Thrombosis model

The IVC was exposed, carefully separated from the aorta, and fully ligated with 5-0 silk suture below the left renal vein. Any side branches close to the IVC ligation site were also ligated, and the back branches were cauterized. The Vevo 2100 Imaging System (FUJIFILM VisualSonics, Toronto, Ontario, Canada) was used to monitor the development of clots at 3 h, 6 h, 24 h, and 48 h after IVC ligation. Clots were harvested at 48 h and weighed.

3.3.3. Scanning electron microscopic (SEM) imaging of venous thrombus composition

Thrombi were processed as described in section 3.1.3. The same imaging method and evaluations were used as for the investigations regarding arterial thrombus composition. However, in this case, each region was classified as occupied by fibrin, red blood cells,

or their combination based on morphological characteristics. Thrombus composition was then calculated as the percentage of regions occupied by each component out of the total area of the image. The morphometric analysis of fibrin fibers in venous thrombi was also performed as described previously in section 3.2.3.

3.3.4. Statistical procedures

Multiple number of measurements on the morphometric characteristics of SEM images (fiber diameter or area occupied by cells) were performed in each of the experimental animals belonging to two groups – tumor (k=1) and control (k=2). These groups were composed of n_1 and n_2 number of mice, respectively. Thus, for the i-th mouse from the k-th group, we performed $m_{i,k}$ measurements of the respective signal (S), organized in the sample $\chi_{i,k} = \left\{S_1^{i,k}, S_2^{i,k}, \ldots, S_{m_{i,k}}^{i,k}\right\}$ and the goal of the statistical procedure was to identify if there was any difference in S measured in the two groups. The distributions of S in the two groups could be compared at different chosen α-quantile levels. Typically we performed comparisons for $\alpha \in \{0.25,\ 0.50,\ 0.75\}$ (bottom quartile, median, top quartile). If $\alpha_{i,k}$ was the α-quantile estimate of the i-th mouse in the k-th group, the random variable α_k (the α-quantile estimate of the k-th group) had n_k realizations calculated from $\chi_{i,k}$ for i=1,2,…,n_k. Then α_1 and α_2 could be compared by any numerical characteristics estimate $NC_{1,\alpha}$ and $NC_{2,\alpha}$ (NC could be median, mean, standard deviation, interquartile range). For example, $med_{2,\alpha} = med\left(\alpha_2\right)$ was the median estimate of the selected α-quantile estimate of the second group, whereas $IQR_{1,\alpha} = IQR\left(\alpha_1\right)$ was the interquartile range estimate of the selected α-quantile estimate of the first group. The random variables $NC_{k,\alpha}$ had a single realization in the described experiment. To compare the distribution of a pair of random variables (e.g. $med_{1,0.5}$ and $med_{2,0.5}$), we created two samples each containing M=200 Bootstrap realizations of each variable. In the r-th pseudo-reality, for each mouse from the k-th group we generated a synthetic Bootstrap sample $\chi_{i,k}^{r,s}$ using drawing with replacement from the original sample $\chi_{i,k}$ (327). We calculated $\alpha_k^{r,s}$ from $\chi_{i,k}^{r,s}$ and then compressed the n_k synthetic quantiles into the selected numerical characteristic $NC_{k,\alpha}^{r,s}$. Finally, for

both groups we had a sample containing M=200 numerical characteristics of the selected α -quantile. The distributions of the two variables $NC_{1,\alpha}$ and $NC_{2,\alpha}$ (represented in the two samples) were compared using Bootstrap Kuiper test with N=10,000 pseudo-realities (311). The evaluation procedure was performed with original functions - available at request - running under Matlab 9.5.0.944444 (R2018b) with Statistics and Machine Learning Toolbox v. 11.4 (The Mathworks, Natick, MA).

DOI:10.14753/SE.2022.2630

4. RESULTS

4.1. Platelet content of arterial thrombi

Table I. summarizes the clinical characteristics and basic laboratory findings of the patient cohort. If atherosclerotic plaques were found during the procedure or via carotid ultrasound (B mode), atherosclerosis was diagnosed. The patients with elevated fasting blood cholesterol or triglyceride levels or on lipid-lowering therapy were considered dyslipidaemic. Thrombophilia was determined from patient history.

Table I. Patient characteristics. Values are provided as median ± IQR or percentages followed in parenthesis by the number of subjects included in the analysis. CAD: coronary artery disease, PAD: peripheral artery disease, AIS: acute ischemic stroke, WBC=white blood cell count, Plt=platelet count, CRP=C-reactive protein, Hgb=hemoglobin, ASA=acetylsalicylic acid, rtPA=recombinant tissue-type plasminogen activator.

	CAD (66)	**PAD (64)**	**AIS (78)**	**All (208)**
Patient characteristics				
Male	68.2% (45/66)	56.3% (36/64)	61.5% (48/78)	62% (129/208)
Patients' age	63.4±16.4 (66)	67.1±13.7 (64)	60.8±15.4 (78)	64.5±15.1 (208)
Laboratory findings				
WBC (10^3/μL)	11.0±6.4 (66)	9.1±4.2 (62)	9.7±5.4 (78)	10.2±4.8 (206)
Plt (10^3 /μL)	227.5±97 (66)	195±135 (62)	208.5±82 (78)	211±103 (206)
CRP (mg/L)	4.9±12.7 (65)	11.6±18.8 (33)	4.0±8.8 (62)	5.1±12.6 (160)
Hgb (g/L)	137±24.2 (66)	128.9±45.1 (62)	138.6±27.4 (78)	8.4±1.8 (206)
Fibrinogen (g/L)	3.7±1.4 (49)	4.1±1.6 (36)	2.2±1.2 (29)	3.4±1.6 (114)
Etiology				
Thrombophilia	0% (0/66)	0% (0/17)	5.2% (4/77)	2.5% (4/159)
Cardiac embolization	0% (0/66)	11.8% (2/17)	49.4% (38/77)	25.2% (40/159)
Atherosclerosis	100% (66/66)	70.6% (12/17)	26% (20/77)	61% (97/159)
Dissection	0% (0/66)	0% (0/17)	3.9% (3/77)	1.9% (3/159)

DOI:10.14753/SE.2022.2630

	CAD (66)	PAD (64)	AIS (78)	All (208)
Cryptogenic	0% (0/66)	17.6% (3/17)	15.6% (12/77)	9.4% (15/159)
Antithrombotic medication (prior to intervention)				
ASA	100% (62/62)	41.9% (26/62)	24.7% (18/73)	53.8% (106/197)
Clopidogrel	100% (62/62)	22.6% (14/62)	12.3% (9/73)	43.1% (85/197)
Oral anticoagulant	-	6.7% (1/15)	19.5% (15/77)	-
rtPA	-	-	51.3% (40/78)	-
Comorbidities and risk factors				
Atherosclerosis	100% (66/66)	79.4% (50/63)	50.6% (39/77)	75.2% (155/206)
Diabetes	25.8% (17/66)	31.7% (20/63)	20.8% (16/77)	25.7% (53/206)
Hypertonia	69.7% (46/66)	79.4% (50/63)	79.2% (61/77)	76.2% (157/206)
Hyperlipidaemia	50% (33/66)	55.6% (35/63)	35.1% (27/77)	46.1% (95/206)
Uremia	18.2% (12/66)	9.5% (6/63)	0% (0/78)	8.7% (18/207)
Thrombophilia	3% (2/66)	1.6% (1/63)	2.6% (2/78)	2.4% (5/207)
Tumor	18.2% (12/66)	11.1% (7/63)	15.6% (12/77)	15% (31/206)
Smoking				
Never	54% (34/63)	41.3% (26/63)	12.5% (2/16)	43.7% (62/142)
Former	7.9% (5/63)	0% (0/63)	6.3% (1/16)	4.2% (6/142)
Currently smoking	38.1% (24/63)	58.7% (37/63)	81.3% (13/16)	52.1% (74/142)

The SEM analysis of cellular components of thrombi retrieved from different locations (AIS, CAD, and PAD patients) revealed a marked difference in their platelet content (sPlt, Figure 6.). AIS thrombi showed 1.8-fold higher median platelet occupancy than PAD thrombi (sPlt 3.9 vs. 2.2%, $p<0.001$), whereas sPlt difference from CAD thrombi was observed only in male patients (4.9% in AIS vs. 2.8% in CAD, $p=0.0032$).

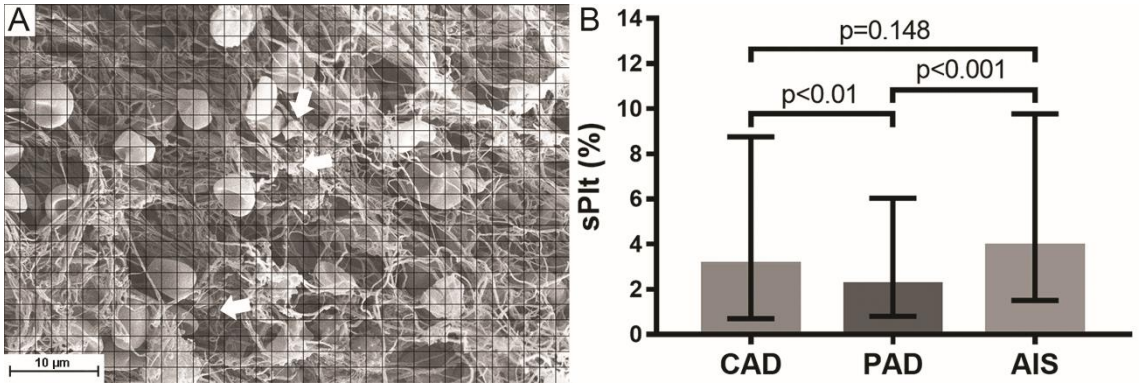

Figure 6. Platelet content of arterial thrombi from coronary (CAD), peripheral artery disease (PAD), and acute ischemic stroke (AIS). The area of scanning electron microscopy images occupied by platelets or platelet conglomerates (indicated by arrows) was determined as a percentage of the total thrombus area (sPlt) as described in section 3.1.3. (A). The number of observations (evaluated thrombus images, #O) were $\#O_{CAD}$=301 (from n=62 patients), $\#O_{PAD}$=298 (n=61) and $\#O_{AIS}$=376 (n=77). B: The columns and bars represent median and interquartile range values. p-values result from one-tailed hypothesis testing for medians (significant if p-value less than 0.05) using Bootstrap resampling of n'=10,000 for each statistical test.

Several factors could be identified as modulators of platelet content (Table 2). In thrombi removed from diabetic patients we measured lower sPlt values (2.1% compared to 3.2% in non-diabetic patients, $p < 0.001$). In AIS with atherosclerotic etiology, the median of the sPlt values (2.7%) was 2-fold lower than in the rest of the AIS cases (5.4%), but no such etiology-related difference was seen in PAD thrombi. The presence of a malignant neoplasm was associated with a decreased median sPlt (1.9%) compared to patients with no malignant comorbidity (4.4%) only in AIS thrombi, but not in CAD and PAD.

In all main groups of sufficiently large size for statistical evaluation, the thrombus occupancy by platelets was more than two-fold lower in active smokers compared to non-smokers, median sPlt 3.6% vs. 1.6% in CAD and 3.2% vs. 1.6% in PAD (there were only 2 documented non-smokers in the AIS group).

Table 2. Platelet content (sPlt) of thrombi from coronary (CAD), cerebral (AIS), and peripheral (PAD) arteries in the presence and absence of comorbidities and

risk factors. The area occupied by platelets on SEM images of thrombi was determined as a percentage of the total thrombus area, as described for Fig. 6. in section 3.1.3. #O=number of observations (evaluated thrombus images); the numbers in parentheses after the #O indicate the numbers of patients included in the respective groups; med=median; no/yes in subscript refers to the presence of the respective comorbidity/risk factor; p_{med}=p-value resulting from one-tailed hypothesis testing for medians (significant if p-value less than 0.05); p_{distr}=p-value from Kuiper-test for distributions performed with Bootstrap resampling of n=10,000 for each statistical test.

Main group	Comorbidity/ risk factor	sPlt % med_{no}	sPlt % med_{yes}	p_{med}	p_{distr}	#O_{no}	#O_{yes}
CAD	**Smoking**	**3.6**	**1.6**	0.011	0.669	166 (33)	99 (21)
	Malignant tumor	2.5	3.9	0.139	0.047	244 (50)	57 (12)
PAD	**Atherosclerosis**	3.0	2.0	0.097	0.728	60 (13)	233 (47)
	Smoking	**3.2**	**1.6**	0.004	0.935	115 (24)	178 (36)
	Malignant tumor	2.0	3.4	0.059	0.207	258 (53)	35 (7)
AIS	**Atherosclerosis**	**5.4**	**2.7**	<0.001	0.072	175 (37)	196 (39)
	Smoking	8.0	2.4	0.164	0.771	11 (2)	67 (13)
	Malignant tumor	**4.4**	**1.9**	<0.001	1.000	308 (64)	63 (12)

4.2. Effects of CypD and CsA on platelet morphology and function

4.2.1. Morphological alterations of platelets activated by 'strong' stimuli

To mimic the environment at the site of vascular injury, platelets were allowed to adhere to a collagen surface, and soluble activators relevant to the core area of the platelet plug (thrombin and ROS) were added. ROS (hydroxyl radicals) were generated using physiological concentrations of Cu^{2+}, homocysteine, and H_2O_2, as described previously in section 3.2.3 (315, 316). Human platelets activated by thrombin and collagen showed flattening and surface spreading, which were accompanied by membrane blebbing and fragmentation (e.g. Fig. 7a, upper left panel, lower right

corner). In the presence of CsA, membrane integrity remained more preserved (Fig. 7a, upper right panel). In the presence of ROS, platelets exhibited dramatic shape changes and extensive shedding of membrane particles, and these effects were markedly counteracted by CsA treatment (compare lower left and right panels of Fig. 7a). Thrombin plus collagen-activated $CypD^{+/+}$ murine platelets also exhibited spreading and membrane disintegration (Fig. 7b, upper left panel, lower region, and middle region, respectively), while platelets isolated from $CypD^{-/-}$ mice showed more preserved membrane integrity. Similarly, differences in membrane integrity, although less pronounced, could be noted between platelets of different genotypes in the presence of ROS (compare lower left and right panels of Fig. 7b).

DOI:10.14753/SE.2022.2630

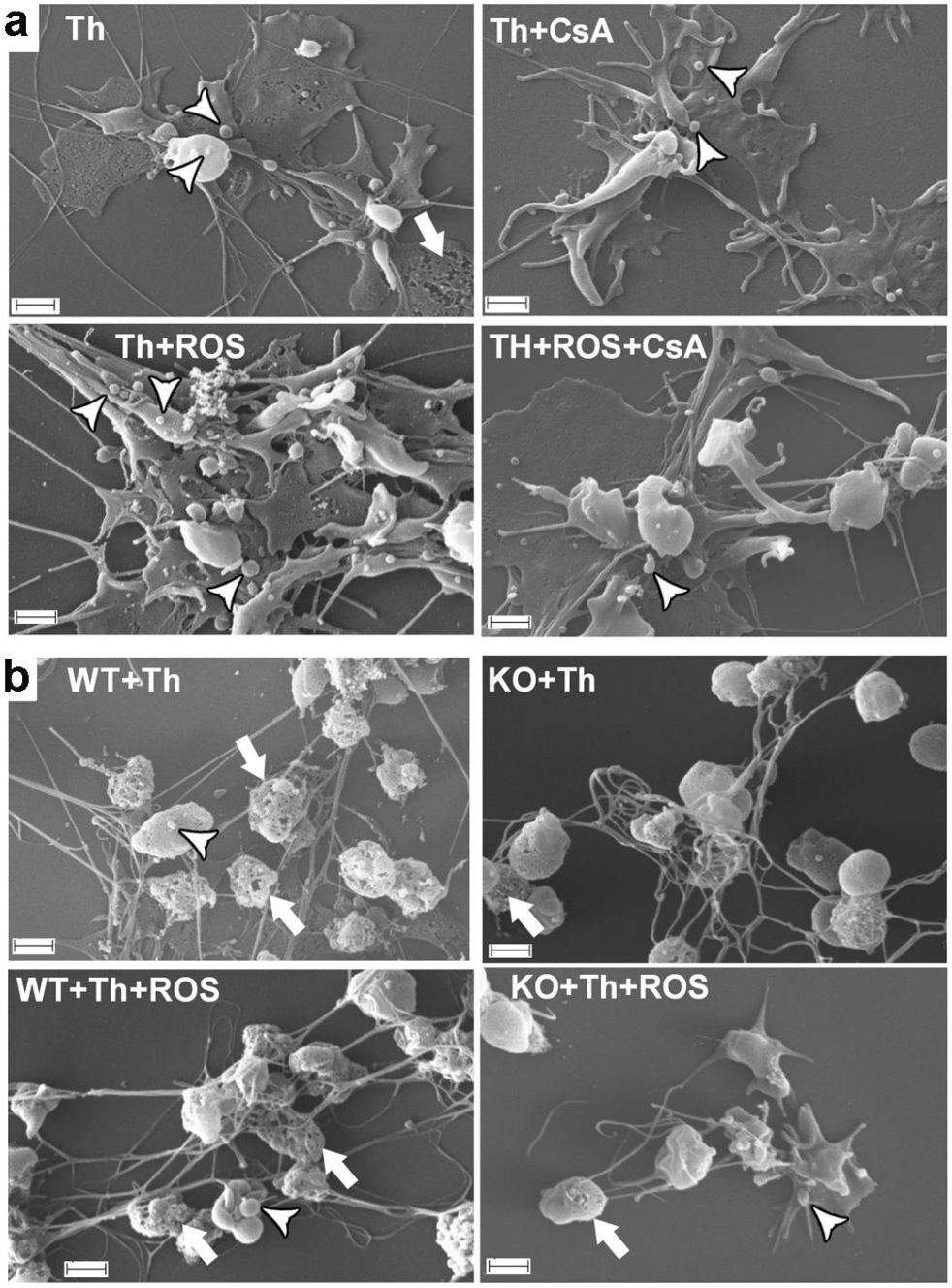

Figure 7. Adhesion and activation of platelets on collagen. (a) Washed human platelets and (b) wild type (WT) or CypD$^{-/-}$ (KO) washed murine platelets were placed on collagen-coated glass surfaces and simultaneously activated with 25 nM thrombin in the presence of additives as indicated (reactive oxygen species, ROS, cyclosporin A CsA). SEM images were taken following fixation with glutaraldehyde. The arrowheads mark representative cases of membrane blebbing and shedding, the arrows point to membrane fragmentation and disintegration. Scale bar = 1 μm.

These qualitative observations warranted further structural investigations. Because of the known influence of CypD and MPTP on cellular integrity (328), TEM imaging was performed to address the effect of CypD and CsA on the intracellular features of platelet activation. This technique requires that cells are activated in a suspension, therefore the collagen surface was replaced by its peptide analog, convulxin. For quantitative assessment of the ultrastructural rearrangements a parameter independent of inherent variances in platelet cross-sections was used: the normalized organelle area, which was defined as the average area of membrane-bearing organelles per unit platelet cross-section area in the TEM micrographs. ROS induced pronounced swelling of organelles in thrombin+convulxin-treated human platelets (Fig. 8a, b) as reflected in the 5-fold increase of the normalized organelle area (Fig. 8h), which could be completely reversed by CsA treatment (Fig. 8c, h). Genetic ablation of CypD also caused a slight decline in the normalized organelle area of murine platelets, however, this tendency failed to reach statistical significance regardless of the presence or absence of ROS (Fig. 8h). On the other hand, disruption of membrane integrity —which was more frequently seen in murine than in human ROS-treated samples— was largely abolished in CypD$^{-/-}$ platelets (compare Fig. 8f and g).

DOI:10.14753/SE.2022.2630

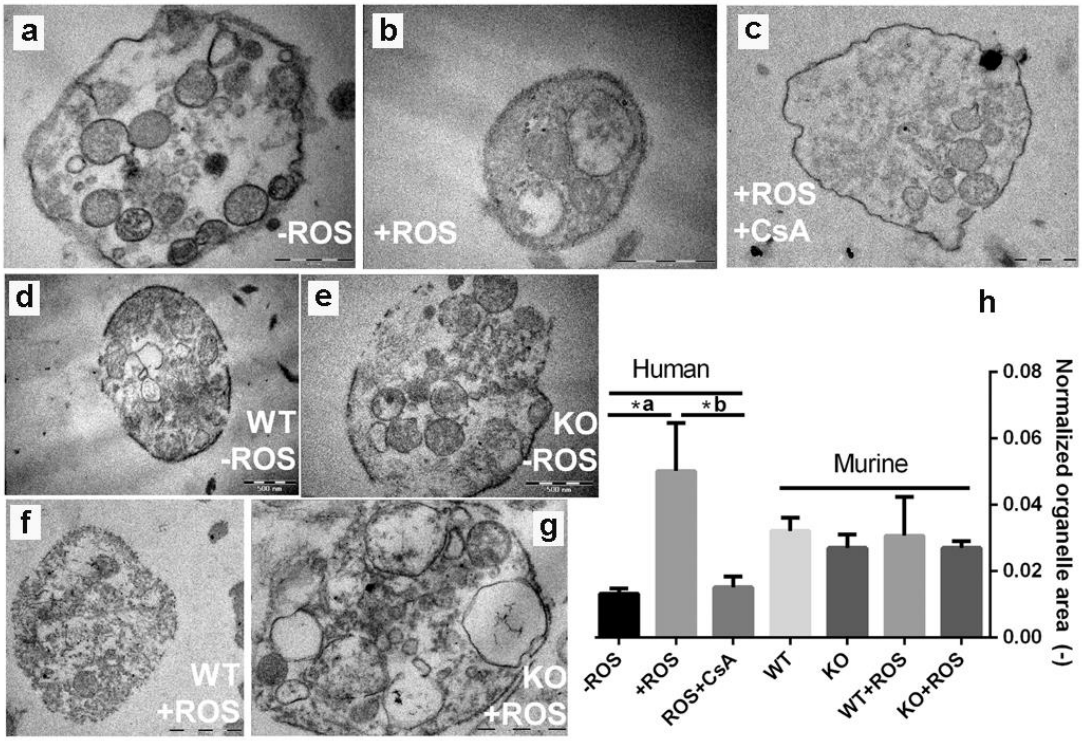

Figure 8. Effects of reactive oxygen species on the subcellular morphology of activated platelets. Human (a–c) as well as wild-type (WT) and CypD$^{-/-}$ (KO) murine platelets (d–g) were activated by thrombin+convulxin in the presence or absence of ROS and examined with TEM. For each treatment regimen, 10–25 images were analyzed. The cumulative area (TO) and number (n) of membrane-bearing organelles, as well as the total platelet cross-section area (TC), were measured and the normalized organelle area was calculated as $TO/(n \times TC)$ and interpreted as an indicator of individual organelle swelling (h). The typical key changes of the organelle area are exemplified by the size and shape of the membrane-bearing organelles of panels (a) and (b). Mean values and SE are shown, the asterisk represents a difference significant at $P < 0.05$ according to a post-hoc Tukey test performed after ANOVA (separately for human and murine datasets). ROS: reactive oxygen species, CsA: cyclosporin A. *a: $P = 0.0003$ *b: $P = 0.0038$. Scale bar = 500 nm.

DOI:10.14753/SE.2022.2630

4.2.2. Structural features of fibrin formed in the presence of 'strongly activated' platelets

In the course of clot formation, stimulated platelets are not only passively entrapped in the fibrin network, but they also modify the clot structure. Therefore, in further studies 'strong' stimuli were applied on platelets recruited to a three-dimensional fibrin matrix. SEM investigation of composite platelet-fibrin clots revealed that the combined stimulus of thrombin and convulxin caused the appearance of fragmented platelets (Fig. 9a, arrowheads) which were surrounded by thicker clusters of fibrin fibers. In contrast, platelets appeared to be more intact in clots containing $CypD^{-/-}$ murine or CsA-treated human platelets with less heterogeneity in the surrounding fibrin fibers (e.g. WT vs. KO in Fig. 9a). Quantification of fibrin fiber diameters confirmed that incorporation of activated murine platelets caused a moderate thickening of fibrin fibers (the median diameter increased from 76.1 to 80.8 nm), while genetic ablation of CypD abolished this effect and reduced the heterogeneity of fiber size (Fig. 9b, left panels). Human platelets activated by thrombin+convulxin in the presence or absence of CsA had a minor influence on fiber diameters when compared with appropriate controls to account for vehicle effects ('HPlt' vs. 'No additive' and 'HPlt+CsA' vs. 'CsA').

DOI:10.14753/SE.2022.2630

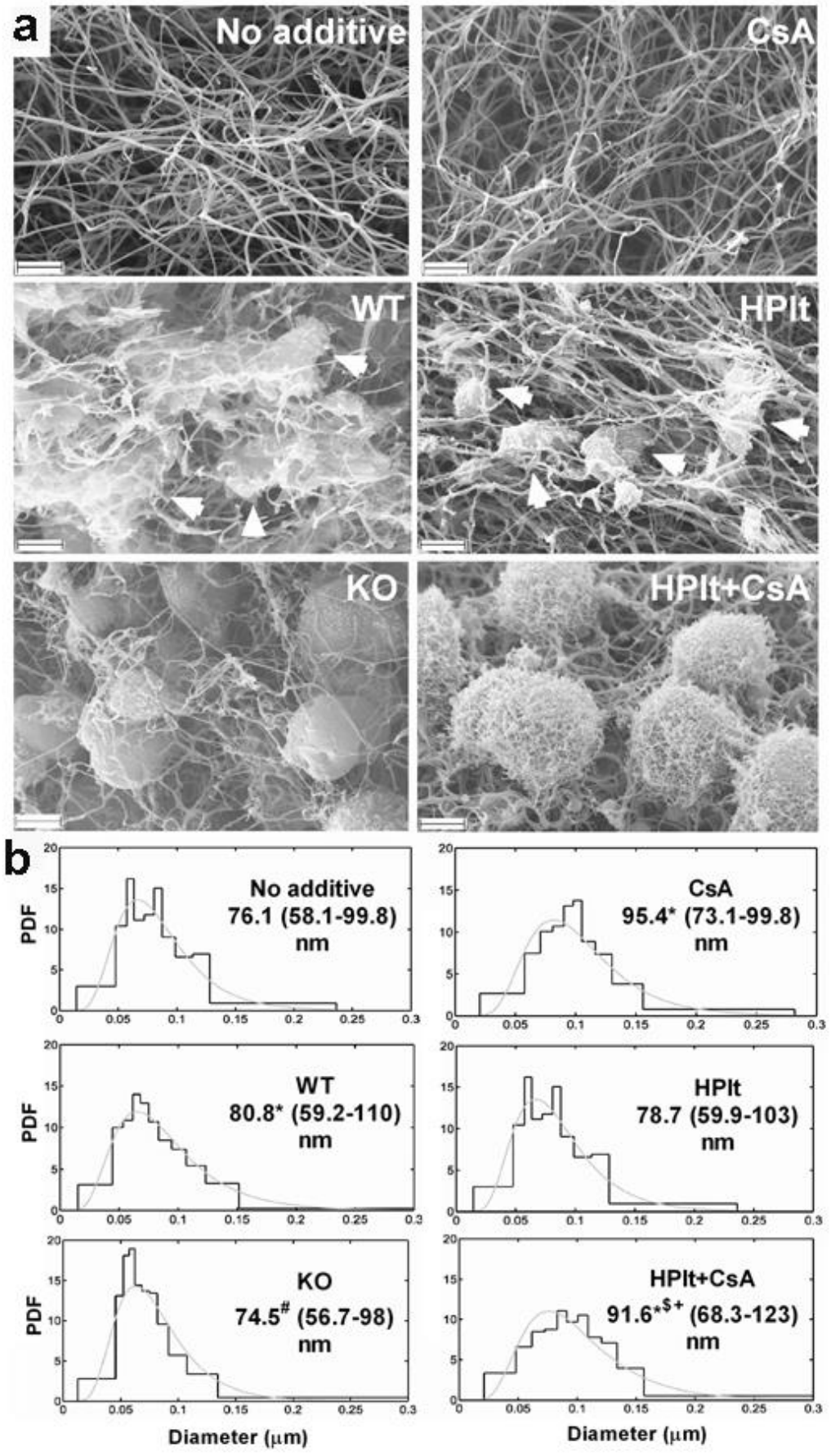

Figure 9. Platelet morphology in a fibrin matrix. (a) Representative SEM images of fibrin clots prepared from 6 μM fibrinogen clotted for 2 h with 15 nM thrombin containing —where indicated— murine (WT: wild type or KO: $CypD^{-/-}$) or human (HPlt) platelets at 0.5×10^5/μl. In all cases, 250 ng/ml convulxin was present in the clots. Where indicated, 1 μM cyclosporin A (CsA) was also added. Scale bar = 2 μm. Arrowheads point to platelet fragments (WT and HPlt panels), in the vicinity of which bundles of fibrin fibers are assembled. This phenomenon is not observed around $CypD^{-/-}$ and CsA-treated platelets (KO and HPlt + CsA panels). (b) The diameter of 300 fibers per image was measured from 2–6 SEM images per clot type using the algorithms described in section 3.2.3. The graphs present the probability density function (PDF) of the empiric distribution (histogram) and the fitted theoretical distribution (gray curves). The numbers under the clot type show the median, as well as the bottom and the top quartile values (in brackets) of the fitted theoretical distributions. Differences significant at $P < 0.05$ level according to Kuiper's test are indicated with the following symbols: *($P < 0.001$) compared to 'No additive'; #($P < 0.001$) compared to 'WT'; $($P = 0.00249$) compared to 'CsA'; +($P < 0.001$) compared to 'HPlt'.

4.2.3. Platelet functions as a response to 'mild' stimuli

While platelets in the core region of thrombi are likely to be exposed to 'strong' activators, 'mild' stimuli, such as ADP play a key role in platelet activation in the peripheral zones. To investigate the effect of CsA and CypD on this process, we carried out functional assays focusing on ADP-induced platelet adhesion, spreading, and aggregation.

To examine real-time platelet-surface interactions, we adopted an impedance-based method described in recent studies (320, 321). Cells were allowed to adhere to and spread on electrodes placed at the bottom of impedimetric wells and the change of impedance on the electrodes was measured. The initial, linear phase of the cell index (CI) curves reflect adhesion, while the maximal CI value corresponds to the area occupied by spreading platelets (321). Genetic ablation of CypD resulted in an increased slope of impedimetric curves (by 210 and 140% without and with ADP, respectively) and in an increased maximum CI (by 40 and 34% without and with ADP, respectively) when compared to wild type (WT) platelets (Fig. 10a, b), reflecting

DOI:10.14753/SE.2022.2630

increased adhesion and spreading of CypD$^{-/-}$ platelets. Similar trends were observed with human platelets: CsA-treatment resulted in increased steepness (by 91 and 76%, without and with ADP, respectively) and maximum CI (by 18 and 10%, without and with ADP, respectively) of impedimetric curves (Fig. 10c, d).

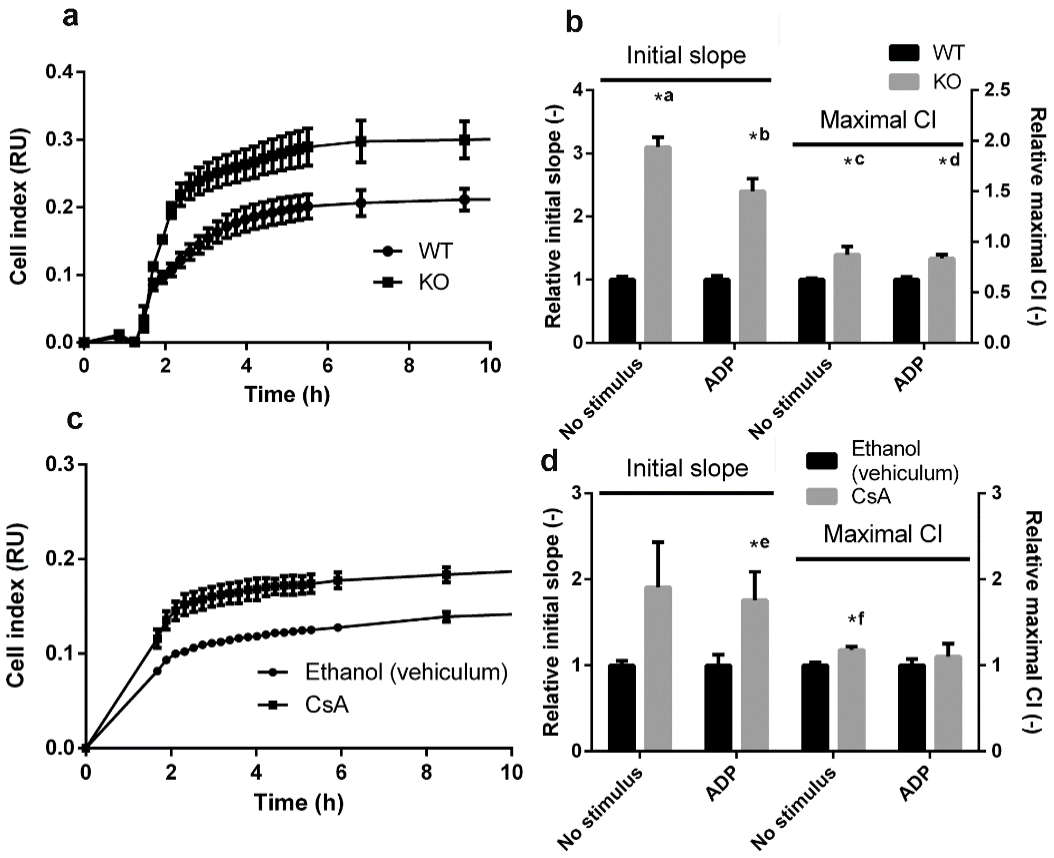

Figure 10. Adhesion and spreading of platelets measured by impedimetry. Impedance changes during adhesion and spreading of murine (a, b) and human (c, d) platelets. The change in impedance is represented as Cell Index (CI), a relative and dimensionless value which is calculated as $CI = (Z_i - Z_0)/F$ where Z_i is the impedance at an individual time point, Z_0 is the impedance at the start of the experiment and F is a constant depending on the applied frequency. (a, c) Impedimetry traces: representative mean curves from 2–3 replicas. Bars represent SE. (b, d) The steepness and maximum Cell Index (CI) value were calculated from the impedimetry traces and are shown in relative units (the mean values of the steepness and maximum CI from the replicas of the vehicle control for human platelets and WT results for murine platelets were considered to be 1 for each independent set of measurements). Data are presented as

means of n = 5–6, bars represent SE. Asterisks mark differences significant at $P < 0.05$ between the respective data pairs according to the Kolmogorov-Smirnov test. *a: $P = 0.0013$ *b: $P = 0.0013$ *c: $P = 0.0013$ *d: $P = 0.0122$ *e: $P = 0.0183$ *f: $P = 0.0122$. CsA: cyclosporin A, WT: wild-type, KO: $CypD^{-/-}$.

Platelet-platelet interactions were tested in an ADP-induced aggregometry assay. In the presence of CsA the initial slope of aggregation curves was almost doubled (1.00 ± 0.08 for control, 1.92 ± 0.26 for CsA) and the maximal aggregation values were also moderately increased (1.28 ± 0.09 with CsA compared to 1.00 ± 0.09) reflecting increased aggregation (Fig. 11a, c). In contrast, the absence of CypD in murine platelets resulted in a decreased aggregation response to ADP (Fig. 11b, d) as initial slope and maximal aggregation values were lower by 35 and 26%, respectively. To clarify the discrepancy between CsA and CypD effects, selective modifiers of calcineurin and mitochondrial energetics were tested in this assay. Bongkrekic acid [Bk, an inhibitor of adenine nucleotide translocator (ANT)] treatment resulted in a pronounced (67%) increase in initial slope values, while maximal aggregation remained essentially unchanged. FK-506 (a selective inhibitor of calcineurin) in the 100–1000 nM range had no effect on aggregation parameters (results not shown), while higher concentrations (5–50 μM) resulted in increased maximal aggregation values (1.47 ± 0.1 with FK-506 compared to 1.00 ± 0.03) (Fig. 11c).

DOI:10.14753/SE.2022.2630

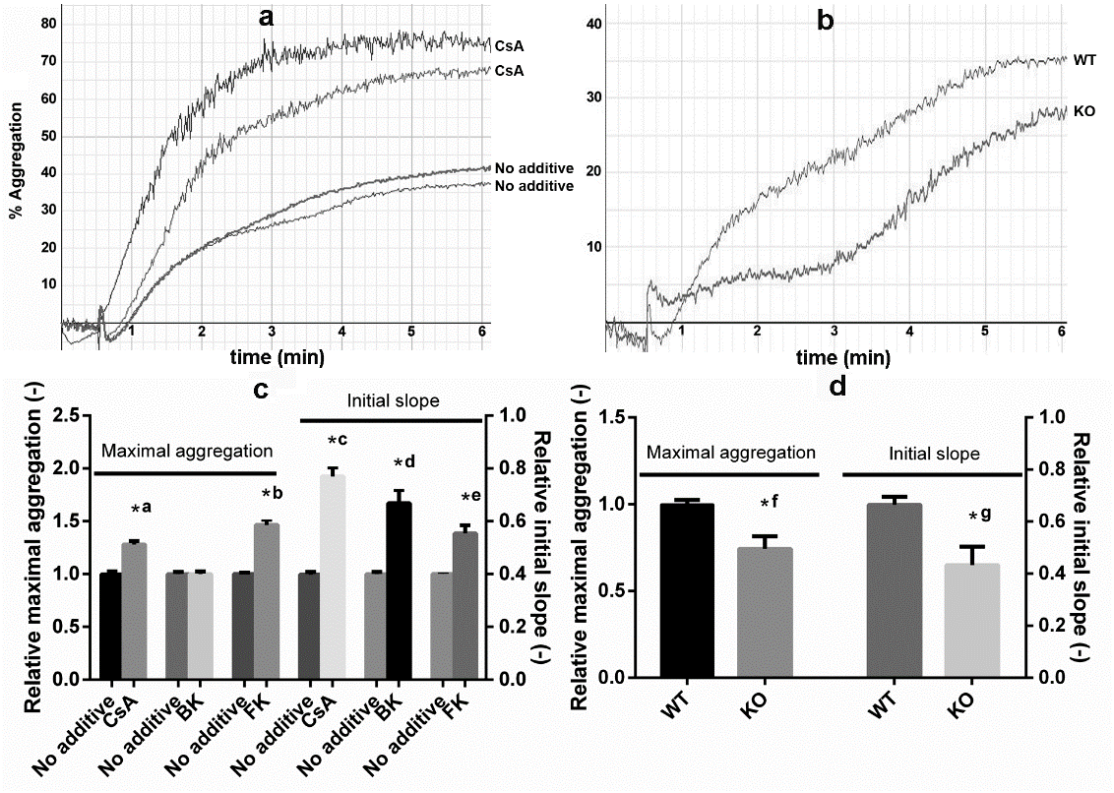

Figure 11. ADP-induced platelet aggregation. Washed human platelets were incubated with 2 µM cyclosporin A (CsA), 20 µM bongkrekic acid (BK) or 10 µM FK-506 (FK), or their respective vehicles (1% ethanol for CsA, 2 mM NH_4OH for bongkrekic acid, and 0.5% DMSO for FK-506) for 30 min at 37 °C. The conditioned human and the washed murine (WT: wild-type, or KO: $CypD^{-/-}$) platelets were supplemented with 6 µM fibrinogen to support aggregation right before it was initiated by the addition of 10–50 µM ADP (to give a maximal aggregation value of at least 30%) and 2.5 mM $CaCl_2$. PBS was used as background for 100% transparency, and aggregation was recorded for 30 min. Aggregation curves from representative experiments using human (a) or murine (b) platelets are shown. (c, d) The measured initial slope and maximal aggregation values are shown in relative units (the mean value of the replicates of the vehicle control in each independent set of measurement was considered to be 1). 'No additive' designates samples incubated with the respective vehiculum of the inhibitors. Data from duplicates from at least three independent experiments and SE are shown. Asterisks mark differences significant at $P < 0.05$ between the indicated pairs of samples according to the Kolmogorov-Smirnov test. *a: $P = 0.0438$, *b: $P = 0.0111$, *c: $P = 0.0026$, *d: $P = 0.0361$, *e: $P = 0.0111$, *f: $P = 0.0275$ *g: $P = 0.0042$.

DOI:10.14753/SE.2022.2630

4.2.4. Fibrin structure modification in the presence of platelets activated by 'mild' stimuli

To test how 'mild' activation of platelets affects the surrounding fibrin structure, platelets pre-treated with various modulators were activated by ADP (Table 3). Pre-treatment of human and WT murine platelets with CsA or Bk resulted in thinner fibers, whereas using CypD$^{-/-}$ platelets Bk-treatment decreased the fiber diameter, but CsA-treatment had no effect. Incorporation of FK-506-treated human and murine platelets resulted in a decrease in the median fiber diameter from 84.9 nm to 78.5 nm with human platelets and an increase with murine platelets (from 85.9 nm to 92.3 nm in the presence of WT and from 91.3 nm to 109.4 nm with CypD$^{-/-}$ platelets). The addition of ROS did not alter these tendencies, although it generally increased the diameter of fibrin fibers, e.g. in clots containing CypD$^{-/-}$ platelets median values were 17–27 nm higher in the presence of ROS than in their absence (compare data for inhibitor-free vehicle samples in Table 3, all $P < 0.0001$).

Table 3. Fibrin fiber thickness in the presence of platelets activated by ' mild' stimuli. The table shows the median fibrin fiber diameters with lower and upper quartiles in brackets determined using the algorithm described in section 3.2.9 from the measurement of diameter of 300 fibrin fibers per image from 2–6 scanning electron microscopic images per clot type. Fibrin was prepared from 6 µM fibrinogen clotted for 2 h with 15 nM thrombin in the presence of human or murine (WT: wild type or $CypD^{-/-}$) platelets at 10^5/µl. Where indicated (+) platelets were incubated with 2 µM cyclosporine A (CsA), 20 µM bongkrekic acid, 10 µM FK-506 or their respective vehicle (1% ethanol for CsA, 2 mM NH_4OH for bongkrekic acid, 0.5% DMSO for FK-506) and 10 µM ADP for 30 min prior to clotting. The P-values refer to Kuiper's statistical test for differences of distributions of the fiber diameters in the presence and absence of the respective inhibitor.

Platelet	cyclosporine A			FK-506			bongkrekic acid		
	-	+	P	-	+	P	-	+	P
Human	94.2 [75.0-118.2]	86.8 [66.9-112.7]	0.0017	84.9 [67.9-106.2]	78.5 [63.4-97.3]	0.0042	86.2 [69.8-106.4]	78.4 [64.4-95.4]	0.0008
WT	97.8 [80.1-119.4]	85.9 [70.4-104.7]	0.0000	85.9 [70.0-105.3]	92.3 [74.5-114.4]	0.0067	99.6 [79.8-124.3]	90.6 [73.4-112.0]	0.0008
$CypD^{-/-}$	96.9 [74.6-125.9]	98.5 [76.4-126.8]	0.7630	91.3 [70.8-117.7]	109.4 [85.3-140.2]	0.0000	107.6 [83.0-139.5]	100.4 [80.2-125.7]	0.0017
Human+ ROS	97.6 [79.4-119.9]	91.3 [72.7-114.8]	0.0133	109.6 [86.6-138.7]	87.2 [67.7-112.3]	0.0000	96.2 [74.2-124.7]	89.7 [71.5-112.5]	0.0075
WT+ ROS	97.6 [77.0-123.7]	88.2 [69.9-111.5]	0.0008	90.8 [71.9-114.8]	107.5 [85.8-134.8]	0.0000	111.8 [87.8-142.4]	98.6 [78.5-123.9]	0.0000
$CypD^{-/-}$ +ROS	115.0 [89.2-148.4]	110.0 [84.6-143.0]	0.2650	108.1 [86.3-135.4]	128.4 [98.3-167.7]	0.0000	134.7 [104.9-172.9]	97.1 [73.5-128.1]	0.0000

DOI:10.14753/SE.2022.2630

DOI:10.14753/SE.2022.2630

4.2.5. Effects of platelets on the tissue factor-induced clotting of plasma

The pro-coagulant effects of platelets were examined in two experimental setups (see section 3.2.7.). Table 4. presents the tissue factor-induced clotting times from the electromechanical coagulometric assay, while Figure 12 shows the time to reach half-maximal absorbance (t50) in the turbidimetric assay. Both assays indicate that the presence of platelets increases the rate of clot formation, however, no differences were seen in relation to the applied modulators of platelet function.

Table 4. Effect of platelets on tissue factor-induced clotting time. Clotting time was measured with an electromechanical coagulometric assay. The table reports the mean±SD values of two independent experiments with three parallel measurements. PPP: human platelet-poor pooled plasma, Plt: platelet. The addition of ADP did not change the clotting time in the presence of platelets ($p>0.05$ for (PPP+Plt) v. (PPP+ADP+Plt), Kolmogorov-Smirnov statistical test).

1.	PPP	PPP+Plt	PPP+ADP+Plt
Clotting time (s)	99.13±1.59	93.47±0.45	93.4±0.7
	84.23±3.68	80.17±0.7	81.63±1.32

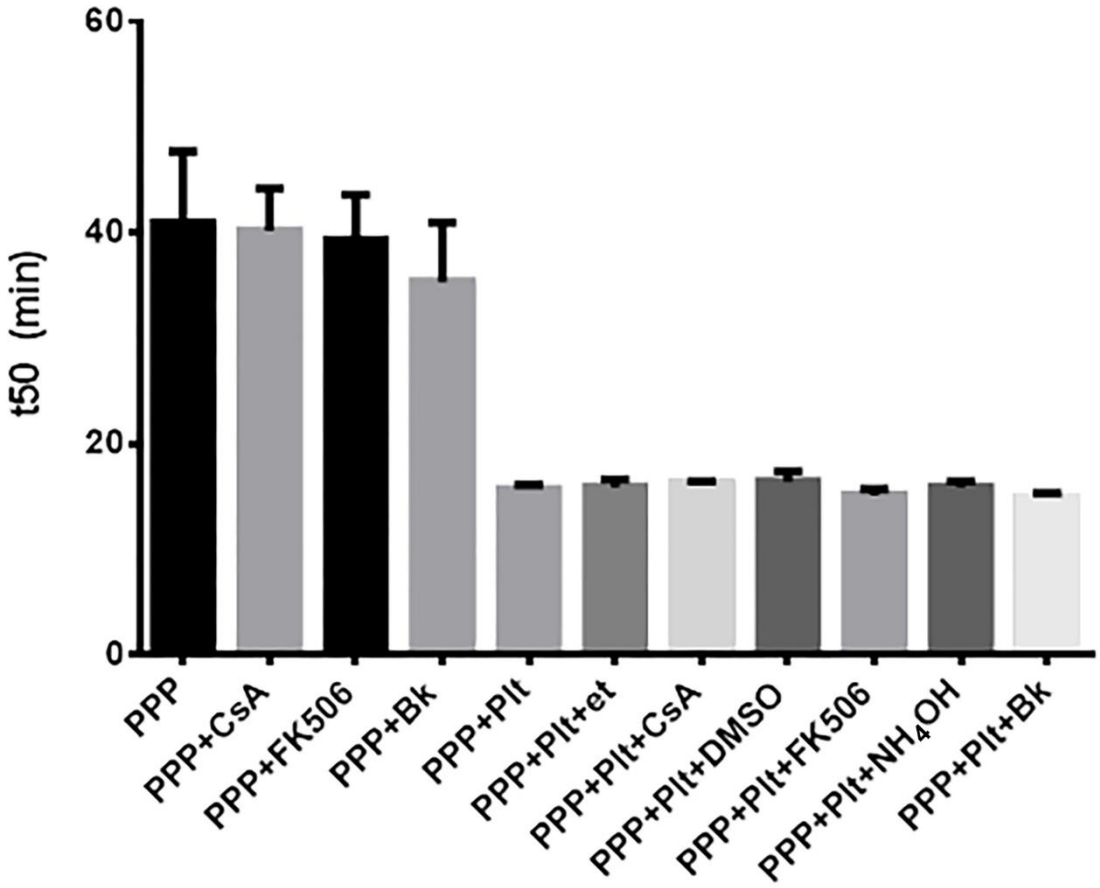

Figure 12. The impact of platelets and modulators of their function on tissue factor-induced clotting of plasma. Tissue factor-induced clotting was followed by measuring the absorbance at 340 nm. Time to reach half of the maximal absorbance value (t50) was calculated. The figure shows mean t50 values with standard deviation of platelet-poor pooled plasma in the absence and presence of platelets and the indicated modulators or their respective vehicles. Each column represents the mean values of eight parallel measurements. The addition of different modulators did not change the t50 values in the presence of platelets ($p>0.05$, Kolmogorov-Smirnov statistical test). PPP: platelet-poor pooled plasma; CsA: Cyclosporin A; Bk: Bongkrekic acid; Plt: platelet; et: ethanol; DMSO: dimethyl-sulfoxide.

4.2.6. Impact on fibrinolytic susceptibility

At sites of their activation platelets interact with a heterogeneous fibrin network forming the scaffold of hemostatic clots and pathological thrombi. There is continuing therapeutic interest in the effective enzymatic dissolution of the fibrin network in

several clinical settings. In view of the role of platelets in fibrin stabilization (reviewed by Longstaff and Kolev (169)), we examined the effects of CsA and CypD on the fibrinolytic susceptibility of model thrombi. Modifying a global turbidity-based assay that has been successfully used in our earlier studies (326), we incorporated platelets at different cell counts into a fibrin matrix containing various activators. (i) Thrombin played a dual role in this assay catalyzing the fibrinogen-fibrin conversion and activating platelets. (ii) In certain cases, ROS were added to represent oxidative agents released from dying cells and neutrophils in thrombi. (iii) The mild activator ADP was used to match the milieu of peripheral regions of thrombi, which are more susceptible to circulating fibrinolytic agents. Proteolytic digestion of the formed clot was initiated by a clinically relevant fibrinolytic agent, tissue-type plasminogen activator (tPA) (Fig. 13a). In all experimental setups, the presence of WT murine platelets caused a delay in fibrinolysis (Fig. 13b, c). Remarkably, genetic ablation of CypD largely reversed this effect: the t10 or t50 values of fibrin containing platelets from $CypD^{-/-}$ mice were shifted towards those of platelet-free fibrin. These tendencies were more evident at higher platelet counts (compare left side of Fig. 13b and c), and the differences were most pronounced in the presence of ROS (right side of Fig. 13b and c). CsA treatment had no effect on the progress of lysis curves in fibrin clot models containing human platelets (data not shown).

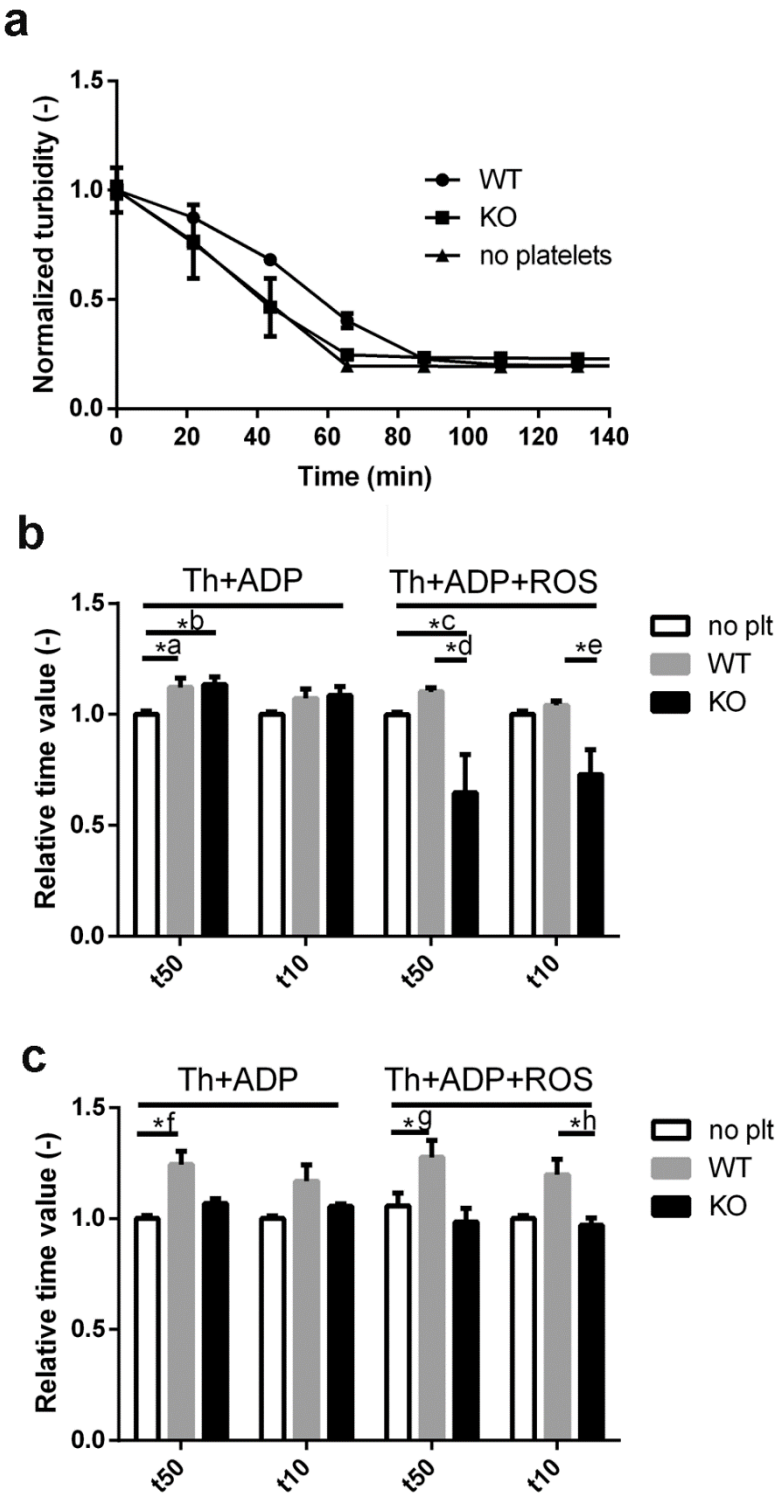

Figure 13. tPA-induced lysis of platelet-containing fibrin clots. Fibrinogen (6 μM) supplemented with 0.5 μM plasminogen, 2.5 mM $CaCl_2$, 10 μM ADP, and in the indicated cases, with murine platelets and modulator additives was clotted with 16 nM

thrombin (Th) for 60 min. Lysis was initiated by the addition of 50 µg/ml tPA to the clot surface and light absorbance at 340 nm was measured. (a) Representative lysis curves of tPA-induced lysis in clots containing reactive oxygen species (ROS) and platelets isolated from wild type (WT) and CypD$^{-/-}$ (KO) mice. The presented turbidity values are the measured absorbance values normalized for the maximal absorbance for each sample (n = 4, every 10th measurement point is shown, bars represent SE values). The time to reach 50% (t50) and 10% (t10) of the initial turbidity was calculated from the lysis curves of clots containing (b) 1×10^5/µl or (c) 2×10^5/µl platelets and presented in relative units: the mean value of the t50 and t10 for platelet-free fibrin (no plt) in each independent set of measurement was considered to be 1. Mean of n = 7–8 replicates and SE values are shown. Asterisks indicate significant differences at $P < 0.05$ according to the post-hoc Dunn test performed after the Kruskal-Wallis test for the respective triplets of data. *a: P = 0.0241, *b: P = 0.0241, *c: P = 0.0154, *d: P = 0.0021, *e: P = 0.0034, *f: P = 0.0009 *g: P = 0.0184, *h: P = 0.0239.

4.3. Structural properties of venous thrombi formed in human pancreatic tumor-bearing mice

The analysis of the composition of venous thrombi by scanning electron microscopy showed decreased red blood cell content in thrombi from tumor-bearing mice compared with thrombi from control mice (Figure 14A). In addition, we observed an increase in fibrin density and a decrease in fibrin fiber thickness in thrombi from tumor-bearing mice compared with thrombi from controls (Figure 14B).

DOI:10.14753/SE.2022.2630

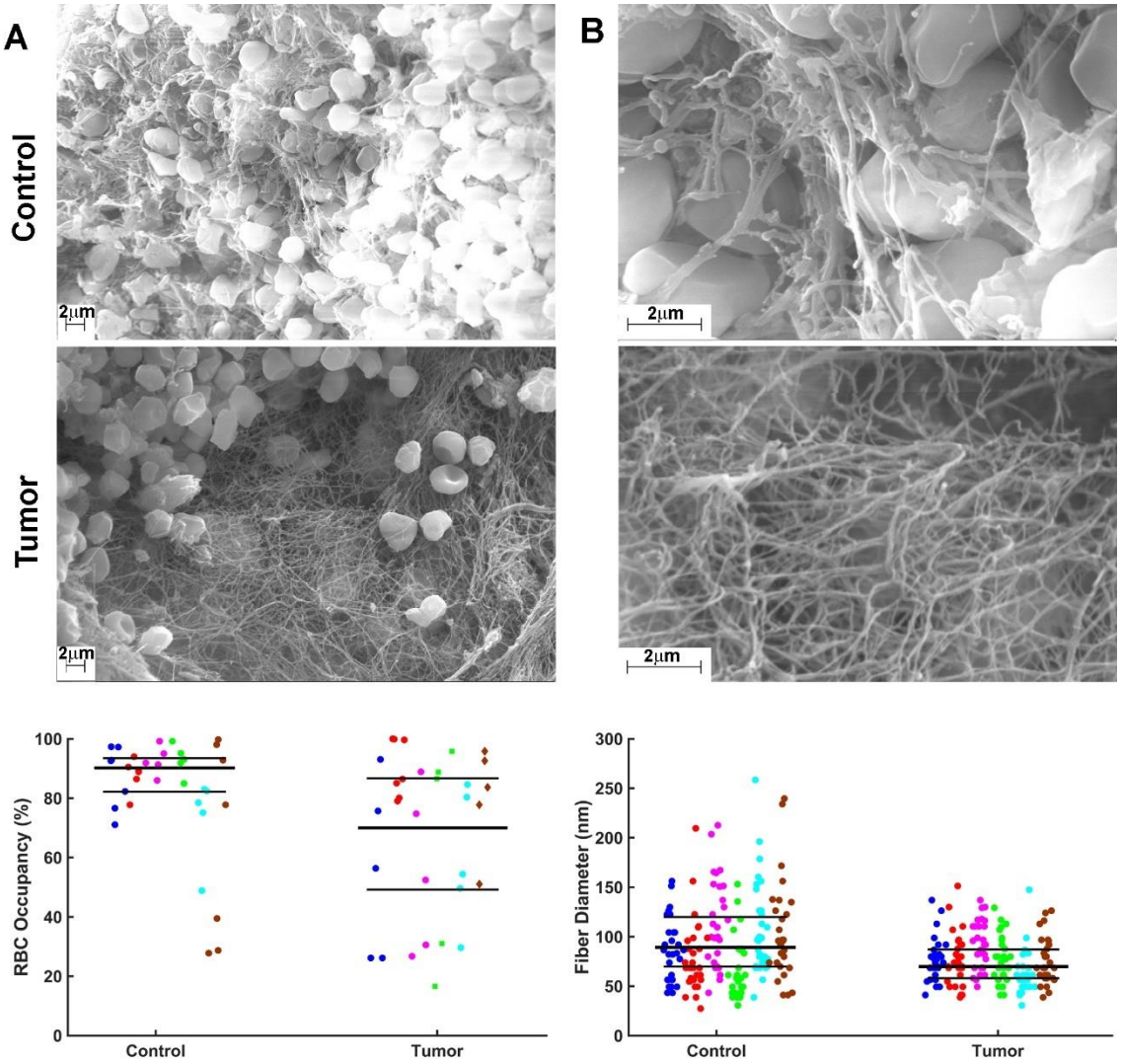

Figure 14. Analysis of thrombi by scanning electron microscopy. (A, B) The red blood cell (RBC) and fibrin content in thrombi from control and tumor-bearing mice were assessed by scanning electron microscopy. Upper panels are representative images of thrombi from control and tumor-bearing mice. RBC occupancy was quantified in 5-7 randomly selected images from each animal (A, data from each thrombus are shown with the same color in the lower panel). The diameter of 300 fibrin fibers from separate parts of each thrombus was measured (B, every 10th measured value is plotted in the same color for each thrombus in the lower panel). Lines indicate the median values of the bottom, median, and top quartiles calculated from the data of six animals from each group (shown in different colors) based on 35 images in the control group and 32 images in the tumor group. Bootstrap Kuiper test $P<0.001$ for all three quartiles of the datasets in the lower panels.

DOI:10.14753/SE.2022.2630

5. DISCUSSION

5.1. Platelet content of arterial thrombi

The development of interventional techniques in the treatment of arterial thrombosis has given us a new opportunity to study the structure of in vivo formed thrombi antemortem. The assessment of patient history, pharmacological anamnesis and comorbidities can provide us with novel information about the modulators of thrombus composition.

The SEM analysis of cellular components of thrombi retrieved from AIS, CAD, and PAD patients revealed a marked difference in their platelet content (sPlt, Fig. 6). AIS thrombi showed 1.8-fold higher median platelet occupancy than PAD thrombi (sPlt 3.9 vs. 2.2%, $p < 0.001$), whereas sPlt difference from CAD thrombi was observed only in male patients (4.9% in AIS vs. 2.8% in CAD, $p=0.0032$). These several-fold differences in sPlt can lead to major downstream alterations through the signal amplification of the coagulation cascade as platelets usually initiate clotting in arteries. Our sPlt results in CAD were similar to those reported before by others (329), however concerning AIS other studies found higher platelet content in thrombi (330, 331). The inconsistency of these data could be a result of many factors: group heterogeneity, the smaller sample size in the earlier AIS studies, variations in the rheological conditions of the culprit sites of emboli causing stroke.

Several factors could be identified as modulators of platelet content (Table 2). In AIS with atherosclerotic etiology, the median of the sPlt values (2.7%) was 2-fold lower than in the rest of the AIS cases (5.4%), but no such etiology-related difference was seen in PAD thrombi (and all CAD cases are considered atherosclerotic). Traditionally, thrombi originating from the heart and caused by atrial fibrillation (cardiac ethiology) were thought to be erythrocyte or fibrin dominant because of the slower flow rates, but so far, this was not proved by histological, or immunohistochemical studies. On the other hand, thrombi formed in stenotic arteries (atherosclerotic ethiology) are supposed to be platelet-dominant due to high shear conditions. Recent studies investigating samples from mechanical thrombectomy found erythrocytes more frequently dominant in atherosclerotic thrombi (331-333), although contradictory results were also presented (330). The relative platelet content in other groups' studies either showed no difference

in thrombi of different etiologies (331, 334) or was higher in cardioembolic thrombi (compared to noncardioembolic cases) (335).

The presence of a malignant neoplasm was associated with a decreased median sPlt (1.9%) compared to patients with no malignant comorbidity (4.4%) only in AIS thrombi, but not in CAD and PAD. Others have found an increased platelet content of stroke thrombi in patients with active cancer compared to inactive cancer and control groups (336). The increased risk of venous thromboembolism in cancer patients is a well-known and extensively studied phenomenon (337). Similarly, a strong relationship between cancer and arterial thrombosis was observed in various studies (338-340). In the first 6 months after cancer diagnosis, the risk for ischemic stroke increased two-fold (341). Cancer cells can interact with platelets causing their activation and aggregation by secreting ADP (342), thrombin (343) or abnormally glycosylated mucins (binding to P-selectin on platelets) (344). Podoplanin expression of cancer-related fibroblasts, or even the release of podoplanin-containing microparticles can mean similar stimulus for platelets through the C-type lectin receptor-2 (345, 346). The physiological role of this interaction is yet unknown as this receptor is exclusively expressed in megakaryocytes and platelets, and its sole known endogenous ligand (podoplanin) (347) has only been identified on tumor cells and lymphatic endothelial cells(348).

Platelet functions are affected by diabetes through many factors, involving insulin resistance, hyperglycemia, oxidative stress, changes in flow conditions and associated metabolic diseases. All of these lead to an enhanced atherosclerosis and a prothrombotic state resulting in various cardiovascular events. Insulin has an inhibitory effect on platelet adhesion and aggregation while stimulating NO synthesis, all of which are lost in patients with insulin resistance (349-351). The increased levels of circulating adipokines (e.g. resistin, leptin, PAI-1) cause a hormone insensitivity by decreasing the gene expression of insulin receptor substrate-1 in megakaryocytes, and thereby disturb signaling pathways in platelets (352). Platelets display a hyperreactivity (353) in chronic hyperglycemia and a decreased sensitivity to inhibitory drugs, such as aspirin (354, 355). The elevated ROS formation in diabetic patients also contributes to the increased activation of platelets (356, 357). In thrombi removed from diabetic patients we measured lower sPlt values (2.1% compared to 3.2% in non-diabetic patients, $p < 0.001$). The SEM images depict the final state of platelets in a formed thrombus and

enable measurements regarding the area occupied by these cells without giving information about their function and reactivity. However, these results showed platelets concentrated to smaller areas within the thrombi, creating more compact aggregates, which might indicate their hyperreactive state in the associated comorbidities.

Smoking is a recognized risk factor in ischemic cardiovascular diseases, but a recent study showed that in ST-elevation myocardial infarction, the platelet content of thrombi was not altered by smoking (358). In the current study we observed that in all main groups, the size of which allowed for statistical evaluation, the thrombus occupancy by platelets was more than two-fold lower in active smokers compared to non-smokers, median sPlt 3.6% vs. 1.6% in CAD and 3.2% vs. 1.6% in PAD (there were only 2 documented non-smokers in the AIS group, thus no statistical evaluation could be done). This surprising finding could be attributed to a phenomenon observed in studies designed to evaluate platelet responsiveness to clopidogrel. Whole blood aggregation-based assays indicated improved drug-response in smokers compared to non-smokers (’smokers' paradox’). However, a careful analysis of the laboratory data revealed that this apparent improvement in the inhibition of platelet reactivity in whole blood aggregation is related to an off-drug effect of hematocrit (359, 360). Smokers are known to have higher hemoglobin levels (361) and in our study, a similar difference was observed with blood hemoglobin of 138.6 g/l in smokers (n=74) versus 127.3 g/l in non-smokers (n=61, p=0.0124), which could contribute to the observed difference in the platelet content of thrombi. Interestingly, blood platelet content was not associated with sPlt.

5.2.Effects of CypD and CsA on platelet morphology and function

Previous studies on the role of MPTP in platelet activation have suggested CypD as an attractive target to influence thrombus formation (63, 306, 307). However, the findings of these studies are controversial, possibly stemming from the spatiotemporal heterogeneity of platelet subpopulations in growing thrombi (9). In a photochemical injury model, genetic ablation of CypD accelerated thrombosis (63), and this was confirmed with megakaryocyte/platelet-specific CypD-knockout platelets in a mesenteric arterial thrombosis model (306). In contrast, deletion of CypD hampered thrombus formation in a study using $FeCl_3$ injury (307). These controversial results

from studies using global in vivo models, as well as the thrombotic complications of patients treated with CsA, warranted further ex vivo investigation of CypD and CsA effects under specific conditions. Accordingly, with the present study, we addressed the consequences of the genetic deletion of CypD and its acute inhibition by pharmacological agents in terms of distinct platelet functions. We found that CypD-deficiency increased spreading (Fig. 10) and impaired aggregation (Fig. 11) of murine platelets in response to a 'mild' stimulus (ADP); and accelerated the resolution of fibrin-platelet clots formed in the presence of 'mild' and 'strong' stimuli (Fig. 13). The effects of pharmacological inhibition of CypD in human platelets generally followed the same trends, however, important differences will also be discussed (see the summary of our results on Fig. 15.).

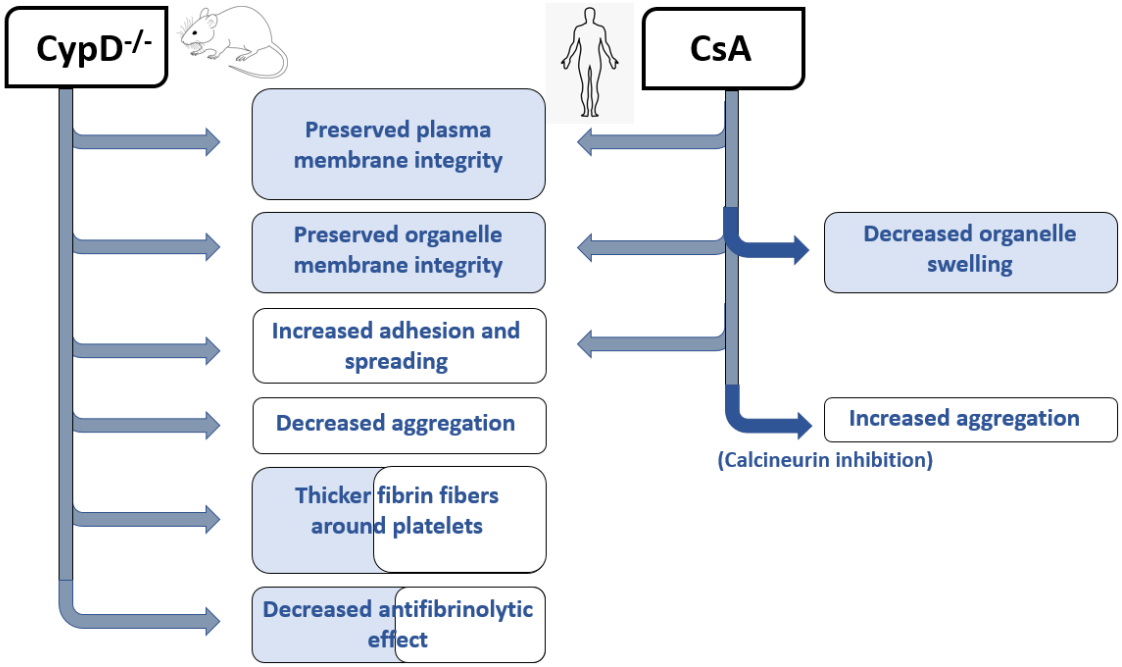

Figure 15. Summary of the effects of CypD genetic deletion or pharmacological inhibition on platelet functions. Light blue background indicates results obtained in the presence of strong activators, while white background indicates 'weak' agonist-induced changes.

MPTP opening is characterized by the loss of ion gradients across the inner mitochondrial membrane, organelle swelling, and eventually, disruption of plasma membrane integrity (328). Platelets activated by 'strong' stimuli that induce MPTP

formation share these characteristics and have been termed ’procoagulant’ or ‘necrotic’ (307). An earlier study (63) showed that membrane integrity of fibrin-adherent murine platelets challenged with ‘strong’ activators could be restored by genetic ablation of CypD. Our SEM studies have expanded this observation using collagen-adherent as well as fibrin-entrapped platelets. Moreover, we report that CsA treatment of human platelets is able to reproduce the ultrastructural effects of CypD deletion under these circumstances.

To detect and quantify another ultrastructural characteristic of MPTP opening (organelle swelling), we utilized TEM. To our knowledge, the aforementioned study (63) has been the only one in this field so far in which TEM investigations were undertaken, however, the authors do not show any micrographs or quantification. According to the evaluation of our TEM images, CsA effectively counteracted ROS effects in terms of organelle swelling in human platelets. Our and others’ (63) failure to detect quantifiable differences in subcellular structures of activated WT and $CypD^{-/-}$ platelets might be explained by chronic metabolic alterations resulting in rupture of membrane-coated vesicles. In our study, only organelles surrounded by membranes were measured, therefore excessively swollen vesicles that lost their membrane integrity were not included in the analysis. Alternatively, the discrepancies between the effects of CypD ablation and CsA effects might underline the importance of CypD-independent CsA effects that protect mitochondrial and cellular integrity (362).

Adhesion and aggregation of platelets are of fundamental importance to prevent blood loss. Platelets are known to adhere to a variety of surfaces (collagen, fibrin, gold (363)) and go through consequential shape changes (flattening known as ‘spreading’). Previous studies have reported increased spreading in the absence of CypD (63, 306). However, these studies were carried out using ‘strong’ stimuli, and the methods used (SEM (63), fluorescent microscopy (306)) do not provide information on adhesion. The impedance-based method enabled us to follow real-time adhesion and spreading dynamics in a single assay, and we found that both aspects of platelet activation were enhanced not only in the absence of CypD but also during its inhibition by CsA in the presence of the ‘mild’ activator ADP. An apparent limitation of this experimental setup is the lack of physiological coating on electrodes. However, it is important to note that (i) for the purposes of our investigation, the isolated assessment of ‘mild’ stimulus (ADP) effects

necessitated the absence of proteins that might interfere with platelet activation (e.g. collagen or fibrinogen); (ii) our impedimetric curves reach maximum CI values almost identical to those reported in other studies (320), where the authors used collagen coating [although the stimuli are naturally different, the platelet counts are very similar in the two studies (10^5/μl versus 1.25×10^5/μl)].

Regarding platelet-platelet interactions, CsA has been long shown to increase aggregation in vitro (364-366), in line with our current data. On the other hand, previous data concerning the effects of CypD-deletion on 'strong' stimulus-induced aggregation are not consistent. CypD-deletion either had no effect (63) or enhanced aggregation (306), while other authors have proposed that the change in light transmission measured in aggregometry assays in response to thrombin + convulxin reflected a shape change of platelets rather than aggregate formation (367). However, to our knowledge, the current study is the first to test aggregation of $CypD^{-/-}$ platelets in response to ADP, a 'mild' trigger acting independently of MPTP formation. Here we report that ADP-activated platelets of $CypD^{-/-}$ mice exhibited lower aggregation propensity compared to WT platelets. We tested two hypotheses that might account for the disparate aggregation patterns with CsA-inhibition and CypD-deletion in our study. (i) CypD-deletion might impair aggregation through alteration of the metabolic status of platelets. It is known that ablation of CypD causes substantial changes in the levels of numerous mitochondrial enzymes involved in intermediary metabolism (368). Such an altered metabolic status might lead to impaired aggregation since this response is of relatively high metabolic cost among ADP-induced activation events (369). As a crude model of this scenario, we used Bk, an inhibitor of mitochondrial ADP-ATP exchange (370). It is important to note that the Bk-target ANT is a well-recognized modulator of MPTP (371). However, in our aggregation assay, where MPTP formation is absent, the effect of Bk on the initial slope of aggregation could be attributed to alteration of the cellular metabolic status by interference with the mitochondrial ADP-ATP exchange. Nevertheless, Bk treatment of human platelets failed to reproduce the impaired aggregation response of $CypD^{-/-}$ platelets, suggesting a significant role for the long-term metabolic adaptation of $CypD^{-/-}$ platelets in their modified functional response (rather than for the acute impairment of ATP generation). (ii) CypA- and not CypD-mediated effects of CsA might dominate the aggregation response seen with human

platelets. It is known that CsA binds to both intra- and extracellular forms of CypA. However, given that extracellular CypA secreted during platelet activation promotes aggregation and adhesion (372), this pathway is likely to have a negligible effect in our and others' (364-366) experimental systems where CsA-treatment enhanced aggregation and adhesion responses —in line with the thrombotic complications observed in patients undergoing CsA-treatment (373). Therefore, we focused on the effects of CsA on the intracellular form of CypA resulting in inhibition of calcineurin. Despite earlier, variable results with calcineurin-inhibition in platelets (365, 366), recently, deletion of an isoform of the catalytic subunit of calcineurin as well as FK-506-treatment have been shown to increase ADP-triggered aggregation (374). In line with this finding, FK-506 and CsA had similar effects in our aggregation assay. Taken together, these results suggest that the positive effect of CsA in our mild stimulus-induced aggregation studies is primarily not exerted through CypD, rather via binding to CypA and consequent inhibition of calcineurin.

During thrombus formation, platelets play a major role in shaping the characteristics of the fibrin scaffold. This effect is based on various mechanisms: modulation of thrombin concentration through the provision of pro-coagulant phospholipid surface, mechanical retraction caused by platelet contraction, promotion of the catalytic activity of factor XIII (as reviewed by Longstaff & Kolev (169)). Our coagulometric assays clearly showed that the pro-coagulant effect of platelets in the tissue-factor-induced clotting of plasma was not affected by the modulators of platelet function applied in our study (CypD-ablation, CsA-, FK-506- or Bk-treatment). Thus, excluding this mechanism, we restricted our evaluation of platelet effects on fibrin structure to a purified system using isolated platelets and thrombin-induced fibrin formation, in which Ca^{2+}-dependent platelet contraction and factor XIII crosslinking are key determinants of fibrin structure. In clots containing human platelets, both CsA and FK-506 resulted in a decreased fibrin fiber diameter consistent with a role for calcineurin signaling in the CsA effects. However, CypD inhibition was also partially accountable for the effects of CsA in this assay, based on the finding that CsA decreased the fibrin diameter in the presence of WT, but not $CypD^{-/-}$ murine platelets. An interesting unexpected finding also supported the primary role of CypD inhibition in the mechanism of CsA action: despite the thinning effect of CsA, selective calcineurin inhibition with FK-506 resulted in thicker

fibers in the presence of both WT and CypD$^{-/-}$ platelets. These disparate effects of FK-506 in platelets of human and murine origin indicate a species-dependent difference in the role of calcineurin in platelet activation. A plausible source of this difference might be the thrombin-sensitizing effect of protease-activated receptor (PAR) 3 on PAR4 activation in mice, an effect absent in human platelets (375, 376).

The therapeutic modality of thrombolysis relies on the administration of agents (e.g. tPA) that promote digestion of the fibrin network (fibrinolysis) resulting in the disassembly of the clot. Thrombolysis is the first-line treatment in ischemic stroke (377), an option in certain cases of deep vein thrombosis (378), as well as for selected patients with acute myocardial infarction (379). However, this therapeutic approach often fails and/or causes bleeding as a side effect (380), which warrants further studies on the determinants of thrombolytic efficacy. As essential constituents of hemostatic plugs and pathological thrombi, platelets are known to render clots resistant to physiological as well as therapeutic fibrinolysis through a variety of mechanisms. In addition to the structural modifications in fibrin discussed above, these mechanisms include secretion of plasminogen activator inhibitor PAI-1 and α_2-plasmin inhibitor, the release of phospholipids, and myosin (as reviewed by Longstaff & Kolev (169)). A recent work of Morrow et al. found that in platelets stimulated by 'strong' activators PAI-1 secretion increases, a significant amount of which remains functionally active and retained on the platelet surface (179). We report that while the incorporation of WT murine platelets in fibrin clots resulted in a delay in tPA-induced fibrinolysis, the absence of CypD largely abolished this effect, specifically under conditions of oxidative stress. Previously, increased retraction was found in plasma clots containing CypD$^{-/-}$ platelets (63), which suggests lytic resistance. However, our study has identified additional factors that can reverse the anti-fibrinolytic effects of enhanced clot retraction in the absence of CypD. (i) Electron microscopy showed preserved ultrastructural integrity of CypD$^{-/-}$ platelets, implying limited release of anti-fibrinolytic constituents (e.g. phospholipids, myosin, PAI-1). (ii) The presence of CypD$^{-/-}$ platelets resulted in larger fibrin fiber diameters compared to WT platelets with a stronger effect under oxidative stress (compare the diameters in the inhibitor-free clots for the respective WT/CypD$^{-/-}$ pairs in Table 3). Since fiber diameter is an important determinant of tPA-induced lysis (coarse meshwork with thicker fibers being more susceptible) (318), this

finding might also contribute to the observed differences in tPA-induced degradation of clots containing WT and CypD$^{-/-}$ platelets.

In summary, our findings —taken together with other published data— suggest that caution is necessary if therapeutic benefit is sought through modulation of CypD-dependent pathways in platelets. Firstly, the outcome of CypD targeting is dependent on the stimulus of platelet activation (e.g. different effects of CypD ablation with 'strong' vs. 'mild' stimulus-induced aggregation). Secondly, the net impact of CypD inhibition on thrombosis is difficult to predict as it is likely to be a result of opposing (pro-thrombotic and pro-fibrinolytic) effects (e.g. increased adhesion of platelets versus decreased fibrinolytic resistance of clots in the absence of CypD). Finally, CsA-treatment of human platelets does not fully reproduce the effects of CypD deletion. In view of the thrombotic complications associated with CsA therapy, these conclusions warrant further in vitro and in vivo research with selective inhibitors of CypD to detect which of the mechanisms identified in different studies can be translated into actual clinical benefit.

5.3. Structural properties of venous thrombi formed in human pancreatic tumor-bearing mice

Cancer patients have a 4- to 7-fold increased risk of venous thromboembolism (VTE) compared with the general population (4). However, the rates of VTE vary in different cancer types. For instance, breast cancer has a low rate, whereas pancreatic cancer has a high rate of VTE (381). This variability suggests that there may be cancer type-specific mechanisms of VTE (337). For instance, Mackman's group found an association between levels of circulating extracellular vesicle tissue factor activity and VTE in pancreatic cancer in two studies and a borderline significance in a third study (382-384). Circulating tumor-derived, tissue factor-positive extracellular vesicles are also observed in mice bearing human pancreatic tumors (385-388). Importantly, these tumor-derived, human tissue factor-positive extracellular vesicles enhance venous thrombosis in mice (385). In the present study, thrombi from tumor-bearing mice had a denser fibrin network with thinner fibrin fibers compared with thrombi from control mice. We know from in vitro experiments that such thrombi are produced by higher thrombin concentrations (389). In our model of cancer-associated thrombosis, it is likely that

tumor-derived, tissue factor-positive extracellular vesicles cause the increase in thrombin concentration and lead to the alteration of fibrin structure.

We observed decreased red blood cell content in thrombi from tumor-bearing mice compared with controls. This is consistent with the recent study of Mackman's group that showed a decrease in red blood cell-rich areas in thrombi from tumor-bearing mice compared with controls (385). This finding could be attributed to a tumor-related shift in the balance of neutrophil and red blood cells in favour of the neutrophils both in circulation (384) and locally in thrombi ([3]): the increased levels of inflammatory cells supercede the red blood cells.

DOI:10.14753/SE.2022.2630

6. CONCLUSIONS

Our most important *conclusions* are the following:

1. The relative platelet content of arterial thrombi is the highest in acute ischemic stroke (compared to peripheral artery disease and coronary artery disease).
2. The presence of certain comorbidities (atherosclerosis, malignant neoplasms, diabetes) or smoking results in more compact platelet aggregates in thrombi possibly caused by increased platelet reactivity.
3. CsA-treatment of human platelets increases the adhesion and aggregation induced by the ’mild’ agonist, ADP.
4. The loss of CypD in murine platelets boosts ADP-induced adhesion but not aggregation.
5. The discrepancies between the effects of CsA-inhibition and CypD-deletion on aggregation suggest a role for long-term metabolic adaptation of $CypD^{-/-}$ platelets. Additionally, the aggregation promoting effects of CsA are exerted via calcineurin inhibition.
6. Lack of CypD function helps preserve the subcellular integration of platelets in a fibrin environment and increases the thickness of the fibers.
7. The stabilizing role of platelets against enzymatic degradation of the fibrin network is lost without CypD function.
8. In human pancreatic tumor-bearing mice, the relative RBC content of venous thrombi is decreased, and thinner fibrin fibers are formed.

Implications

1. Atherosclerosis, smoking, diabetes mellitus and malignant neoplasms are modulators of the platelet content of arterial thrombi.
2. Targeting CypD-dependent pathways in platelets to prevent thrombotic events may lead to unpredictable outcomes as the net results depend on both the stimulus of platelet activation (’mild’ or ’strong’) and on the balance of the pro-thrombotic and pro-fibrinolytic effects.

3. Human pancreatic tumor cells affect the fibrin structure and RBC content of venous thrombi formed in mice.

DOI:10.14753/SE.2022.2630

7. SUMMARY

The recent advances in thrombectomy have given a new opportunity to study the contribution of platelets to arterial thrombus structure. Assessing the composition of arterial thrombi removed during interventional treatment from coronary (CAD), peripheral artery disease (PAD) and acute ischemic stroke (AIS) patients, we identified modulators of platelet content; diabetes mellitus, atherosclerosis (in AIS), smoking (in CAD and PAD) and malignancy (in AIS). In the thrombi of patients with these comorbidities platelets assembled in more compact conglomerates.

Different platelet populations form as a response to heterogeneous stimuli. 'Strong' activators (e.g. thrombin+collagen or reactive oxygen species) lead to the opening of the mitochondrial permeability transition pore (MPTP) and results in a procoagulant platelet phenotype. When 'mild' activators (such as ADP) are present, a discoid platelet population forms without MPTP opening. Cyclophilin D (CypD) is a sensitizer of the MPTP. We investigated the effects of CypD inhibition on platelet functions in the presence of 'mild' agonist, ADP using CypD-deficient murine, and CsA-treated human platelets.

Our results showed that platelets without functional CypD respond to ADP signal with increased adhesion and spreading, as well as an impaired anti-fibrinolytic effect in both species. The change in ADP-induced aggregation showed a different trend in the two groups (decreased in $CypD^{-/-}$ and increased in CsA-inhibited platelets), and our results with the selective calcineurin inhibitor FK506 highlighted the importance of CypD-independent pathways regulated by CsA. We found that fibrin fibers formed in the presence of CypD-deficient murine or CsA-treated human platelets are thinner, while the inhibition of calcineurin has a species-specific impact on their structure.

Lastly, we examined venous thrombi formed in human pancreatic cancer-bearing mice and found decreased erythrocyte content and thinner fibrin fibers compared to the control group.

In summary, we identified modulators of platelet content in arterial thrombi and altered venous thrombus composition in the presence of pancreatic cancer. We found that CypD affects platelet activation initiated by 'mild' stimulus and the platelet-dependent regulation of fibrinolysis. In view of the pro-thrombotic and pro-fibrinolytic effects of CypD inhibition, we suggest a cautious approach by the therapeutic targeting of CypD.

DOI:10.14753/SE.2022.2630

8. ÖSSZEFOGLALÁS

A trombektómiás technikák fejlődésével vizsgálhatóvá vált a vérlemezkék hozzájárulása artériás trombusok szerkezetéhez. Elemezve intervenciós terápia során koszorúér betegségben (CAD), perifériás artériás betegségben (PAD), illetve ischaemiás stroke-ban (AIS) szenvedő betegek artériáiból eltávolított trombusok szerkezetét, a következő, vérlemezketartalmat meghatározó modulátorokat azonosítottuk: diabetes mellitus, érelmeszesedés (AIS betegekben), dohányzás (CAD és PAD betegekben) és malignus tumorok (AIS betegekben) jelenlétében a vizsgált trombusokban a vérlemezkék kompaktabb konglomerátumokba tömörültek, mint ezek hiányában.

Heterogén stimulusra adott válaszként különböző vérlemezke-populációk keletkeznek. „Erős" aktivátorok (pl. trombin és kollagén, illetve reaktív oxigéngyökök) mitokondriális permeabilitási tranzíciós pórus (MPTP) megnyílását idézik elő, ami prokoaguláns vérlemezke-fenotípust eredményez. „Gyenge" aktivátorok (pl. ADP) jelenlétében azonban diszkoid vérlemezkék keletkeznek MPTP-nyitás nélkül. A Cyclophilin D (CypD) fehérje érzékenyítő hatású az MPTP-re. Munkám második részében a CypD-gátlás vérlemezke funkciókra kifejtett hatását vizsgáltam ADP jelenlétében CypD-génhiányos egér-, illetve CsA-kezelt humán vérlemezkékben.

CypD hiányában ADP-stimulusra mindkét fajban fokozott vérlemezke-adhéziót és szétterülést, valamint csökkent antifibrinolítikus hatást találtunk. Az aggregáció eltérő tendenciát mutatott a két csoportban (csökkent $CypD^{-/-}$ és nőtt CsA-gátolt vérlemezkékben). A szelektív kalcineuringátló FK506-tal végzett kísérleteink rámutattak a CsA által regulált, CypD-független útvonalak aggregációban betöltött szerepére. $CypD^{-/-}$, illetve CsA-kezelt vérlemezkék jelenlétében vékonyabb fibrinszálak jöttek létre, míg a kalcineurin gátlása fajfüggő módon befolyásolta a fibrin szerkezetét.

Végül, humán tumorsejteket hordozó egerekben képződött vénás trombusok elemzése során csökkent vörösvértesttartalmat és vékonyabb fibrinszálakat találtunk.

Összefoglalva, munkánk során az artériás trombusok vérlemezketartalmát befolyásoló modulátorokat azonosítottunk, és megváltozott vénás trombusszerkezetet találtunk tumor jelenlétében. Igazoltuk a CypD szerepét „gyenge" agonista-indukálta vérlemezke-aktivációban, valamint a fibrinolízis vérlemezkefüggő szabályozásában. Figyelembevéve a CypD-gátlás protrombotikus és profibrinolítikus hatásait, óvatos megközelítést javaslunk a CypD-t célzó terápiás beavatkozások során.

9. BIBLIOGRAPHY

1 World Health Organization - The top 10 causes of death. Available at: https://www.who.int/news-room/fact-sheets/detail/the-top-10-causes-of-death Accessed 2021 Apr 13.

2 Song P, Rudan D, Zhu Y, Fowkes FJI, Rahimi K, Fowkes FGR and Rudan I. (2019) Global, regional, and national prevalence and risk factors for peripheral artery disease in 2015: an updated systematic review and analysis. Lancet Glob Health, 7: e1020-e1030.

3 Cohen AT, Agnelli G, Anderson FA, Arcelus JI, Bergqvist D, Brecht JG, Greer IA, Heit JA, Hutchinson JL, Kakkar AK, Mottier D, Oger E, Samama MM, Spannagl M and Europe VTEIAGi. (2007) Venous thromboembolism (VTE) in Europe. The number of VTE events and associated morbidity and mortality. Thromb Haemost, 98: 756-64.

4 Timp JF, Braekkan SK, Versteeg HH and Cannegieter SC. (2013) Epidemiology of cancer-associated venous thrombosis. Blood, 122: 1712-23.

5 Machlus KR and Italiano JE, Jr. (2013) The incredible journey: From megakaryocyte development to platelet formation. J Cell Biol, 201: 785-96.

6 Grozovsky R, Giannini S, Falet H and Hoffmeister KM. (2015) Regulating billions of blood platelets: glycans and beyond. Blood, 126: 1877-84.

7 Kaser A, Brandacher G, Steurer W, Kaser S, Offner FA, Zoller H, Theurl I, Widder W, Molnar C, Ludwiczek O, Atkins MB, Mier JW and Tilg H. (2001) Interleukin-6 stimulates thrombopoiesis through thrombopoietin: role in inflammatory thrombocytosis. Blood, 98: 2720-5.

8 Kroll MH and Schafer AI. (1989) Biochemical mechanisms of platelet activation. Blood, 74: 1181-95.

9 Ivanciu L and Stalker TJ. (2015) Spatiotemporal regulation of coagulation and platelet activation during the hemostatic response in vivo. J Thromb Haemost, 13: 1949-59.

10 Kaplan JE and Saba TM. (1978) Platelet removal from the circulation by the liver and spleen. Am J Physiol, 235: H314-20.

11 Isermann B and Nawroth PP. (2007) [Relevance of platelets in placental development and function]. Hamostaseologie, 27: 263-7.

12 Wagner DD and Burger PC. (2003) Platelets in inflammation and thrombosis. Arterioscler Thromb Vasc Biol, 23: 2131-7.

13 Nash GF, Turner LF, Scully MF and Kakkar AK. (2002) Platelets and cancer. Lancet Oncol, 3: 425-30.

14 Gay LJ and Felding-Habermann B. (2011) Contribution of platelets to tumour metastasis. Nat Rev Cancer, 11: 123-34.

15 Hangge P, Stone J, Albadawi H, Zhang YS, Khademhosseini A and Oklu R. (2017) Hemostasis and nanotechnology. Cardiovasc Diagn Ther, 7: S267-S275.

16 Kiefer TL and Becker RC. (2009) Inhibitors of platelet adhesion. Circulation, 120: 2488-95.

17 Houdijk WP, de Groot PG, Nievelstein PF, Sakariassen KS and Sixma JJ. (1986) Subendothelial proteins and platelet adhesion. von Willebrand factor and fibronectin, not thrombospondin, are involved in platelet adhesion to extracellular matrix of human vascular endothelial cells. Arteriosclerosis, 6: 24-33.

18 Hindriks G, Ijsseldijk MJ, Sonnenberg A, Sixma JJ and de Groot PG. (1992) Platelet adhesion to laminin: role of Ca2+ and Mg2+ ions, shear rate, and platelet membrane glycoproteins. Blood, 79: 928-35.

19 Bornstein P. (2001) Thrombospondins as matricellular modulators of cell function. J Clin Invest, 107: 929-34.

20 Ruggeri ZM and Mendolicchio GL. (2007) Adhesion mechanisms in platelet function. Circ Res, 100: 1673-85.

21 Savage B, Saldivar E and Ruggeri ZM. (1996) Initiation of platelet adhesion by arrest onto fibrinogen or translocation on von Willebrand factor. Cell, 84: 289-97.

22 De Meyer SF, Deckmyn H and Vanhoorelbeke K. (2009) von Willebrand factor to the rescue. Blood, 113: 5049-57.

23 Lankhof H, van Hoeij M, Schiphorst ME, Bracke M, Wu YP, Ijsseldijk MJ, Vink T, de Groot PG and Sixma JJ. (1996) A3 domain is essential for interaction of von Willebrand factor with collagen type III. Thromb Haemost, 75: 950-8.

24 Hoylaerts MF, Yamamoto H, Nuyts K, Vreys I, Deckmyn H and Vermylen J. (1997) von Willebrand factor binds to native collagen VI primarily via its A1 domain. Biochem J, 324 (Pt 1): 185-91.

25 Schneider SW, Nuschele S, Wixforth A, Gorzelanny C, Alexander-Katz A, Netz RR and Schneider MF. (2007) Shear-induced unfolding triggers adhesion of von Willebrand factor fibers. Proc Natl Acad Sci U S A, 104: 7899-903.

26 Yuan Y, Kulkarni S, Ulsemer P, Cranmer SL, Yap CL, Nesbitt WS, Harper I, Mistry N, Dopheide SM, Hughan SC, Williamson D, de la Salle C, Salem HH, Lanza F and Jackson SP. (1999) The von Willebrand factor-glycoprotein Ib/V/IX interaction induces actin polymerization and cytoskeletal reorganization in rolling platelets and glycoprotein Ib/V/IX-transfected cells. J Biol Chem, 274: 36241-51.

27 Hartwig JH. (1992) Mechanisms of actin rearrangements mediating platelet activation. J Cell Biol, 118: 1421-42.

28 Farndale RW, Siljander PR, Onley DJ, Sundaresan P, Knight CG and Barnes MJ. (2003) Collagen-platelet interactions: recognition and signalling. Biochem Soc Symp, 81-94.

29 Lockyer S, Okuyama K, Begum S, Le S, Sun B, Watanabe T, Matsumoto Y, Yoshitake M, Kambayashi J and Tandon NN. (2006) GPVI-deficient mice lack collagen responses and are protected against experimentally induced pulmonary thromboembolism. Thromb Res, 118: 371-80.

30 Nieswandt B, Brakebusch C, Bergmeier W, Schulte V, Bouvard D, Mokhtari-Nejad R, Lindhout T, Heemskerk JW, Zirngibl H and Fassler R. (2001) Glycoprotein VI but not alpha2beta1 integrin is essential for platelet interaction with collagen. EMBO J, 20: 2120-30.

31 Chen H and Kahn ML. (2003) Reciprocal signaling by integrin and nonintegrin receptors during collagen activation of platelets. Mol Cell Biol, 23: 4764-77.

32 Atkinson BT, Jarvis GE and Watson SP. (2003) Activation of GPVI by collagen is regulated by alpha2beta1 and secondary mediators. J Thromb Haemost, 1: 1278-87.

33 Jung SM and Moroi M. (2000) Signal-transducing mechanisms involved in activation of the platelet collagen receptor integrin alpha(2)beta(1). J Biol Chem, 275: 8016-26.

34 Lecut C, Schoolmeester A, Kuijpers MJ, Broers JL, van Zandvoort MA, Vanhoorelbeke K, Deckmyn H, Jandrot-Perrus M and Heemskerk JW. (2004) Principal role of glycoprotein VI in alpha2beta1 and alphaIIbbeta3 activation during collagen-induced thrombus formation. Arterioscler Thromb Vasc Biol, 24: 1727-33.

35 Monroe DM and Hoffman M. (2006) What does it take to make the perfect clot? Arterioscler Thromb Vasc Biol, 26: 41-8.

36 Nolte C, Eigenthaler M, Schanzenbacher P and Walter U. (1991) Endothelial cell-dependent phosphorylation of a platelet protein mediated by cAMP- and cGMP-elevating factors. J Biol Chem, 266: 14808-12.

37 Canobbio I, Balduini C and Torti M. (2004) Signalling through the platelet glycoprotein Ib-V-IX complex. Cell Signal, 16: 1329-44.

38 Li Z, Zhang G, Liu J, Stojanovic A, Ruan C, Lowell CA and Du X. (2010) An important role of the SRC family kinase Lyn in stimulating platelet granule secretion. J Biol Chem, 285: 12559-70.

39 Lian L, Wang Y, Draznin J, Eslin D, Bennett JS, Poncz M, Wu D and Abrams CS. (2005) The relative role of PLCbeta and PI3Kgamma in platelet activation. Blood, 106: 110-7.

40 Li Z, Zhang G, Feil R, Han J and Du X. (2006) Sequential activation of p38 and ERK pathways by cGMP-dependent protein kinase leading to activation of the platelet integrin alphaIIb beta3. Blood, 107: 965-72.

41 Estevez B, Stojanovic-Terpo A, Delaney MK, O'Brien KA, Berndt MC, Ruan C and Du X. (2013) LIM kinase-1 selectively promotes glycoprotein Ib-IX-mediated TXA2 synthesis, platelet activation, and thrombosis. Blood, 121: 4586-94.

42 Li Z, Xi X, Gu M, Feil R, Ye RD, Eigenthaler M, Hofmann F and Du X. (2003) A stimulatory role for cGMP-dependent protein kinase in platelet activation. Cell, 112: 77-86.

43 Ezumi Y, Shindoh K, Tsuji M and Takayama H. (1998) Physical and functional association of the Src family kinases Fyn and Lyn with the collagen receptor glycoprotein VI-Fc receptor gamma chain complex on human platelets. J Exp Med, 188: 267-76.

44 Quek LS, Pasquet JM, Hers I, Cornall R, Knight G, Barnes M, Hibbs ML, Dunn AR, Lowell CA and Watson SP. (2000) Fyn and Lyn phosphorylate the Fc receptor gamma chain downstream of glycoprotein VI in murine platelets, and Lyn regulates a novel feedback pathway. Blood, 96: 4246-53.

45 Watson SP, Auger JM, McCarty OJ and Pearce AC. (2005) GPVI and integrin alphaIIb beta3 signaling in platelets. J Thromb Haemost, 3: 1752-62.

46 Watson SP, Herbert JM and Pollitt AY. (2010) GPVI and CLEC-2 in hemostasis and vascular integrity. J Thromb Haemost, 8: 1456-67.

47 Daniel JL, Dangelmaier C and Smith JB. (1994) Evidence for a role for tyrosine phosphorylation of phospholipase C gamma 2 in collagen-induced platelet cytosolic calcium mobilization. Biochem J, 302 (Pt 2): 617-22.

48 Inoue O, Suzuki-Inoue K, Dean WL, Frampton J and Watson SP. (2003) Integrin alpha2beta1 mediates outside-in regulation of platelet spreading on collagen through activation of Src kinases and PLCgamma2. J Cell Biol, 160: 769-80.

49 Bhagwat SS, Hamann PR, Still WC, Bunting S and Fitzpatrick FA. (1985) Synthesis and structure of the platelet aggregation factor thromboxane A2. Nature, 315: 511-3.

50 FitzGerald GA. (1991) Mechanisms of platelet activation: thromboxane A2 as an amplifying signal for other agonists. Am J Cardiol, 68: 11B-15B.

51 Offermanns S. (2006) Activation of platelet function through G protein-coupled receptors. Circ Res, 99: 1293-304.

52 Oldham WM and Hamm HE. (2008) Heterotrimeric G protein activation by G-protein-coupled receptors. Nat Rev Mol Cell Biol, 9: 60-71.

53 Cho MJ, Liu J, Pestina TI, Steward SA, Thomas DW, Coffman TM, Wang D, Jackson CW and Gartner TK. (2003) The roles of alpha IIb beta 3-mediated outside-in signal transduction, thromboxane A2, and adenosine diphosphate in collagen-induced platelet aggregation. Blood, 101: 2646-51.

54 Moers A, Wettschureck N, Gruner S, Nieswandt B and Offermanns S. (2004) Unresponsiveness of platelets lacking both Galpha(q) and Galpha(13). Implications for collagen-induced platelet activation. J Biol Chem, 279: 45354-9.

55 Kahn ML, Nakanishi-Matsui M, Shapiro MJ, Ishihara H and Coughlin SR. (1999) Protease-activated receptors 1 and 4 mediate activation of human platelets by thrombin. J Clin Invest, 103: 879-87.

56 Ossovskaya VS and Bunnett NW. (2004) Protease-activated receptors: contribution to physiology and disease. Physiol Rev, 84: 579-621.

57 Vu TK, Hung DT, Wheaton VI and Coughlin SR. (1991) Molecular cloning of a functional thrombin receptor reveals a novel proteolytic mechanism of receptor activation. Cell, 64: 1057-68.

58 Hung DT, Wong YH, Vu TK and Coughlin SR. (1992) The cloned platelet thrombin receptor couples to at least two distinct effectors to stimulate phosphoinositide hydrolysis and inhibit adenylyl cyclase. J Biol Chem, 267: 20831-4.

59 Estevez B, Kim K, Delaney MK, Stojanovic-Terpo A, Shen B, Ruan C, Cho J, Ruggeri ZM and Du X. (2016) Signaling-mediated cooperativity between glycoprotein Ib-IX and protease-activated receptors in thrombin-induced platelet activation. Blood, 127: 626-36.

60 Davlouros P, Xanthopoulou I, Mparampoutis N, Giannopoulos G, Deftereos S and Alexopoulos D. (2016) Role of Calcium in Platelet Activation: Novel Insights and Pharmacological Implications. Med Chem, 12: 131-8.

61 Mammadova-Bach E, Nagy M, Heemskerk JWM, Nieswandt B and Braun A. (2019) Store-operated calcium entry in thrombosis and thrombo-inflammation. Cell Calcium, 77: 39-48.

62 Harper MT, Londono JE, Quick K, Londono JC, Flockerzi V, Philipp SE, Birnbaumer L, Freichel M and Poole AW. (2013) Transient receptor potential channels function as a coincidence signal detector mediating phosphatidylserine exposure. Sci Signal, 6: ra50.

63 Jobe SM, Wilson KM, Leo L, Raimondi A, Molkentin JD, Lentz SR and Di Paola J. (2008) Critical role for the mitochondrial permeability transition pore and cyclophilin D in platelet activation and thrombosis. Blood, 111: 1257-65.

64 Abbasian N, Millington-Burgess SL, Chabra S, Malcor JD and Harper MT. (2020) Supramaximal calcium signaling triggers procoagulant platelet formation. Blood Adv, 4: 154-164.

65 Heemskerk JW, Vis P, Feijge MA, Hoyland J, Mason WT and Sage SO. (1993) Roles of phospholipase C and Ca(2+)-ATPase in calcium responses of single, fibrinogen-bound platelets. J Biol Chem, 268: 356-63.

66 Heemskerk JW, Siljander P, Vuist WM, Breikers G, Reutelingsperger CP, Barnes MJ, Knight CG, Lassila R and Farndale RW. (1999) Function of glycoprotein VI and integrin alpha2beta1 in the procoagulant response of single, collagen-adherent platelets. Thromb Haemost, 81: 782-92.

67 Broos K, Feys HB, De Meyer SF, Vanhoorelbeke K and Deckmyn H. (2011) Platelets at work in primary hemostasis. Blood Rev, 25: 155-67.

68 Hartwig JH, Barkalow K, Azim A and Italiano J. (1999) The elegant platelet: signals controlling actin assembly. Thromb Haemost, 82: 392-8.

69 Steiner M and Ikeda Y. (1979) Quantitative assessment of polymerized and depolymerized platelet microtubules. Changes caused by aggregating agents. J Clin Invest, 63: 443-8.

70 Mattila PK and Lappalainen P. (2008) Filopodia: molecular architecture and cellular functions. Nat Rev Mol Cell Biol, 9: 446-54.

71 Calaminus SD, Auger JM, McCarty OJ, Wakelam MJ, Machesky LM and Watson SP. (2007) MyosinIIa contractility is required for maintenance of platelet structure during spreading on collagen and contributes to thrombus stability. J Thromb Haemost, 5: 2136-45.

72 Lee D, Fong KP, King MR, Brass LF and Hammer DA. (2012) Differential dynamics of platelet contact and spreading. Biophys J, 102: 472-82.

73 Schwarz Henriques S, Sandmann R, Strate A and Koster S. (2012) Force field evolution during human blood platelet activation. J Cell Sci, 125: 3914-20.

74 Lam WA, Chaudhuri O, Crow A, Webster KD, Li TD, Kita A, Huang J and Fletcher DA. (2011) Mechanics and contraction dynamics of single platelets and implications for clot stiffening. Nat Mater, 10: 61-6.

75 Vinogradova O, Velyvis A, Velyviene A, Hu B, Haas T, Plow E and Qin J. (2002) A structural mechanism of integrin alpha(IIb)beta(3) "inside-out" activation as regulated by its cytoplasmic face. Cell, 110: 587-97.

76 Crittenden JR, Bergmeier W, Zhang Y, Piffath CL, Liang Y, Wagner DD, Housman DE and Graybiel AM. (2004) CalDAG-GEFI integrates signaling for platelet aggregation and thrombus formation. Nat Med, 10: 982-6.

77 Han J, Lim CJ, Watanabe N, Soriani A, Ratnikov B, Calderwood DA, Puzon-McLaughlin W, Lafuente EM, Boussiotis VA, Shattil SJ and Ginsberg MH. (2006) Reconstructing and deconstructing agonist-induced activation of integrin alphaIIbbeta3. Curr Biol, 16: 1796-806.

78 Banno A and Ginsberg MH. (2008) Integrin activation. Biochem Soc Trans, 36: 229-34.

79 Anthis NJ, Wegener KL, Ye F, Kim C, Goult BT, Lowe ED, Vakonakis I, Bate N, Critchley DR, Ginsberg MH and Campbell ID. (2009) The structure of an

integrin/talin complex reveals the basis of inside-out signal transduction. EMBO J, 28: 3623-32.

80 Shattil SJ, Kim C and Ginsberg MH. (2010) The final steps of integrin activation: the end game. Nat Rev Mol Cell Biol, 11: 288-300.

81 Hanby HA, Bao J, Noh JY, Jarocha D, Poncz M, Weiss MJ and Marks MS. (2017) Platelet dense granules begin to selectively accumulate mepacrine during proplatelet formation. Blood Adv, 1: 1478-1490.

82 King SM and Reed GL. (2002) Development of platelet secretory granules. Semin Cell Dev Biol, 13: 293-302.

83 Italiano JE, Jr., Richardson JL, Patel-Hett S, Battinelli E, Zaslavsky A, Short S, Ryeom S, Folkman J and Klement GL. (2008) Angiogenesis is regulated by a novel mechanism: pro- and antiangiogenic proteins are organized into separate platelet alpha granules and differentially released. Blood, 111: 1227-33.

84 Eckly A, Rinckel JY, Proamer F, Ulas N, Joshi S, Whiteheart SW and Gachet C. (2016) Respective contributions of single and compound granule fusion to secretion by activated platelets. Blood, 128: 2538-2549.

85 White JG. (1998) Use of the electron microscope for diagnosis of platelet disorders. Semin Thromb Hemost, 24: 163-8.

86 Maynard DM, Heijnen HF, Gahl WA and Gunay-Aygun M. (2010) The alpha-granule proteome: novel proteins in normal and ghost granules in gray platelet syndrome. J Thromb Haemost, 8: 1786-96.

87 Maynard DM, Heijnen HF, Horne MK, White JG and Gahl WA. (2007) Proteomic analysis of platelet alpha-granules using mass spectrometry. J Thromb Haemost, 5: 1945-55.

88 Gralnick HR, Williams SB, McKeown LP, Krizek DM, Shafer BC and Rick ME. (1985) Platelet von Willebrand factor: comparison with plasma von Willebrand factor. Thromb Res, 38: 623-33.

89 Kuijpers MJ, de Witt S, Nergiz-Unal R, van Kruchten R, Korporaal SJ, Verhamme P, Febbraio M, Tjwa M, Voshol PJ, Hoylaerts MF, Cosemans JM and Heemskerk JW. (2014) Supporting roles of platelet thrombospondin-1 and CD36 in thrombus formation on collagen. Arterioscler Thromb Vasc Biol, 34: 1187-92.

90 Rendu F and Brohard-Bohn B. (2001) The platelet release reaction: granules' constituents, secretion and functions. Platelets, 12: 261-73.

91 Ambrosio AL and Di Pietro SM. (2017) Storage pool diseases illuminate platelet dense granule biogenesis. Platelets, 28: 138-146.

92 Kahner BN, Shankar H, Murugappan S, Prasad GL and Kunapuli SP. (2006) Nucleotide receptor signaling in platelets. J Thromb Haemost, 4: 2317-26.

93 Jin J, Quinton TM, Zhang J, Rittenhouse SE and Kunapuli SP. (2002) Adenosine diphosphate (ADP)-induced thromboxane A(2) generation in human platelets requires coordinated signaling through integrin alpha(IIb)beta(3) and ADP receptors. Blood, 99: 193-8.

94 Nakahata N. (2008) Thromboxane A2: physiology/pathophysiology, cellular signal transduction and pharmacology. Pharmacol Ther, 118: 18-35.

95 Hu H and Hoylaerts MF. (2010) The P2X1 ion channel in platelet function. Platelets, 21: 153-66.

96 De Clerck F, Xhonneux B, Leysen J and Janssen PA. (1984) Evidence for functional 5-HT2 receptor sites on human blood platelets. Biochem Pharmacol, 33: 2807-11.

97 Smith SA, Choi SH, Davis-Harrison R, Huyck J, Boettcher J, Rienstra CM and Morrissey JH. (2010) Polyphosphate exerts differential effects on blood clotting, depending on polymer size. Blood, 116: 4353-9.

98 Ruiz FA, Lea CR, Oldfield E and Docampo R. (2004) Human platelet dense granules contain polyphosphate and are similar to acidocalcisomes of bacteria and unicellular eukaryotes. J Biol Chem, 279: 44250-7.

99 Verhoef JJ, Barendrecht AD, Nickel KF, Dijkxhoorn K, Kenne E, Labberton L, McCarty OJ, Schiffelers R, Heijnen HF, Hendrickx AP, Schellekens H, Fens MH, de Maat S, Renne T and Maas C. (2017) Polyphosphate nanoparticles on the platelet surface trigger contact system activation. Blood, 129: 1707-1717.

100 Smith SA, Mutch NJ, Baskar D, Rohloff P, Docampo R and Morrissey JH. (2006) Polyphosphate modulates blood coagulation and fibrinolysis. Proc Natl Acad Sci U S A, 103: 903-8.

101 Choi SH, Smith SA and Morrissey JH. (2011) Polyphosphate is a cofactor for the activation of factor XI by thrombin. Blood, 118: 6963-70.

102 Caen J and Wu Q. (2010) Hageman factor, platelets and polyphosphates: early history and recent connection. J Thromb Haemost, 8: 1670-4.

103 Day HJ, Holmsen H and Hovig T. (1969) Subcellular particles of human platelets. A biochemical and electron microscopic study with particular reference to the influence of fractionation techniques. Scand J Haematol Suppl, 7: 3-35.

104 Ciferri S, Emiliani C, Guglielmini G, Orlacchio A, Nenci GG and Gresele P. (2000) Platelets release their lysosomal content in vivo in humans upon activation. Thromb Haemost, 83: 157-64.

105 Williamson P, Bevers EM, Smeets EF, Comfurius P, Schlegel RA and Zwaal RF. (1995) Continuous analysis of the mechanism of activated transbilayer lipid movement in platelets. Biochemistry, 34: 10448-55.

106 Fujii T, Sakata A, Nishimura S, Eto K and Nagata S. (2015) TMEM16F is required for phosphatidylserine exposure and microparticle release in activated mouse platelets. Proc Natl Acad Sci U S A, 112: 12800-5.

107 Wolfs JL, Comfurius P, Rasmussen JT, Keuren JF, Lindhout T, Zwaal RF and Bevers EM. (2005) Activated scramblase and inhibited aminophospholipid translocase cause phosphatidylserine exposure in a distinct platelet fraction. Cell Mol Life Sci, 62: 1514-25.

108 Schoenwaelder SM, Yuan Y, Josefsson EC, White MJ, Yao Y, Mason KD, O'Reilly LA, Henley KJ, Ono A, Hsiao S, Willcox A, Roberts AW, Huang DC, Salem HH, Kile BT and Jackson SP. (2009) Two distinct pathways regulate platelet phosphatidylserine exposure and procoagulant function. Blood, 114: 663-6.

109 Malhotra OP, Nesheim ME and Mann KG. (1985) The kinetics of activation of normal and gamma-carboxyglutamic acid-deficient prothrombins. J Biol Chem, 260: 279-87.

110 Zwaal RF and Schroit AJ. (1997) Pathophysiologic implications of membrane phospholipid asymmetry in blood cells. Blood, 89: 1121-32.

111 Miletich JP, Jackson CM and Majerus PW. (1978) Properties of the factor Xa binding site on human platelets. J Biol Chem, 253: 6908-16.

112 Rawala-Sheikh R, Ahmad SS, Ashby B and Walsh PN. (1990) Kinetics of coagulation factor X activation by platelet-bound factor IXa. Biochemistry, 29: 2606-11.

113 Zwaal RF, Comfurius P and Bevers EM. (1998) Lipid-protein interactions in blood coagulation. Biochim Biophys Acta, 1376: 433-53.

114 van Rijn JL, Govers-Riemslag JW, Zwaal RF and Rosing J. (1984) Kinetic studies of prothrombin activation: effect of factor Va and phospholipids on the formation of the enzyme-substrate complex. Biochemistry, 23: 4557-64.

115 Haynes LM, Bouchard BA, Tracy PB and Mann KG. (2012) Prothrombin activation by platelet-associated prothrombinase proceeds through the prethrombin-2 pathway via a concerted mechanism. J Biol Chem, 287: 38647-55.

116 Lentz BR. (2003) Exposure of platelet membrane phosphatidylserine regulates blood coagulation. Prog Lipid Res, 42: 423-38.

117 Bevers EM and Williamson PL. (2016) Getting to the Outer Leaflet: Physiology of Phosphatidylserine Exposure at the Plasma Membrane. Physiol Rev, 96: 605-45.

118 Heijnen HF, Schiel AE, Fijnheer R, Geuze HJ and Sixma JJ. (1999) Activated platelets release two types of membrane vesicles: microvesicles by surface shedding and exosomes derived from exocytosis of multivesicular bodies and alpha-granules. Blood, 94: 3791-9.

119 Boilard E. (2018) Extracellular vesicles and their content in bioactive lipid mediators: more than a sack of microRNA. J Lipid Res, 59: 2037-2046.

120 Lindemann S, Tolley ND, Dixon DA, McIntyre TM, Prescott SM, Zimmerman GA and Weyrich AS. (2001) Activated platelets mediate inflammatory signaling by regulated interleukin 1beta synthesis. J Cell Biol, 154: 485-90.

121 Boudreau LH, Duchez AC, Cloutier N, Soulet D, Martin N, Bollinger J, Pare A, Rousseau M, Naika GS, Levesque T, Laflamme C, Marcoux G, Lambeau G, Farndale RW, Pouliot M, Hamzeh-Cognasse H, Cognasse F, Garraud O, Nigrovic PA, Guderley H, Lacroix S, Thibault L, Semple JW, Gelb MH and Boilard E. (2014) Platelets release mitochondria serving as substrate for bactericidal group IIA-secreted phospholipase A2 to promote inflammation. Blood, 124: 2173-83.

122 Bei JJ, Liu C, Peng S, Liu CH, Zhao WB, Qu XL, Chen Q, Zhou Z, Yu ZP, Peter K and Hu HY. (2016) Staphylococcal SSL5-induced platelet microparticles provoke proinflammatory responses via the CD40/TRAF6/NFkappaB signalling pathway in monocytes. Thromb Haemost, 115: 632-45.

123 Tang K, Liu J, Yang Z, Zhang B, Zhang H, Huang C, Ma J, Shen GX, Ye D and Huang B. (2010) Microparticles mediate enzyme transfer from platelets to mast cells: a new pathway for lipoxin A4 biosynthesis. Biochem Biophys Res Commun, 400: 432-6.

124 Melki I, Tessandier N, Zufferey A and Boilard E. (2017) Platelet microvesicles in health and disease. Platelets, 28: 214-221.

125 Michael JV, Wurtzel JGT, Mao GF, Rao AK, Kolpakov MA, Sabri A, Hoffman NE, Rajan S, Tomar D, Madesh M, Nieman MT, Yu J, Edelstein LC, Rowley JW, Weyrich AS and Goldfinger LE. (2017) Platelet microparticles infiltrating solid tumors transfer miRNAs that suppress tumor growth. Blood, 130: 567-580.

126 Chargaff E and West R. (1946) The biological significance of the thromboplastic protein of blood. J Biol Chem, 166: 189-97.

127 Zwaal RF, Comfurius P and Bevers EM. (1992) Platelet procoagulant activity and microvesicle formation. Its putative role in hemostasis and thrombosis. Biochim Biophys Acta, 1180: 1-8.

128 Dahlback B, Wiedmer T and Sims PJ. (1992) Binding of anticoagulant vitamin K-dependent protein S to platelet-derived microparticles. Biochemistry, 31: 12769-77.

129 Tans G, Rosing J, Thomassen MC, Heeb MJ, Zwaal RF and Griffin JH. (1991) Comparison of anticoagulant and procoagulant activities of stimulated platelets and platelet-derived microparticles. Blood, 77: 2641-8.

130 Berckmans RJ, Lacroix R, Hau CM, Sturk A and Nieuwland R. (2019) Extracellular vesicles and coagulation in blood from healthy humans revisited. J Extracell Vesicles, 8: 1688936.

131 Milioli M, Ibanez-Vea M, Sidoli S, Palmisano G, Careri M and Larsen MR. (2015) Quantitative proteomics analysis of platelet-derived microparticles reveals distinct protein signatures when stimulated by different physiological agonists. J Proteomics, 121: 56-66.

132 Munnix IC, Cosemans JM, Auger JM and Heemskerk JW. (2009) Platelet response heterogeneity in thrombus formation. Thromb Haemost, 102: 1149-56.

133 Ruggeri ZM. (1997) Mechanisms initiating platelet thrombus formation. Thromb Haemost, 78: 611-6.

134 Brill A, Fuchs TA, Chauhan AK, Yang JJ, De Meyer SF, Kollnberger M, Wakefield TW, Lammle B, Massberg S and Wagner DD. (2011) von Willebrand factor-

mediated platelet adhesion is critical for deep vein thrombosis in mouse models. Blood, 117: 1400-7.

135 Maxwell MJ, Westein E, Nesbitt WS, Giuliano S, Dopheide SM and Jackson SP. (2007) Identification of a 2-stage platelet aggregation process mediating shear-dependent thrombus formation. Blood, 109: 566-76.

136 Dopheide SM, Maxwell MJ and Jackson SP. (2002) Shear-dependent tether formation during platelet translocation on von Willebrand factor. Blood, 99: 159-67.

137 Cosemans JM, Iserbyt BF, Deckmyn H and Heemskerk JW. (2008) Multiple ways to switch platelet integrins on and off. J Thromb Haemost, 6: 1253-61.

138 Mazzucato M, Pradella P, Cozzi MR, De Marco L and Ruggeri ZM. (2002) Sequential cytoplasmic calcium signals in a 2-stage platelet activation process induced by the glycoprotein Ibalpha mechanoreceptor. Blood, 100: 2793-800.

139 Nesbitt WS, Kulkarni S, Giuliano S, Goncalves I, Dopheide SM, Yap CL, Harper IS, Salem HH and Jackson SP. (2002) Distinct glycoprotein Ib/V/IX and integrin alpha IIbbeta 3-dependent calcium signals cooperatively regulate platelet adhesion under flow. J Biol Chem, 277: 2965-72.

140 Ma YQ, Qin J and Plow EF. (2007) Platelet integrin alpha(IIb)beta(3): activation mechanisms. J Thromb Haemost, 5: 1345-52.

141 Ni H, Yuen PS, Papalia JM, Trevithick JE, Sakai T, Fassler R, Hynes RO and Wagner DD. (2003) Plasma fibronectin promotes thrombus growth and stability in injured arterioles. Proc Natl Acad Sci U S A, 100: 2415-9.

142 Ni H, Denis CV, Subbarao S, Degen JL, Sato TN, Hynes RO and Wagner DD. (2000) Persistence of platelet thrombus formation in arterioles of mice lacking both von Willebrand factor and fibrinogen. J Clin Invest, 106: 385-92.

143 Weisel JW and Nagaswami C. (1992) Computer modeling of fibrin polymerization kinetics correlated with electron microscope and turbidity observations: clot structure and assembly are kinetically controlled. Biophys J, 63: 111-28.

144 Ryan EA, Mockros LF, Weisel JW and Lorand L. (1999) Structural origins of fibrin clot rheology. Biophys J, 77: 2813-26.

145 Bagoly Z, Koncz Z, Harsfalvi J and Muszbek L. (2012) Factor XIII, clot structure, thrombosis. Thromb Res, 129: 382-7.

146 Muszbek L, Adany R and Mikkola H. (1996) Novel aspects of blood coagulation factor XIII. I. Structure, distribution, activation, and function. Crit Rev Clin Lab Sci, 33: 357-421.

147 Hethershaw EL, Cilia La Corte AL, Duval C, Ali M, Grant PJ, Ariens RA and Philippou H. (2014) The effect of blood coagulation factor XIII on fibrin clot structure and fibrinolysis. J Thromb Haemost, 12: 197-205.

148 Mutch NJ, Engel R, Uitte de Willige S, Philippou H and Ariens RA. (2010) Polyphosphate modifies the fibrin network and down-regulates fibrinolysis by attenuating binding of tPA and plasminogen to fibrin. Blood, 115: 3980-8.

149 Shattil SJ, Kashiwagi H and Pampori N. (1998) Integrin signaling: the platelet paradigm. Blood, 91: 2645-57.

150 Jenkins AL, Nannizzi-Alaimo L, Silver D, Sellers JR, Ginsberg MH, Law DA and Phillips DR. (1998) Tyrosine phosphorylation of the beta3 cytoplasmic domain mediates integrin-cytoskeletal interactions. J Biol Chem, 273: 13878-85.

151 Law DA, DeGuzman FR, Heiser P, Ministri-Madrid K, Killeen N and Phillips DR. (1999) Integrin cytoplasmic tyrosine motif is required for outside-in alphaIIbbeta3 signalling and platelet function. Nature, 401: 808-11.

152 Phillips DR, Jennings LK and Edwards HH. (1980) Identification of membrane proteins mediating the interaction of human platelets. J Cell Biol, 86: 77-86.

153 Jen CJ and McIntire LV. (1982) The structural properties and contractile force of a clot. Cell Motil, 2: 445-55.

154 Carvalho FA, Connell S, Miltenberger-Miltenyi G, Pereira SV, Tavares A, Ariens RA and Santos NC. (2010) Atomic force microscopy-based molecular recognition of a fibrinogen receptor on human erythrocytes. ACS Nano, 4: 4609-20.

155 Carvalho FA, de Oliveira S, Freitas T, Goncalves S and Santos NC. (2011) Variations on fibrinogen-erythrocyte interactions during cell aging. PLoS One, 6: e18167.

156 Sokolova IA, Muravyov AV, Khokhlova MD, Rikova SY, Lyubin EV, Gafarova MA, Skryabina MN, Fedyanin AA, Kryukova DV and Shahnazarov AA. (2014) An effect of glycoprotein IIb/IIIa inhibitors on the kinetics of red blood cells aggregation. Clin Hemorheol Microcirc, 57: 291-302.

157 Cines DB, Lebedeva T, Nagaswami C, Hayes V, Massefski W, Litvinov RI, Rauova L, Lowery TJ and Weisel JW. (2014) Clot contraction: compression of erythrocytes into tightly packed polyhedra and redistribution of platelets and fibrin. Blood, 123: 1596-603.

158 Muthard RW and Diamond SL. (2012) Blood clots are rapidly assembled hemodynamic sensors: flow arrest triggers intraluminal thrombus contraction. Arterioscler Thromb Vasc Biol, 32: 2938-45.

159 Wautier MP, Heron E, Picot J, Colin Y, Hermine O and Wautier JL. (2011) Red blood cell phosphatidylserine exposure is responsible for increased erythrocyte adhesion to endothelium in central retinal vein occlusion. J Thromb Haemost, 9: 1049-55.

160 Whelihan MF, Zachary V, Orfeo T and Mann KG. (2012) Prothrombin activation in blood coagulation: the erythrocyte contribution to thrombin generation. Blood, 120: 3837-45.

161 Wohner N, Sotonyi P, Machovich R, Szabo L, Tenekedjiev K, Silva MM, Longstaff C and Kolev K. (2011) Lytic resistance of fibrin containing red blood cells. Arterioscler Thromb Vasc Biol, 31: 2306-13.

162 Aleman MM, Walton BL, Byrnes JR and Wolberg AS. (2014) Fibrinogen and red blood cells in venous thrombosis. Thromb Res, 133 Suppl 1: S38-40.

163 Silvain J, Collet JP, Nagaswami C, Beygui F, Edmondson KE, Bellemain-Appaix A, Cayla G, Pena A, Brugier D, Barthelemy O, Montalescot G and Weisel JW. (2011) Composition of coronary thrombus in acute myocardial infarction. J Am Coll Cardiol, 57: 1359-67.

164 Liebeskind DS, Sanossian N, Yong WH, Starkman S, Tsang MP, Moya AL, Zheng DD, Abolian AM, Kim D, Ali LK, Shah SH, Towfighi A, Ovbiagele B, Kidwell CS, Tateshima S, Jahan R, Duckwiler GR, Vinuela F, Salamon N, Villablanca JP, Vinters HV, Marder VJ and Saver JL. (2011) CT and MRI early vessel signs reflect clot composition in acute stroke. Stroke, 42: 1237-43.

165 Saksela O. (1985) Plasminogen activation and regulation of pericellular proteolysis. Biochim Biophys Acta, 823: 35-65.

166 Pennica D, Holmes WE, Kohr WJ, Harkins RN, Vehar GA, Ward CA, Bennett WF, Yelverton E, Seeburg PH, Heyneker HL, Goeddel DV and Collen D. (1983)

Cloning and expression of human tissue-type plasminogen activator cDNA in E. coli. Nature, 301: 214-21.

167 Kasai S, Arimura H, Nishida M and Suyama T. (1985) Primary structure of single-chain pro-urokinase. J Biol Chem, 260: 12382-9.

168 Goldsmith GH, Jr., Saito H and Ratnoff OS. (1978) The activation of plasminogen by Hageman factor (Factor XII) and Hageman factor fragments. J Clin Invest, 62: 54-60.

169 Longstaff C and Kolev K. (2015) Basic mechanisms and regulation of fibrinolysis. J Thromb Haemost, 13 Suppl 1: S98-105.

170 Reed GL, Matsueda GR and Haber E. (1991) Fibrin-fibrin and alpha 2-antiplasmin-fibrin cross-linking by platelet factor XIII increases the resistance of platelet clots to fibrinolysis. Trans Assoc Am Physicians, 104: 21-8.

171 Aoki N. (1993) Clot retraction increases clot resistance to fibrinolysis by condensing alpha 2-plasmin inhibitor crosslinked to fibrin. Thromb Haemost, 70: 376.

172 Kunitada S, FitzGerald GA and Fitzgerald DJ. (1992) Inhibition of clot lysis and decreased binding of tissue-type plasminogen activator as a consequence of clot retraction. Blood, 79: 1420-7.

173 Sabovic M, Lijnen HR, Keber D and Collen D. (1989) Effect of retraction on the lysis of human clots with fibrin specific and non-fibrin specific plasminogen activators. Thromb Haemost, 62: 1083-7.

174 Collet JP, Montalescot G, Lesty C and Weisel JW. (2002) A structural and dynamic investigation of the facilitating effect of glycoprotein IIb/IIIa inhibitors in dissolving platelet-rich clots. Circ Res, 90: 428-34.

175 Booth NA, Simpson AJ, Croll A, Bennett B and MacGregor IR. (1988) Plasminogen activator inhibitor (PAI-1) in plasma and platelets. Br J Haematol, 70: 327-33.

176 Robbie LA, Young SP, Bennett B and Booth NA. (1997) Thrombi formed in a Chandler loop mimic human arterial thrombi in structure and RAI-1 content and distribution. Thromb Haemost, 77: 510-5.

177 Booth NA, Robbie LA, Croll AM and Bennett B. (1992) Lysis of platelet-rich thrombi: the role of PAI-1. Ann N Y Acad Sci, 667: 70-80.

178 Robbie LA, Bennett B, Croll AM, Brown PA and Booth NA. (1996) Proteins of the fibrinolytic system in human thrombi. Thromb Haemost, 75: 127-33.

179 Morrow GB, Whyte CS and Mutch NJ. (2020) Functional plasminogen activator inhibitor 1 is retained on the activated platelet membrane following platelet activation. Haematologica, 105: 2824-2833.

180 Kooistra T, Sprengers ED and van Hinsbergh VW. (1986) Rapid inactivation of the plasminogen-activator inhibitor upon secretion from cultured human endothelial cells. Biochem J, 239: 497-503.

181 Declerck PJ, De Mol M, Alessi MC, Baudner S, Paques EP, Preissner KT, Muller-Berghaus G and Collen D. (1988) Purification and characterization of a plasminogen activator inhibitor 1 binding protein from human plasma. Identification as a multimeric form of S protein (vitronectin). J Biol Chem, 263: 15454-61.

182 Podor TJ, Peterson CB, Lawrence DA, Stefansson S, Shaughnessy SG, Foulon DM, Butcher M and Weitz JI. (2000) Type 1 plasminogen activator inhibitor binds to fibrin via vitronectin. J Biol Chem, 275: 19788-94.

183 Huisman LG, van Griensven JM and Kluft C. (1995) On the role of C1-inhibitor as inhibitor of tissue-type plasminogen activator in human plasma. Thromb Haemost, 73: 466-71.

184 Boulaftali Y, Ho-Tin-Noe B, Pena A, Loyau S, Venisse L, Francois D, Richard B, Arocas V, Collet JP, Jandrot-Perrus M and Bouton MC. (2011) Platelet protease nexin-1, a serpin that strongly influences fibrinolysis and thrombolysis. Circulation, 123: 1326-34.

185 Jones AL, Hulett MD, Altin JG, Hogg P and Parish CR. (2004) Plasminogen is tethered with high affinity to the cell surface by the plasma protein, histidine-rich glycoprotein. J Biol Chem, 279: 38267-76.

186 Nesheim M. (1998) Fibrinolysis and the plasma carboxypeptidase. Curr Opin Hematol, 5: 309-13.

187 Schadinger SL, Lin JH, Garand M and Boffa MB. (2010) Secretion and antifibrinolytic function of thrombin-activatable fibrinolysis inhibitor from human platelets. J Thromb Haemost, 8: 2523-9.

188 Komorowicz E, Balazs N, Tanka-Salamon A, Varga Z, Szabo L, Bota A, Longstaff C and Kolev K. (2020) Biorelevant polyanions stabilize fibrin against

mechanical and proteolytic decomposition: Effects of polymer size and electric charge. J Mech Behav Biomed Mater, 102: 103459.

189 Engel R, Brain CM, Paget J, Lionikiene AS and Mutch NJ. (2014) Single-chain factor XII exhibits activity when complexed to polyphosphate. J Thromb Haemost, 12: 1513-22.

190 Konings J, Hoving LR, Ariens RS, Hethershaw EL, Ninivaggi M, Hardy LJ, de Laat B, Ten Cate H, Philippou H and Govers-Riemslag JW. (2015) The role of activated coagulation factor XII in overall clot stability and fibrinolysis. Thromb Res, 136: 474-80.

191 Mitchell JL, Lionikiene AS, Georgiev G, Klemmer A, Brain C, Kim PY and Mutch NJ. (2016) Polyphosphate colocalizes with factor XII on platelet-bound fibrin and augments its plasminogen activator activity. Blood, 128: 2834-2845.

192 Whyte CS and Mutch NJ. (2021) uPA-mediated plasminogen activation is enhanced by polyphosphate. Haematologica, 106: 522-531.

193 den Dekker E, van Abel M, van der Vuurst H, van Eys GJ, Akkerman JW and Heemskerk JW. (2003) Cell-to-cell variability in the differentiation program of human megakaryocytes. Biochim Biophys Acta, 1643: 85-94.

194 Long MW. (1993) Population heterogeneity among cells of the megakaryocyte lineage. Stem Cells, 11: 33-40.

195 Versteeg HH, Heemskerk JW, Levi M and Reitsma PH. (2013) New fundamentals in hemostasis. Physiol Rev, 93: 327-58.

196 Gilio K, van Kruchten R, Braun A, Berna-Erro A, Feijge MA, Stegner D, van der Meijden PE, Kuijpers MJ, Varga-Szabo D, Heemskerk JW and Nieswandt B. (2010) Roles of platelet STIM1 and Orai1 in glycoprotein VI- and thrombin-dependent procoagulant activity and thrombus formation. J Biol Chem, 285: 23629-38.

197 Stehbens WE and Biscoe TJ. (1967) The ultrastructure of early platelet aggregation in vivo. Am J Pathol, 50: 219-43.

198 Jorgensen L, Rowsell HC, Hovig T and Mustard JF. (1967) Resolution and organization of platelet-rich mural thrombi in carotid arteries of swine. Am J Pathol, 51: 681-719.

199 Heemskerk JW, Mattheij NJ and Cosemans JM. (2013) Platelet-based coagulation: different populations, different functions. J Thromb Haemost, 11: 2-16.

200 Stalker TJ, Traxler EA, Wu J, Wannemacher KM, Cermignano SL, Voronov R, Diamond SL and Brass LF. (2013) Hierarchical organization in the hemostatic response and its relationship to the platelet-signaling network. Blood, 121: 1875-85.

201 Kempton CL, Hoffman M, Roberts HR and Monroe DM. (2005) Platelet heterogeneity: variation in coagulation complexes on platelet subpopulations. Arterioscler Thromb Vasc Biol, 25: 861-6.

202 Agbani EO, Williams CM, Hers I and Poole AW. (2017) Membrane Ballooning in Aggregated Platelets is Synchronised and Mediates a Surge in Microvesiculation. Sci Rep, 7: 2770.

203 Agbani EO, van den Bosch MT, Brown E, Williams CM, Mattheij NJ, Cosemans JM, Collins PW, Heemskerk JW, Hers I and Poole AW. (2015) Coordinated Membrane Ballooning and Procoagulant Spreading in Human Platelets. Circulation, 132: 1414-24.

204 Bevers EM, Rosing J and Zwaal RF. (1985) Development of procoagulant binding sites on the platelet surface. Adv Exp Med Biol, 192: 359-71.

205 Welsh JD, Colace TV, Muthard RW, Stalker TJ, Brass LF and Diamond SL. (2012) Platelet-targeting sensor reveals thrombin gradients within blood clots forming in microfluidic assays and in mouse. J Thromb Haemost, 10: 2344-53.

206 Baaten C, Swieringa F, Misztal T, Mastenbroek TG, Feijge MAH, Bock PE, Donners M, Collins PW, Li R, van der Meijden PEJ and Heemskerk JWM. (2018) Platelet heterogeneity in activation-induced glycoprotein shedding: functional effects. Blood Adv, 2: 2320-2331.

207 Mattheij NJ, Gilio K, van Kruchten R, Jobe SM, Wieschhaus AJ, Chishti AH, Collins P, Heemskerk JW and Cosemans JM. (2013) Dual mechanism of integrin alphaIIbbeta3 closure in procoagulant platelets. J Biol Chem, 288: 13325-36.

208 Yakimenko AO, Verholomova FY, Kotova YN, Ataullakhanov FI and Panteleev MA. (2012) Identification of different proaggregatory abilities of activated platelet subpopulations. Biophys J, 102: 2261-9.

209 Agbani EO, Hers I and Poole AW. (2017) Temporal contribution of the platelet body and balloon to thrombin generation. Haematologica, 102: e379-e381.

210 Abaeva AA, Canault M, Kotova YN, Obydennyy SI, Yakimenko AO, Podoplelova NA, Kolyadko VN, Chambost H, Mazurov AV, Ataullakhanov FI, Nurden

AT, Alessi MC and Panteleev MA. (2013) Procoagulant platelets form an alpha-granule protein-covered "cap" on their surface that promotes their attachment to aggregates. J Biol Chem, 288: 29621-32.

211 Podoplelova NA, Sveshnikova AN, Kotova YN, Eckly A, Receveur N, Nechipurenko DY, Obydennyi SI, Kireev, II, Gachet C, Ataullakhanov FI, Mangin PH and Panteleev MA. (2016) Coagulation factors bound to procoagulant platelets concentrate in cap structures to promote clotting. Blood, 128: 1745-55.

212 Mitchell JL, Lionikiene AS, Fraser SR, Whyte CS, Booth NA and Mutch NJ. (2014) Functional factor XIII-A is exposed on the stimulated platelet surface. Blood, 124: 3982-90.

213 Whyte CS, Swieringa F, Mastenbroek TG, Lionikiene AS, Lance MD, van der Meijden PE, Heemskerk JW and Mutch NJ. (2015) Plasminogen associates with phosphatidylserine-exposing platelets and contributes to thrombus lysis under flow. Blood, 125: 2568-78.

214 Alberio L, Safa O, Clemetson KJ, Esmon CT and Dale GL. (2000) Surface expression and functional characterization of alpha-granule factor V in human platelets: effects of ionophore A23187, thrombin, collagen, and convulxin. Blood, 95: 1694-702.

215 Dale GL, Friese P, Batar P, Hamilton SF, Reed GL, Jackson KW, Clemetson KJ and Alberio L. (2002) Stimulated platelets use serotonin to enhance their retention of procoagulant proteins on the cell surface. Nature, 415: 175-9.

216 Dale GL. (2005) Coated-platelets: an emerging component of the procoagulant response. J Thromb Haemost, 3: 2185-92.

217 Jobe SM, Leo L, Eastvold JS, Dickneite G, Ratliff TL, Lentz SR and Di Paola J. (2005) Role of FcRgamma and factor XIIIA in coated platelet formation. Blood, 106: 4146-51.

218 van Kruchten R, Mattheij NJ, Saunders C, Feijge MA, Swieringa F, Wolfs JL, Collins PW, Heemskerk JW and Bevers EM. (2013) Both TMEM16F-dependent and TMEM16F-independent pathways contribute to phosphatidylserine exposure in platelet apoptosis and platelet activation. Blood, 121: 1850-7.

219 Wang P and Heitman J. (2005) The cyclophilins. Genome Biol, 6: 226.

220 Connern CP and Halestrap AP. (1992) Purification and N-terminal sequencing of peptidyl-prolyl cis-trans-isomerase from rat liver mitochondrial matrix reveals the existence of a distinct mitochondrial cyclophilin. Biochem J, 284 (Pt 2): 381-5.

221 Johnson N, Khan A, Virji S, Ward JM and Crompton M. (1999) Import and processing of heart mitochondrial cyclophilin D. Eur J Biochem, 263: 353-9.

222 Connern CP and Halestrap AP. (1996) Chaotropic agents and increased matrix volume enhance binding of mitochondrial cyclophilin to the inner mitochondrial membrane and sensitize the mitochondrial permeability transition to [Ca2+]. Biochemistry, 35: 8172-80.

223 Connern CP and Halestrap AP. (1994) Recruitment of mitochondrial cyclophilin to the mitochondrial inner membrane under conditions of oxidative stress that enhance the opening of a calcium-sensitive non-specific channel. Biochem J, 302 (Pt 2): 321-4.

224 Davis TL, Walker JR, Campagna-Slater V, Finerty PJ, Paramanathan R, Bernstein G, MacKenzie F, Tempel W, Ouyang H, Lee WH, Eisenmesser EZ and Dhe-Paganon S. (2010) Structural and biochemical characterization of the human cyclophilin family of peptidyl-prolyl isomerases. PLoS Biol, 8: e1000439.

225 Walsh CT, Zydowsky LD and McKeon FD. (1992) Cyclosporin A, the cyclophilin class of peptidylprolyl isomerases, and blockade of T cell signal transduction. J Biol Chem, 267: 13115-8.

226 Handschumacher RE, Harding MW, Rice J, Drugge RJ and Speicher DW. (1984) Cyclophilin: a specific cytosolic binding protein for cyclosporin A. Science, 226: 544-7.

227 Gutierrez-Aguilar M, Douglas DL, Gibson AK, Domeier TL, Molkentin JD and Baines CP. (2014) Genetic manipulation of the cardiac mitochondrial phosphate carrier does not affect permeability transition. J Mol Cell Cardiol, 72: 316-25.

228 Tanveer A, Virji S, Andreeva L, Totty NF, Hsuan JJ, Ward JM and Crompton M. (1996) Involvement of cyclophilin D in the activation of a mitochondrial pore by Ca2+ and oxidant stress. Eur J Biochem, 238: 166-72.

229 Beutner G, Eliseev RA and Porter GA, Jr. (2014) Initiation of electron transport chain activity in the embryonic heart coincides with the activation of mitochondrial complex 1 and the formation of supercomplexes. PLoS One, 9: e113330.

230 Etzler JC, Bollo M, Holstein D, Deng JJ, Perez V, Lin DT, Richardson A, Bai Y and Lechleiter JD. (2017) Cyclophilin D over-expression increases mitochondrial complex III activity and accelerates supercomplex formation. Arch Biochem Biophys, 613: 61-68.

231 Beutner G, Alanzalon RE and Porter GA, Jr. (2017) Cyclophilin D regulates the dynamic assembly of mitochondrial ATP synthase into synthasomes. Sci Rep, 7: 14488.

232 Mitchell P. (1966) Chemiosmotic coupling in oxidative and photosynthetic phosphorylation. Biol Rev Camb Philos Soc, 41: 445-502.

233 Jonas EA, Porter GA, Jr., Beutner G, Mnatsakanyan N and Alavian KN. (2015) Cell death disguised: The mitochondrial permeability transition pore as the c-subunit of the F(1)F(O) ATP synthase. Pharmacol Res, 99: 382-92.

234 Demine S, Renard P and Arnould T. (2019) Mitochondrial Uncoupling: A Key Controller of Biological Processes in Physiology and Diseases. Cells, 8:

235 Nicholls DG and Locke RM. (1984) Thermogenic mechanisms in brown fat. Physiol Rev, 64: 1-64.

236 Andreyev A, Bondareva TO, Dedukhova VI, Mokhova EN, Skulachev VP, Tsofina LM, Volkov NI and Vygodina TV. (1989) The ATP/ADP-antiporter is involved in the uncoupling effect of fatty acids on mitochondria. Eur J Biochem, 182: 585-92.

237 Haworth RA and Hunter DR. (1979) The Ca2+-induced membrane transition in mitochondria. II. Nature of the Ca2+ trigger site. Arch Biochem Biophys, 195: 460-7.

238 Hunter DR and Haworth RA. (1979) The Ca2+-induced membrane transition in mitochondria. I. The protective mechanisms. Arch Biochem Biophys, 195: 453-9.

239 Hunter DR and Haworth RA. (1979) The Ca2+-induced membrane transition in mitochondria. III. Transitional Ca2+ release. Arch Biochem Biophys, 195: 468-77.

240 Kowaltowski AJ, Castilho RF and Vercesi AE. (1996) Opening of the mitochondrial permeability transition pore by uncoupling or inorganic phosphate in the presence of Ca2+ is dependent on mitochondrial-generated reactive oxygen species. FEBS Lett, 378: 150-2.

241 Takeyama N, Matsuo N and Tanaka T. (1993) Oxidative damage to mitochondria is mediated by the Ca(2+)-dependent inner-membrane permeability transition. Biochem J, 294 (Pt 3): 719-25.

242 Petronilli V, Cola C and Bernardi P. (1993) Modulation of the mitochondrial cyclosporin A-sensitive permeability transition pore. II. The minimal requirements for pore induction underscore a key role for transmembrane electrical potential, matrix pH, and matrix Ca2+. J Biol Chem, 268: 1011-6.

243 Wieckowski MR, Brdiczka D and Wojtczak L. (2000) Long-chain fatty acids promote opening of the reconstituted mitochondrial permeability transition pore. FEBS Lett, 484: 61-4.

244 Marzo I, Brenner C, Zamzami N, Jurgensmeier JM, Susin SA, Vieira HL, Prevost MC, Xie Z, Matsuyama S, Reed JC and Kroemer G. (1998) Bax and adenine nucleotide translocator cooperate in the mitochondrial control of apoptosis. Science, 281: 2027-31.

245 Halestrap AP, Woodfield KY and Connern CP. (1997) Oxidative stress, thiol reagents, and membrane potential modulate the mitochondrial permeability transition by affecting nucleotide binding to the adenine nucleotide translocase. J Biol Chem, 272: 3346-54.

246 Block MR, Lauguin GJ and Vignais PV. (1981) Atractyloside and bongkrekic acid sites in the mitochondrial ADP/ATP carrier protein. An appraisal of their unicity by chemical modifications. FEBS Lett, 131: 213-8.

247 Bonora M, Wieckowski MR, Chinopoulos C, Kepp O, Kroemer G, Galluzzi L and Pinton P. (2015) Molecular mechanisms of cell death: central implication of ATP synthase in mitochondrial permeability transition. Oncogene, 34: 1475-86.

248 Ichas F, Jouaville LS and Mazat JP. (1997) Mitochondria are excitable organelles capable of generating and conveying electrical and calcium signals. Cell, 89: 1145-53.

249 Huser J, Rechenmacher CE and Blatter LA. (1998) Imaging the permeability pore transition in single mitochondria. Biophys J, 74: 2129-37.

250 Kwong JQ, Davis J, Baines CP, Sargent MA, Karch J, Wang X, Huang T and Molkentin JD. (2014) Genetic deletion of the mitochondrial phosphate carrier desensitizes the mitochondrial permeability transition pore and causes cardiomyopathy. Cell Death Differ, 21: 1209-17.

251 Kokoszka JE, Waymire KG, Levy SE, Sligh JE, Cai J, Jones DP, MacGregor GR and Wallace DC. (2004) The ADP/ATP translocator is not essential for the mitochondrial permeability transition pore. Nature, 427: 461-5.

252 Vyssokikh MY and Brdiczka D. (2003) The function of complexes between the outer mitochondrial membrane pore (VDAC) and the adenine nucleotide translocase in regulation of energy metabolism and apoptosis. Acta Biochim Pol, 50: 389-404.

253 Sileikyte J, Blachly-Dyson E, Sewell R, Carpi A, Menabo R, Di Lisa F, Ricchelli F, Bernardi P and Forte M. (2014) Regulation of the mitochondrial permeability transition pore by the outer membrane does not involve the peripheral benzodiazepine receptor (Translocator Protein of 18 kDa (TSPO)). J Biol Chem, 289: 13769-81.

254 Baines CP, Kaiser RA, Sheiko T, Craigen WJ and Molkentin JD. (2007) Voltage-dependent anion channels are dispensable for mitochondrial-dependent cell death. Nat Cell Biol, 9: 550-5.

255 Krauskopf A, Eriksson O, Craigen WJ, Forte MA and Bernardi P. (2006) Properties of the permeability transition in VDAC1(-/-) mitochondria. Biochim Biophys Acta, 1757: 590-5.

256 Baines CP, Kaiser RA, Purcell NH, Blair NS, Osinska H, Hambleton MA, Brunskill EW, Sayen MR, Gottlieb RA, Dorn GW, Robbins J and Molkentin JD. (2005) Loss of cyclophilin D reveals a critical role for mitochondrial permeability transition in cell death. Nature, 434: 658-62.

257 Basso E, Fante L, Fowlkes J, Petronilli V, Forte MA and Bernardi P. (2005) Properties of the permeability transition pore in mitochondria devoid of Cyclophilin D. J Biol Chem, 280: 18558-61.

258 Nakagawa T, Shimizu S, Watanabe T, Yamaguchi O, Otsu K, Yamagata H, Inohara H, Kubo T and Tsujimoto Y. (2005) Cyclophilin D-dependent mitochondrial permeability transition regulates some necrotic but not apoptotic cell death. Nature, 434: 652-8.

259 Basso E, Petronilli V, Forte MA and Bernardi P. (2008) Phosphate is essential for inhibition of the mitochondrial permeability transition pore by cyclosporin A and by cyclophilin D ablation. J Biol Chem, 283: 26307-11.

260 Giorgio V, von Stockum S, Antoniel M, Fabbro A, Fogolari F, Forte M, Glick GD, Petronilli V, Zoratti M, Szabo I, Lippe G and Bernardi P. (2013) Dimers of mitochondrial ATP synthase form the permeability transition pore. Proc Natl Acad Sci U S A, 110: 5887-92.

261 Bonora M, Morganti C, Morciano G, Pedriali G, Lebiedzinska-Arciszewska M, Aquila G, Giorgi C, Rizzo P, Campo G, Ferrari R, Kroemer G, Wieckowski MR, Galluzzi L and Pinton P. (2017) Mitochondrial permeability transition involves dissociation of F1FO ATP synthase dimers and C-ring conformation. EMBO Rep, 18: 1077-1089.

262 He J, Carroll J, Ding S, Fearnley IM and Walker JE. (2017) Permeability transition in human mitochondria persists in the absence of peripheral stalk subunits of ATP synthase. Proc Natl Acad Sci U S A, 114: 9086-9091.

263 Carroll J, He J, Ding S, Fearnley IM and Walker JE. (2019) Persistence of the permeability transition pore in human mitochondria devoid of an assembled ATP synthase. Proc Natl Acad Sci U S A, 116: 12816-12821.

264 Neginskaya MA, Solesio ME, Berezhnaya EV, Amodeo GF, Mnatsakanyan N, Jonas EA and Pavlov EV. (2019) ATP Synthase C-Subunit-Deficient Mitochondria Have a Small Cyclosporine A-Sensitive Channel, but Lack the Permeability Transition Pore. Cell Rep, 26: 11-17 e2.

265 He J, Ford HC, Carroll J, Ding S, Fearnley IM and Walker JE. (2017) Persistence of the mitochondrial permeability transition in the absence of subunit c of human ATP synthase. Proc Natl Acad Sci U S A, 114: 3409-3414.

266 Karch J, Bround MJ, Khalil H, Sargent MA, Latchman N, Terada N, Peixoto PM and Molkentin JD. (2019) Inhibition of mitochondrial permeability transition by deletion of the ANT family and CypD. Sci Adv, 5: eaaw4597.

267 Colombo D and Ammirati E. (2011) Cyclosporine in transplantation - a history of converging timelines. J Biol Regul Homeost Agents, 25: 493-504.

268 Wenger RM and Payne T. (1989) Cyclosporine: intrinsic binding energies to interpret structure-activity relationships. Prog Clin Biol Res, 291: 301-5.

269 Borel JF, Feurer C, Gubler HU and Stahelin H. (1976) Biological effects of cyclosporin A: a new antilymphocytic agent. Agents Actions, 6: 468-75.

270 Faulds D, Goa KL and Benfield P. (1993) Cyclosporin. A review of its pharmacodynamic and pharmacokinetic properties, and therapeutic use in immunoregulatory disorders. Drugs, 45: 953-1040.

271 Tokuda M, Kurata N, Mizoguchi A, Inoh M, Seto K, Kinashi M and Takahara J. (1994) Effect of low-dose cyclosporin A on systemic lupus erythematosus disease activity. Arthritis Rheum, 37: 551-8.

272 Zeidler HK, Kvien TK, Hannonen P, Wollheim FA, Forre O, Geidel H, Hafstrom I, Kaltwasser JP, Leirisalo-Repo M, Manger B, Laasonen L, Markert ER, Prestele H and Kurki P. (1998) Progression of joint damage in early active severe rheumatoid arthritis during 18 months of treatment: comparison of low-dose cyclosporin and parenteral gold. Br J Rheumatol, 37: 874-82.

273 Remuzzi G and Bertani T. (1989) Renal vascular and thrombotic effects of cyclosporine. Am J Kidney Dis, 13: 261-72.

274 Dodhia N, Rodby RA, Jensik SC and Korbet SM. (1991) Renal transplant arterial thrombosis: association with cyclosporine. Am J Kidney Dis, 17: 532-6.

275 Schreiber SL and Crabtree GR. (1992) The mechanism of action of cyclosporin A and FK506. Immunol Today, 13: 136-42.

276 Solbach W, Lange CE, Rollinghoff M and Wagner H. (1984) Growth, interleukin-2 production, and responsiveness to IL-2 in T4-positive T Lymphocyte populations from malignant cutaneous T cell lymphoma (Sezary's syndrome): the effect of cyclosporin A. Blood, 64: 1022-7.

277 Ho S, Clipstone N, Timmermann L, Northrop J, Graef I, Fiorentino D, Nourse J and Crabtree GR. (1996) The mechanism of action of cyclosporin A and FK506. Clin Immunol Immunopathol, 80: S40-5.

278 Granucci F, Feau S, Angeli V, Trottein F and Ricciardi-Castagnoli P. (2003) Early IL-2 production by mouse dendritic cells is the result of microbial-induced priming. J Immunol, 170: 5075-81.

279 Campelo SR, da Silva MB, Vieira JL, da Silva JP and Salgado CG. (2011) Effects of immunomodulatory drugs on TNF-alpha and IL-12 production by purified epidermal langerhans cells and peritoneal macrophages. BMC Res Notes, 4: 24.

280 Greenblatt MB, Aliprantis A, Hu B and Glimcher LH. (2010) Calcineurin regulates innate antifungal immunity in neutrophils. J Exp Med, 207: 923-31.

281 Schlatter D, Thoma R, Kung E, Stihle M, Muller F, Borroni E, Cesura A and Hennig M. (2005) Crystal engineering yields crystals of cyclophilin D diffracting to 1.7 A resolution. Acta Crystallogr D Biol Crystallogr, 61: 513-9.

282 Kajitani K, Fujihashi M, Kobayashi Y, Shimizu S, Tsujimoto Y and Miki K. (2008) Crystal structure of human cyclophilin D in complex with its inhibitor, cyclosporin A at 0.96-A resolution. Proteins, 70: 1635-9.

283 Schreiber SL. (1991) Chemistry and biology of the immunophilins and their immunosuppressive ligands. Science, 251: 283-7.

284 Garcia RA, Hotchkiss JH and Steinkraus KH. (1999) The effect of lipids on bongkrekic (Bongkrek) acid toxin production by Burkholderia cocovenenans in coconut media. Food Addit Contam, 16: 63-9.

285 Halestrap AP and Pasdois P. (2009) The role of the mitochondrial permeability transition pore in heart disease. Biochim Biophys Acta, 1787: 1402-15.

286 Heemskerk JW, Vuist WM, Feijge MA, Reutelingsperger CP and Lindhout T. (1997) Collagen but not fibrinogen surfaces induce bleb formation, exposure of phosphatidylserine, and procoagulant activity of adherent platelets: evidence for regulation by protein tyrosine kinase-dependent Ca2+ responses. Blood, 90: 2615-25.

287 Heemskerk JW, Bevers EM and Lindhout T. (2002) Platelet activation and blood coagulation. Thromb Haemost, 88: 186-93.

288 Heemskerk JW, Feijge MA, Henneman L, Rosing J and Hemker HC. (1997) The Ca2+-mobilizing potency of alpha-thrombin and thrombin-receptor-activating peptide on human platelets -- concentration and time effects of thrombin-induced Ca2+ signaling. Eur J Biochem, 249: 547-55.

289 Andersen H, Greenberg DL, Fujikawa K, Xu W, Chung DW and Davie EW. (1999) Protease-activated receptor 1 is the primary mediator of thrombin-stimulated platelet procoagulant activity. Proc Natl Acad Sci U S A, 96: 11189-93.

290 Griendling KK and Ushio-Fukai M. (1997) NADH/NADPH Oxidase and Vascular Function. Trends Cardiovasc Med, 7: 301-7.

291 Suzuki YJ and Ford GD. (1999) Redox regulation of signal transduction in cardiac and smooth muscle. J Mol Cell Cardiol, 31: 345-53.

292 Marcus AJ, Silk ST, Safier LB and Ullman HL. (1977) Superoxide production and reducing activity in human platelets. J Clin Invest, 59: 149-58.

293 Pratico D, Iuliano L, Alessandri C, Camastra C and Violi F. (1993) Polymorphonuclear leukocyte-derived O2-reactive species activate primed platelets in human whole blood. Am J Physiol, 264: H1582-7.

294 Iwakami M. (1965) Peroxides as a factor of atherosclerosis. Nagoya J Med Sci, 28: 50-66.

295 Forstermann U, Xia N and Li H. (2017) Roles of Vascular Oxidative Stress and Nitric Oxide in the Pathogenesis of Atherosclerosis. Circ Res, 120: 713-735.

296 Wolff SP and Dean RT. (1987) Glucose autoxidation and protein modification. The potential role of 'autoxidative glycosylation' in diabetes. Biochem J, 245: 243-50.

297 Maritim AC, Sanders RA and Watkins JB, 3rd. (2003) Diabetes, oxidative stress, and antioxidants: a review. J Biochem Mol Toxicol, 17: 24-38.

298 McStay GP, Clarke SJ and Halestrap AP. (2002) Role of critical thiol groups on the matrix surface of the adenine nucleotide translocase in the mechanism of the mitochondrial permeability transition pore. Biochem J, 367: 541-8.

299 Cosemans JM, Schols SE, Stefanini L, de Witt S, Feijge MA, Hamulyak K, Deckmyn H, Bergmeier W and Heemskerk JW. (2011) Key role of glycoprotein Ib/V/IX and von Willebrand factor in platelet activation-dependent fibrin formation at low shear flow. Blood, 117: 651-60.

300 Nergiz-Unal R, Lamers MM, Van Kruchten R, Luiken JJ, Cosemans JM, Glatz JF, Kuijpers MJ and Heemskerk JW. (2011) Signaling role of CD36 in platelet activation and thrombus formation on immobilized thrombospondin or oxidized low-density lipoprotein. J Thromb Haemost, 9: 1835-46.

301 Choo HJ, Saafir TB, Mkumba L, Wagner MB and Jobe SM. (2012) Mitochondrial calcium and reactive oxygen species regulate agonist-initiated platelet phosphatidylserine exposure. Arterioscler Thromb Vasc Biol, 32: 2946-55.

302 Yang H, Kim A, David T, Palmer D, Jin T, Tien J, Huang F, Cheng T, Coughlin SR, Jan YN and Jan LY. (2012) TMEM16F forms a Ca2+-activated cation channel required for lipid scrambling in platelets during blood coagulation. Cell, 151: 111-22.

303 Malvezzi M, Chalat M, Janjusevic R, Picollo A, Terashima H, Menon AK and Accardi A. (2013) Ca2+-dependent phospholipid scrambling by a reconstituted TMEM16 ion channel. Nat Commun, 4: 2367.

304 Kwong JQ and Molkentin JD. (2015) Physiological and pathological roles of the mitochondrial permeability transition pore in the heart. Cell Metab, 21: 206-214.

305 Remenyi G, Szasz R, Friese P and Dale GL. (2005) Role of mitochondrial permeability transition pore in coated-platelet formation. Arterioscler Thromb Vasc Biol, 25: 467-71.

306 Liu F, Gamez G, Myers DR, Clemmons W, Lam WA and Jobe SM. (2013) Mitochondrially mediated integrin alphaIIbbeta3 protein inactivation limits thrombus growth. J Biol Chem, 288: 30672-81.

307 Hua VM, Abeynaike L, Glaros E, Campbell H, Pasalic L, Hogg PJ and Chen VM. (2015) Necrotic platelets provide a procoagulant surface during thrombosis. Blood,

308 Kovacs A, Sotonyi P, Nagy AI, Tenekedjiev K, Wohner N, Komorowicz E, Kovacs E, Nikolova N, Szabo L, Kovalszky I, Machovich R, Szelid Z, Becker D, Merkely B and Kolev K. (2015) Ultrastructure and composition of thrombi in coronary and peripheral artery disease: correlations with clinical and laboratory findings. Thromb Res, 135: 760-6.

309 Varju I, Sotonyi P, Machovich R, Szabo L, Tenekedjiev K, Silva MM, Longstaff C and Kolev K. (2011) Hindered dissolution of fibrin formed under mechanical stress. J Thromb Haemost, 9: 979-86.

310 Longstaff C, Varju I, Sotonyi P, Szabo L, Krumrey M, Hoell A, Bota A, Varga Z, Komorowicz E and Kolev K. (2013) Mechanical stability and fibrinolytic resistance of clots containing fibrin, DNA, and histones. J Biol Chem, 288: 6946-56.

311 Nikolova N, Chai S, Ivanova SD, Kolev K and Tenekedjiev K. (2015) Bootstrap Kuiper Testing of the Identity of 1D Continuous Distributions using Fuzzy Samples. International Journal of Computational Intelligence Systems, 8(Suppl. 2): 63-75.

312 Nikolova N, Mihaylova N and Tenekedjiev K. (2015) Bootstrap tests for mean value differences over fuzzy samples. IFAC-PapersOnLine, 48: 7-14.

313 Lundblad RL, Kingdon HS and Mann KG. (1976) Thrombin. Methods Enzymol, 45: 156-76.

314 Longstaff C, Wong MY and Gaffney PJ. (1993) An international collaborative study to investigate standardisation of hirudin potency. Thromb Haemost, 69: 430-5.

315 Heinecke JW, Kawamura M, Suzuki L and Chait A. (1993) Oxidation of low density lipoprotein by thiols: superoxide-dependent and -independent mechanisms. J Lipid Res, 34: 2051-61.

316 Jomova K and Valko M. (2011) Advances in metal-induced oxidative stress and human disease. Toxicology, 283: 65-87.

317 Manevich Y, Held KD and Biaglow JE. (1997) Coumarin-3-carboxylic acid as a detector for hydroxyl radicals generated chemically and by gamma radiation. Radiat Res, 148: 580-91.

318 Longstaff C, Thelwell C, Williams SC, Silva MM, Szabo L and Kolev K. (2011) The interplay between tissue plasminogen activator domains and fibrin structures in the regulation of fibrinolysis: kinetic and microscopic studies. Blood, 117: 661-8.

319 Nikolova N, Toneva-Zheynova D, Tenekedjiev K and Kolev K. Monte Carlo Statistical Tests for Identity of Theoretical and Empirical Distributions of Experimental Data, Theory and Applications of Monte Carlo Simulations. In: W. K. V. Chan (Ed.), Theory and Applications of Monte Carlo Simulations. InTech, London, 2013: 1-26.

320 Jarvis GE, Bihan D, Hamaia S, Pugh N, Ghevaert CJ, Pearce AC, Hughes CE, Watson SP, Ware J, Rudd CE and Farndale RW. (2012) A role for adhesion and degranulation-promoting adapter protein in collagen-induced platelet activation mediated via integrin alpha(2) beta(1). J Thromb Haemost, 10: 268-77.

321 Kho D, MacDonald C, Johnson R, Unsworth CP, O'Carroll SJ, du Mez E, Angel CE and Graham ES. (2015) Application of xCELLigence RTCA Biosensor Technology for Revealing the Profile and Window of Drug Responsiveness in Real Time. Biosensors (Basel), 5: 199-222.

322 Wohner N, Kovacs A, Machovich R and Kolev K. (2012) Modulation of the von Willebrand factor-dependent platelet adhesion through alternative proteolytic pathways. Thromb Res, 129: e41-6.

323 Iwasaki K. (2007) Metabolism of tacrolimus (FK506) and recent topics in clinical pharmacokinetics. Drug Metab Pharmacokinet, 22: 328-35.

324 Dumont FJ. (2000) FK506, an immunosuppressant targeting calcineurin function. Curr Med Chem, 7: 731-48.

325 Deutsch DG and Mertz ET. (1970) Plasminogen: purification from human plasma by affinity chromatography. Science, 170: 1095-6.

326 Varju I, Longstaff C, Szabo L, Farkas AZ, Varga-Szabo VJ, Tanka-Salamon A, Machovich R and Kolev K. (2015) DNA, histones and neutrophil extracellular traps exert anti-fibrinolytic effects in a plasma environment. Thromb Haemost, 113: 1289-98.

327 Efron B TR. An introduction to the Bootstrap. Taylor & Francis, New York, NY, USA, 1993: 10-16.

328 Jackson SP and Schoenwaelder SM. (2010) Procoagulant platelets: are they necrotic? Blood, 116: 2011-8.

329 Zalewski J, Bogaert J, Sadowski M, Woznicka O, Doulaptsis K, Ntoumpanaki M, Zabczyk M, Nessler J and Undas A. (2015) Plasma fibrin clot phenotype independently affects intracoronary thrombus ultrastructure in patients with acute myocardial infarction. Thromb Haemost, 113: 1258-69.

330 Kim SK, Yoon W, Kim TS, Kim HS, Heo TW and Park MS. (2015) Histologic Analysis of Retrieved Clots in Acute Ischemic Stroke: Correlation with Stroke Etiology and Gradient-Echo MRI. AJNR Am J Neuroradiol, 36: 1756-62.

331 Niesten JM, van der Schaaf IC, van Dam L, Vink A, Vos JA, Schonewille WJ, de Bruin PC, Mali WP and Velthuis BK. (2014) Histopathologic composition of cerebral thrombi of acute stroke patients is correlated with stroke subtype and thrombus attenuation. PLoS One, 9: e88882.

332 Ahn SH, Hong R, Choo IS, Heo JH, Nam HS, Kang HG, Kim HW and Kim JH. (2016) Histologic features of acute thrombi retrieved from stroke patients during mechanical reperfusion therapy. Int J Stroke, 11: 1036-1044.

333 Maekawa K, Shibata M, Nakajima H, Mizutani A, Kitano Y, Seguchi M, Yamasaki M, Kobayashi K, Sano T, Mori G, Yabana T, Naito Y, Shimizu S and Miya F. (2018) Erythrocyte-Rich Thrombus Is Associated with Reduced Number of Maneuvers and Procedure Time in Patients with Acute Ischemic Stroke Undergoing Mechanical Thrombectomy. Cerebrovasc Dis Extra, 8: 39-49.

334 Sato Y, Ishibashi-Ueda H, Iwakiri T, Ikeda Y, Matsuyama T, Hatakeyama K and Asada Y. (2012) Thrombus components in cardioembolic and atherothrombotic strokes. Thromb Res, 130: 278-80.

335 Boeckh-Behrens T, Kleine JF, Zimmer C, Neff F, Scheipl F, Pelisek J, Schirmer L, Nguyen K, Karatas D and Poppert H. (2016) Thrombus Histology Suggests Cardioembolic Cause in Cryptogenic Stroke. Stroke, 47: 1864-71.

336 Park H, Kim J, Ha J, Hwang IG, Song TJ, Yoo J, Ahn SH, Kim K, Kim BM, Kim DJ, Kim YD, Nam HS, Kwon I, Choi HJ, Sohn SI, Lee HS and Heo JH. (2019) Histological features of intracranial thrombi in stroke patients with cancer. Ann Neurol, 86: 143-149.

337 Hisada Y and Mackman N. (2017) Cancer-associated pathways and biomarkers of venous thrombosis. Blood, 130: 1499-1506.

338 Wang J, Kim YD and Kim CH. (2021) Incidence and Risk of Various Types of Arterial Thromboembolism in Patients With Cancer. Mayo Clin Proc, 96: 592-600.

339 Navi BB, Reiner AS, Kamel H, Iadecola C, Okin PM, Elkind MSV, Panageas KS and DeAngelis LM. (2017) Risk of Arterial Thromboembolism in Patients With Cancer. J Am Coll Cardiol, 70: 926-938.

340 Zoller B, Ji J, Sundquist J and Sundquist K. (2012) Risk of coronary heart disease in patients with cancer: a nationwide follow-up study from Sweden. Eur J Cancer, 48: 121-8.

341 Zoller B, Ji J, Sundquist J and Sundquist K. (2012) Risk of haemorrhagic and ischaemic stroke in patients with cancer: a nationwide follow-up study from Sweden. Eur J Cancer, 48: 1875-83.

342 Grignani G and Jamieson GA. (1988) Platelets in tumor metastasis: generation of adenosine diphosphate by tumor cells is specific but unrelated to metastatic potential. Blood, 71: 844-9.

343 Heinmoller E, Weinel RJ, Heidtmann HH, Salge U, Seitz R, Schmitz I, Muller KM and Zirngibl H. (1996) Studies on tumor-cell-induced platelet aggregation in human lung cancer cell lines. J Cancer Res Clin Oncol, 122: 735-44.

344 Wahrenbrock M, Borsig L, Le D, Varki N and Varki A. (2003) Selectin-mucin interactions as a probable molecular explanation for the association of Trousseau syndrome with mucinous adenocarcinomas. J Clin Invest, 112: 853-62.

345 Suzuki-Inoue K, Kato Y, Inoue O, Kaneko MK, Mishima K, Yatomi Y, Yamazaki Y, Narimatsu H and Ozaki Y. (2007) Involvement of the snake toxin receptor CLEC-2, in podoplanin-mediated platelet activation, by cancer cells. J Biol Chem, 282: 25993-6001.

346 Tsuruo T and Fujita N. (2008) Platelet aggregation in the formation of tumor metastasis. Proc Jpn Acad Ser B Phys Biol Sci, 84: 189-98.

347 Suzuki-Inoue K. (2009) CLEC-2, the novel platelet activation receptor and its internal ligand, podoplanin. Rinsho Ketsueki, 50: 389-98.

348 Wetterwald A, Hoffstetter W, Cecchini MG, Lanske B, Wagner C, Fleisch H and Atkinson M. (1996) Characterization and cloning of the E11 antigen, a marker expressed by rat osteoblasts and osteocytes. Bone, 18: 125-32.

349 Russo I, Massucco P, Mattiello L, Anfossi G and Trovati M. (2003) Comparison between the effects of the rapid recombinant insulin analog Lispro (Lys B28, Pro B29) and those of human regular insulin on platelet cyclic nucleotides and aggregation. Thromb Res, 109: 323-7.

350 Westerbacka J, Yki-Jarvinen H, Turpeinen A, Rissanen A, Vehkavaara S, Syrjala M and Lassila R. (2002) Inhibition of platelet-collagen interaction: an in vivo action of insulin abolished by insulin resistance in obesity. Arterioscler Thromb Vasc Biol, 22: 167-72.

351 Trovati M, Anfossi G, Massucco P, Mattiello L, Costamagna C, Piretto V, Mularoni E, Cavalot F, Bosia A and Ghigo D. (1997) Insulin stimulates nitric oxide synthesis in human platelets and, through nitric oxide, increases platelet concentrations of both guanosine-3', 5'-cyclic monophosphate and adenosine-3', 5'-cyclic monophosphate. Diabetes, 46: 742-9.

352 Gerrits AJ, Gitz E, Koekman CA, Visseren FL, van Haeften TW and Akkerman JW. (2012) Induction of insulin resistance by the adipokines resistin, leptin, plasminogen activator inhibitor-1 and retinol binding protein 4 in human megakaryocytes. Haematologica, 97: 1149-57.

353 Watala C. (2005) Blood platelet reactivity and its pharmacological modulation in (people with) diabetes mellitus. Curr Pharm Des, 11: 2331-65.

354 Davi G, Catalano I, Averna M, Notarbartolo A, Strano A, Ciabattoni G and Patrono C. (1990) Thromboxane biosynthesis and platelet function in type II diabetes mellitus. N Engl J Med, 322: 1769-74.

355 Finamore F, Reny JL, Malacarne S, Fontana P and Sanchez JC. (2019) A high glucose level is associated with decreased aspirin-mediated acetylation of platelet cyclooxygenase (COX)-1 at serine 529: A pilot study. J Proteomics, 192: 258-266.

356 Wachowicz B, Olas B, Zbikowska HM and Buczynski A. (2002) Generation of reactive oxygen species in blood platelets. Platelets, 13: 175-82.

357 Chung SS, Ho EC, Lam KS and Chung SK. (2003) Contribution of polyol pathway to diabetes-induced oxidative stress. J Am Soc Nephrol, 14: S233-6.

358 Fuijkschot WW, Groothuizen WE, Appelman Y, Radonic T, van Royen N, van Leeuwen MA, Krijnen PA, van der Wal AC, Smulders YM and Niessen HW. (2017) Inflammatory cell content of coronary thrombi is dependent on thrombus age in patients with ST-elevation myocardial infarction. J Cardiol, 69: 394-400.

359 Kim YG, Suh JW, Kang SH, Park JJ, Yoon CH, Cho YS, Youn TJ, Chae IH, Choi DJ and Kim HS. (2016) Cigarette Smoking Does Not Enhance Clopidogrel Responsiveness After Adjusting VerifyNow P2Y12 Reaction Unit for the Influence of Hemoglobin Level. JACC Cardiovasc Interv, 9: 1680-90.

360 Kim YG, Suh JW, Sibbing D, Kastrati A, Ko YG, Jang Y, Cho YS, Youn TJ, Chae IH, Choi DJ and Kim HS. (2017) A laboratory association between hemoglobin and VerifyNow P2Y12 reaction unit: A systematic review and meta-analysis. Am Heart J, 188: 53-64.

361 Nordenberg D, Yip R and Binkin NJ. (1990) The effect of cigarette smoking on hemoglobin levels and anemia screening. JAMA, 264: 1556-9.

362 Cereghetti GM, Stangherlin A, Martins de Brito O, Chang CR, Blackstone C, Bernardi P and Scorrano L. (2008) Dephosphorylation by calcineurin regulates translocation of Drp1 to mitochondria. Proc Natl Acad Sci U S A, 105: 15803-8.

363 Kanagaraja S, Lundstrom I, Nygren H and Tengvall P. (1996) Platelet binding and protein adsorption to titanium and gold after short time exposure to heparinized plasma and whole blood. Biomaterials, 17: 2225-32.

364 Grace AA, Barradas MA, Mikhailidis DP, Jeremy JY, Moorhead JF, Sweny P and Dandona P. (1987) Cyclosporine A enhances platelet aggregation. Kidney Int, 32: 889-95.

365 Fernandes JB, Naik UP, Markell MS and Kornecki E. (1993) Comparative investigation of the effects of the immunosuppressants cyclosporine A, cyclosporine G, and FK-506 on platelet activation. Cell Mol Biol Res, 39: 265-74.

366 Malyszko J, Malyszko JS, Takada A and Mysliwiec M. (2002) Effects of immunosuppressive drugs on platelet aggregation in vitro. Ann Transplant, 7: 55-68.

367 Mattheij NJ, Gilio K, van Kruchten R, Jobe SM, Wieschhaus AJ, Chishti AH, Collins P, Heemskerk JW and Cosemans JM. (2013) Dual mechanism of integrin αIIbβ3 closure in procoagulant platelets. J Biol Chem, 288: 13325-36.

368 Menazza S, Wong R, Nguyen T, Wang G, Gucek M and Murphy E. (2013) CypD(-/-) hearts have altered levels of proteins involved in Krebs cycle, branch chain amino acid degradation and pyruvate metabolism. J Mol Cell Cardiol, 56: 81-90.

369 Verhoeven AJ, Mommersteeg ME and Akkerman JW. (1986) Comparative studies on the energetics of platelet responses induced by different agonists. Biochem J, 236: 879-87.

370 Klingenberg M. (2008) The ADP and ATP transport in mitochondria and its carrier. Biochim Biophys Acta, 1778: 1978-2021.

371 Doczi J, Torocsik B, Echaniz-Laguna A, Mousson de Camaret B, Starkov A, Starkova N, Gal A, Molnar MJ, Kawamata H, Manfredi G, Adam-Vizi V and Chinopoulos C. (2016) Alterations in voltage-sensing of the mitochondrial permeability transition pore in ANT1-deficient cells. Sci Rep, 6: 26700.

372 Seizer P, Ungern-Sternberg SN, Schonberger T, Borst O, Munzer P, Schmidt EM, Mack AF, Heinzmann D, Chatterjee M, Langer H, Malesevic M, Lang F, Gawaz M, Fischer G and May AE. (2015) Extracellular cyclophilin A activates platelets via EMMPRIN (CD147) and PI3K/Akt signaling, which promotes platelet adhesion and thrombus formation in vitro and in vivo. Arterioscler Thromb Vasc Biol, 35: 655-63.

373 Lopez E, Rosado JA and Redondo PC. (2011) Immunophilins and thrombotic disorders. Curr Med Chem, 18: 5414-23.

374 Khatlani T, Pradhan S, Da Q, Gushiken FC, Bergeron AL, Langlois KW, Molkentin JD, Rumbaut RE and Vijayan KV. (2014) The beta isoform of the catalytic subunit of protein phosphatase 2B restrains platelet function by suppressing outside-in alphaII b beta3 integrin signaling. J Thromb Haemost, 12: 2089-101.

375 Nakanishi-Matsui M, Zheng YW, Sulciner DJ, Weiss EJ, Ludeman MJ and Coughlin SR. (2000) PAR3 is a cofactor for PAR4 activation by thrombin. Nature, 404: 609-13.

376 Kahn ML, Zheng YW, Huang W, Bigornia V, Zeng D, Moff S, Farese RV, Jr., Tam C and Coughlin SR. (1998) A dual thrombin receptor system for platelet activation. Nature, 394: 690-4.

377 Adams HP, Jr., del Zoppo G, Alberts MJ, Bhatt DL, Brass L, Furlan A, Grubb RL, Higashida RT, Jauch EC, Kidwell C, Lyden PD, Morgenstern LB, Qureshi AI, Rosenwasser RH, Scott PA, Wijdicks EF, American Heart A, American Stroke Association Stroke C, Clinical Cardiology C, Cardiovascular R, Intervention C, Atherosclerotic Peripheral Vascular D and Quality of Care Outcomes in Research Interdisciplinary Working G. (2007) Guidelines for the early management of adults with ischemic stroke: a guideline from the American Heart Association/American Stroke Association Stroke Council, Clinical Cardiology Council, Cardiovascular Radiology and Intervention Council, and the Atherosclerotic Peripheral Vascular Disease and Quality of Care Outcomes in Research Interdisciplinary Working Groups: the American Academy of Neurology affirms the value of this guideline as an educational tool for neurologists. Stroke, 38: 1655-711.

378 Keeling D, Klok FA and Le Gal G. (2016) Controversies in venous thromboembolism--2015. Blood Rev, 30: 27-33.

379 Armstrong PW, Gershlick AH, Goldstein P, Wilcox R, Danays T, Lambert Y, Sulimov V, Rosell Ortiz F, Ostojic M, Welsh RC, Carvalho AC, Nanas J, Arntz HR, Halvorsen S, Huber K, Grajek S, Fresco C, Bluhmki E, Regelin A, Vandenberghe K, Bogaerts K, Van de Werf F and Team SI. (2013) Fibrinolysis or primary PCI in ST-segment elevation myocardial infarction. N Engl J Med, 368: 1379-87.

380 Dannenberg S, Scheitz JF, Rozanski M, Erdur H, Brunecker P, Werring DJ, Fiebach JB and Nolte CH. (2014) Number of cerebral microbleeds and risk of intracerebral hemorrhage after intravenous thrombolysis. Stroke, 45: 2900-5.

381 Horsted F, West J and Grainge MJ. (2012) Risk of venous thromboembolism in patients with cancer: a systematic review and meta-analysis. PLoS Med, 9: e1001275.

382 Khorana AA, Francis CW, Menzies KE, Wang JG, Hyrien O, Hathcock J, Mackman N and Taubman MB. (2008) Plasma tissue factor may be predictive of venous thromboembolism in pancreatic cancer. J Thromb Haemost, 6: 1983-5.

383 Thaler J, Ay C, Mackman N, Bertina RM, Kaider A, Marosi C, Key NS, Barcel DA, Scheithauer W, Kornek G, Zielinski C and Pabinger I. (2012) Microparticle-associated tissue factor activity, venous thromboembolism and mortality in pancreatic, gastric, colorectal and brain cancer patients. J Thromb Haemost, 10: 1363-70.

384 Bharthuar A, Khorana AA, Hutson A, Wang JG, Key NS, Mackman N and Iyer RV. (2013) Circulating microparticle tissue factor, thromboembolism and survival in pancreaticobiliary cancers. Thromb Res, 132: 180-4.

385 Hisada Y, Ay C, Auriemma AC, Cooley BC and Mackman N. (2017) Human pancreatic tumors grown in mice release tissue factor-positive microvesicles that increase venous clot size. J Thromb Haemost, 15: 2208-2217.

386 Davila M, Amirkhosravi A, Coll E, Desai H, Robles L, Colon J, Baker CH and Francis JL. (2008) Tissue factor-bearing microparticles derived from tumor cells: impact on coagulation activation. J Thromb Haemost, 6: 1517-24.

387 Wang JG, Geddings JE, Aleman MM, Cardenas JC, Chantrathammachart P, Williams JC, Kirchhofer D, Bogdanov VY, Bach RR, Rak J, Church FC, Wolberg AS, Pawlinski R, Key NS, Yeh JJ and Mackman N. (2012) Tumor-derived tissue factor activates coagulation and enhances thrombosis in a mouse xenograft model of human pancreatic cancer. Blood, 119: 5543-52.

388 Geddings JE, Hisada Y, Boulaftali Y, Getz TM, Whelihan M, Fuentes R, Dee R, Cooley BC, Key NS, Wolberg AS, Bergmeier W and Mackman N. (2016) Tissue factor-positive tumor microvesicles activate platelets and enhance thrombosis in mice. J Thromb Haemost, 14: 153-66.

389 Wolberg AS. (2007) Thrombin generation and fibrin clot structure. Blood Rev, 21: 131-42.

10. BIBLIOGRAPHY OF THE CANDIDATE'S PUBLICATIONS

10. 1. Publications related to the PhD thesis

[1] Farkas AZ*, Farkas VJ*, Gubucz I, Szabo L, Balint K, Tenekedjiev K, Nagy AI, Sotonyi P, Hidi L, Nagy Z, Szikora I, Merkely B and Kolev K. (2019) Neutrophil extracellular traps in thrombi retrieved during interventional treatment of ischemic arterial diseases. Thromb Res, 175: 46-52.

Impact factor: 2.869

[2] Varju I*, Farkas VJ*, Kohidai L, Szabo L, Farkas AZ, Polgar L, Chinopoulos C and Kolev K. (2018) Functional cyclophilin D moderates platelet adhesion, but enhances the lytic resistance of fibrin. Sci Rep, 8: 5366.

Impact factor: 4.011

[3] Hisada Y, Grover SP, Maqsood A, Houston R, Ay C, Noubouossie DF, Cooley BC, Wallen H, Key NS, Thalin C, Farkas AZ, Farkas VJ, Tenekedjiev K, Kolev K and Mackman N. (2020) Neutrophils and neutrophil extracellular traps enhance venous thrombosis in mice bearing human pancreatic tumors. Haematologica, 105: 218-225.

Impact factor: 7.116

10. 2. Publications not related to the PhD thesis

[1] Varju I, Longstaff C, Szabo L, Farkas AZ, Varga-Szabo VJ, Tanka-Salamon A, Machovich R and Kolev K. (2015) DNA, histones and neutrophil extracellular traps exert anti-fibrinolytic effects in a plasma environment. Thromb Haemost, 113: 1289-98.

[2] Farkas AZ, Farkas VJ, Szabo L, Wacha A, Bota A, Csehi L, Kolev K and Thelwell C. (2019) Structure, Mechanical, and Lytic Stability of Fibrin and Plasma Coagulum Generated by Staphylocoagulase From Staphylococcus aureus. Front Immunol, 10: 2967.

[3] Kolonics F, Kajdacsi E, Farkas VJ, Veres DS, Khamari D, Kittel A, Merchant ML, McLeish KR, Lorincz AM and Ligeti E. (2021) Neutrophils produce proinflammatory or anti-inflammatory extracellular vesicles depending on the environmental conditions. J Leukoc Biol, 109: 793-806.

[4] Varjú I, Sorvillo N, Cherpokova D, Farkas ÁZ, Farkas VJ, Komorowicz E, Feller T, Kiss B, Kellermayer M, Szabó L, Wacha A, Bóta A, Longstaff C, Wagner DD, Kolev K. (2021) Citrullinated fibrinogen renders clots mechanically less stable, but lysis-resistant. Circ Res, doi: 10.1161/CIRCRESAHA.121.319061. Online ahead of print.

DOI:10.14753/SE.2022.2630

11. ACKNOWLEDGEMENTS

I would like to express my sincere gratitude to all the people who supported and encouraged me during my research and writing this dissertation.

I am deeply grateful to my supervisor, Prof. Kraszimir Kolev, who patiently guided me ever since my first lab experiments in biochemistry. His immense knowledge and inexhaustible scientific curiosity inspired me to pursue research in this field, and his profound belief in my abilities motivated me throughout my work.

I would also like to thank Dr. Imre Varjú, with whom I performed many experiments in this work, for his invaluable contribution, his unwavering support, and for the lighthearted atmosphere he created in our lab.

I am thankful for Prof. Veronika Ádám-Vizi, Prof. László Tretter, and Prof. László Csanády for giving me the opportunity to work at the Department of Medical Biochemistry at Semmelweis University.

I had great pleasure working with every member of the Hemostasis Research Division; they created a positive work environment that encouraged communication and collaboration. I would like to acknowledge the exceptional technical support provided by our assistant, Györgyi Oravecz. I also highly appreciate the continuous help of Krisztián Bálint and his contribution to the evaluation of our scanning electron microscopic images. Dr. Anna Tanka-Salamon was instrumental in my work with thrombus composition; she introduced me to the methodology and frequently provided valuable, practical suggestions, for which I am grateful. I also wish to thank Dr. Erzsébet Komorowicz for her expert help and advice in my experiments. I'd like to recognize the friendly support of Dr. Beáta Törőcsik throughout my work, as well as the insightful input provided by Dr. Dóra Ravasz while writing my thesis.

I highly appreciate the work of our collaborators Dr. László Kőhidai, Dr. Lívia Polgár, Dr. Christos Chinopoulos, and I am grateful for Dr. István Gubucz, Dr. Péter Sótonyi, Dr. Anikó Nagy, Dr. László Hidi, Dr. Zoltán Nagy, Dr. István Szikora, and Prof. Béla Merkely who made our studies with arterial thrombi possible. I would also like to thank Dr. Yohei Hisada and all the members of Prof. Nigel Mackman's lab for their work providing us with venous thrombi samples. Without the contribution of Dr. László Szabó to our electron microscopic studies and Prof. Kiril Tenekedjiev's work

establishing a mathematical background for our studies, my work would not have been possible.

I would also like to acknowledge OTKA for providing the financial background of the work presented here.

Finally, I cannot begin to express my gratitude to my whole family for their love and encouragement. Thank you for your tremendous understanding and belief in me in the past few years. Special thanks to my husband (and colleague) for his contribution to my work and his unparalleled support.